

University of Louisville

ThinkIR: The University of Louisville's Institutional Repository

Electronic Theses and Dissertations

8-2011

DNA polymerase iota promotes G2/M checkpoint activation and genetic stability after UV-induced DNA damage.

Lindsey Jay Stallons 1983-
University of Louisville

Follow this and additional works at: <https://ir.library.louisville.edu/etd>

Recommended Citation

Stallons, Lindsey Jay 1983-, "DNA polymerase iota promotes G2/M checkpoint activation and genetic stability after UV-induced DNA damage." (2011). *Electronic Theses and Dissertations*. Paper 1369.
<https://doi.org/10.18297/etd/1369>

This Doctoral Dissertation is brought to you for free and open access by ThinkIR: The University of Louisville's Institutional Repository. It has been accepted for inclusion in Electronic Theses and Dissertations by an authorized administrator of ThinkIR: The University of Louisville's Institutional Repository. This title appears here courtesy of the author, who has retained all other copyrights. For more information, please contact thinkir@louisville.edu.

DNA POLYMERASE IOTA PROMOTES G2/M CHECKPOINT ACTIVATION AND
GENETIC STABILITY AFTER UV-INDUCED DNA DAMAGE

By

Lindsey Jay Stallons
B.S., University of Louisville, 2006
M.S., Pharmacology and Toxicology, 2008

A Dissertation
Submitted to the Faculty of the
School of Medicine of the University of Louisville
In Partial Fulfillment of the Requirements
for the Degree of

Doctor of Philosophy

Department of Pharmacology and Toxicology
University of Louisville
Louisville, Kentucky

August 2011

**DNA POLYMERASE IOTA PROMOTES G2/M CHECKPOINT ACTIVATION AND
GENETIC STABILITY AFTER UV-INDUCED DNA DAMAGE**

By

Lindsey Jay Stallons
B.S., University of Louisville, 2006
M.S., University of Louisville, 2008

A Dissertation Approved on

June 3, 2011

by the following Dissertation Committee:

J. Christopher States, Ph.D.

Jason Chesney, M.D., Ph.D.

Ramesh Gupta, Ph.D.

Brian Wattenberg, Ph.D.

Wolfgang Zacharias, Ph.D.

DEDICATION

This dissertation is dedicated to my high school chemistry teacher

Mr. Tim Whitley

for instilling in me a passion for science, and for endowing me with the humor to deal
with the life such passion would bring.

ACKNOWLEDGMENTS

I would like to thank my mentor, Dr. Chris States, for his guidance and support during my graduate career. I am also grateful to my dissertation committee members, Drs. Jason Chesney, Ramesh Gupta, Binks Wattenberg, and Wolfgang Zacharias, for their help in the development and evaluation of my dissertation project. I give additional thanks to Dr. Glenn McGregor for his instruction in the field of mutagenesis, to Drs. Raju Kucherlapati and Tom Kunkel for the generous gift of mouse cell strains, and to Tom Burke, Caleb Greenwell, and Brian Sils for valued technical assistance. Finally, I thank my wife, Stacey, for her constant and unfailing support which has provided my motivation over the past five years.

ABSTRACT

DNA POLYMERASE IOTA PROMOTES G2/M CHECKPOINT ACTIVATION AND GENETIC STABILITY AFTER UV-INDUCED DNA DAMAGE

By: Lindsey Jay Stallons

June 3, 2011

Unrepaired DNA damage poses a serious threat to the genetic stability of a replicating cell. One mechanism of tolerating this damage is translesion DNA synthesis (TLS), in which an accessory polymerase synthesizes DNA directly across from a damaged template. TLS is carried out by polymerase η (Pol η), ι , κ , and REV1 in the Y-family and Pol ζ in the B-family. Pol η has the well-characterized ability to perform accurate bypass of the most common UV-induced DNA lesion; loss of Pol η results in hypermutability and severely increased risk of skin cancer. The high mutation frequency in Pol η -deficient cells has been attributed to the mutagenic TLS activity of Pol ι . Deletion of Pol ι in the Pol η -deficient background results in greatly reduced UV-induced mutation frequencies, but unexpectedly the double knockout mice develop cancer *faster* than mice deficient in Pol η alone. This unexpected finding suggests that Pol ι may have a cellular role outside of TLS, which we investigated using a gene expression approach. Pol ι -proficient and -deficient cells showed markedly different mRNA and microRNA expression changes after UV treatment. Bioinformatics analysis revealed that the G2/M checkpoint was the main point of divergence in the transcriptional response. Western

blotting showed that G2/M markers were increased and G1/S markers were decreased 24 hours after UV treatment in Pol ι -proficient cells, indicating an active checkpoint. Loss of Pol ι reversed these trends. FACS analysis of cell cycle kinetics showed a time-dependent increase in the number of aneuploid Pol ι -deficient cells after UV treatment; this degree of genetic instability was not seen in Pol ι -proficient cells. We also examined the effects of Pol ι on UV carcinogenesis in isogenic mice lacking *Xpa*, a gene central to the repair of UV-induced DNA damage. Loss of Pol ι caused a trend towards reduced tumor latency ($p=0.057$), while Pol η -deficiency caused a highly significant reduction in tumor latency ($p<0.01$). These results indicate that Pol ι plays a role in G2/M checkpoint regulation and suppressing UV carcinogenesis. At the cost of frequent point mutations, Pol ι could help cells avoid death by resolving stalled replication forks and preventing double strand breaks.

TABLE OF CONTENTS

	PAGE
ACKNOWLEDGMENTS	iv
ABSTRACT	v
LIST OF FIGURES	ix
CHAPTER	
I. INTRODUCTION	1
II. CELL CYCLE CHECKPOINT REGULATION	30
INTRODUCTION	30
MATERIALS AND METHODS	32
RESULTS	36
DISCUSSION	53
III. UV CARCINOGENESIS	60
INTRODUCTION	69
MATERIALS AND METHODS	65
RESULTS	66
DISCUSSION	69
IV. BPDE MUTAGENESIS	72
INTRODUCTION	72

MATERIALS AND METHODS	74
RESULTS	76
DISCUSSION	82
V. CONCLUSIONS AND FUTURE DIRECTIONS	86
REFERENCES	89
LIST OF ABBREVIATIONS	112
CURRICULUM VITAE	114

LIST OF FIGURES

FIGURE

1-1	Regulation of DNA lesion bypasses in <i>Sacchomyces cerevisiae</i>	4
1-2	Frequency of 6-thioguanine-resistant clones as a function of survival after UV irradiation	14
1-3	UV light-induced skin cancer in mice	16
1-4	Immunohistochemical analysis of Pol κ , Pol ι , and Pol η expression in primary gliomas tissues and normal brain tissues	21
1-5	Nucleotide excision repair	25
2-1	UV-induced mRNA expression changes in <i>Polη^{-/-} Polι^{+/+}</i> and <i>Polη^{-/-} Polι^{-/-}</i> cells	37
2-2	UV-induced microRNA expression changes in <i>Polη^{-/-} Polι^{+/+}</i> and <i>Polη^{-/-} Polι^{-/-}</i> cells	38
2-3	Confirmation of microarrays by RT-qPCR	40
2-4	Combining mRNA and microRNA expression datasets	41
2-5	Polo-like kinase signaling pathway is enriched in gene lists analyzed	43
2-6	mRNA expression changes of PLK signaling pathway members 24 hours after UV	45
2-7	Alterations in G2/M checkpoint pathway proteins after UV	46
2-8	UV-induced accumulation of mitotic markers is reversed by <i>Polι</i> -knockout	49
2-9	<i>Polι</i> -deficient cells display polyploidy after UV treatment	50

2-10	<i>Poh</i> -deficient cells display a failure in cytokinesis	52
3-1	UV spectrum and effects of terrestrial absorption	61
3-2	Skin Cancer Utrecht-Philadelphia action spectrum for hairless albino mice	62
3-3	UV-induced carcinogenesis in <i>Xpa</i> ^{-/-} mice	67
3-4	Histopathology of squamous cell carcinoma in <i>Xpa</i> ^{-/-} mice	68
4-1	Loss of Pol η or Pol ι does not affect BPDE-induced cytotoxicity	78
4-2	Loss of Pol η or Pol ι dramatically reduces BPDE-induced mutagenesis	79

CHAPTER I

INTRODUCTION

Segments of this chapter were published in the Journal of Nucleic Acids (2010).

General Introduction

Tumorigenesis is a multi-step process beginning with the transformation of a single cell by the accumulation of at least six distinct characteristics. These include infinite lifespan, resistance to anti-growth signals, resistance to apoptosis, autocrine production of growth signals, sustained angiogenesis, and tissue invasion [1]. These properties are regulated by genes in two categories: protooncogenes and tumor suppressors. Protooncogenes are normal cellular genes that can be overexpressed due to genetic changes, causing cellular transformation. A tumor suppressor is a gene that protects a cell from transformation, and loss of expression of these genes can, in concert with other genetic changes, lead to carcinogenesis.

Most environmental carcinogens induce transformation by causing mutations in the DNA that alter the activity of protooncogenes or tumor suppressors. These mutations are formed when residual, unrepaired DNA damage stalls progression of the replication fork during S phase. Stalled replication forks are most frequently resolved using error-free mechanisms that include homologous recombination or use of the homologous nascent strand as a template. Nevertheless, replication may proceed using the damaged

strand as a template in an error-prone process known as translesion DNA synthesis (TLS). TLS is defined as the incorporation of a nucleotide across from DNA damage followed by extension of the potentially mispaired primer-template, and can be error-free or error-prone.

Cellular commitment to error-free, recombinatorial damage avoidance or error-prone TLS is modulated by the molecular switch proliferating cell nuclear antigen (PCNA) (Fig. 1-1). Bulky DNA lesions can cause blockage of replicative polymerases and replication fork stalling. The ubiquitin conjugase/ubiquitin ligase pair Rad6/Rad18 is recruited to stalled replication forks where the proteins catalyze monoubiquitylation of PCNA at lysine 164. TLS proteins such as REV1 and Pol η have increased affinity for monoubiquitylated PCNA, which facilitates their recruitment and the completion of TLS [2]. In yeast, Rad5 and the MMS2-Ubc13 complex (UBE2V2-UBE2N in humans) can catalyze polyubiquitylation of PCNA via lysine 63 of ubiquitin, which blocks TLS and activates error-free damage avoidance [3]. Damage avoidance includes template switching, during which the nascent DNA strand from the sister duplex is used as an undamaged homologous template to replicate past the lesion. Humans express two Rad5 homologs, SHPRH and HLTF, and both catalyze K-63-linked polyubiquitylation of PCNA in human cells [4,5,6,7]. In yeast, Ubc9-Siz1 can attach the small ubiquitin-like modifier (SUMO) to lysine 164 of PCNA in a reaction that competes with Rad6/Rad18-mediated monoubiquitylation. PCNA SUMOylation at K-164 attracts the helicase Srs2 and prevents error-prone RAD52-dependent recombination [8].

Cells presumably risk mutations caused by TLS to relieve replication fork blockage at DNA adducts and to avoid the potential formation of extremely cytotoxic

double strand breaks (DSB). Although it accounts for less than 10% of all bypass synthesis events in yeast [9], the frequency of potentially mutagenic TLS may be as high as 50% in higher eukaryotes [10,11,12]. The propensity and mutagenic potential of TLS explain why it is etiologic in most environmentally-induced cancers and has been the focus of numerous investigations over the past decade.

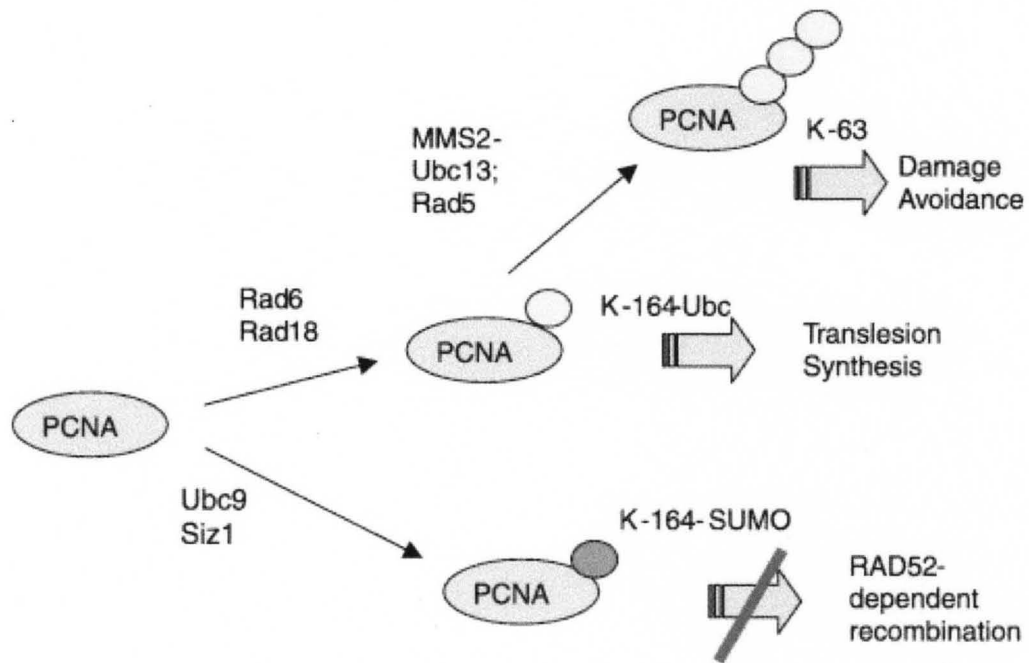


Fig. 1-1. Regulation of DNA lesion bypass in *Saccharomyces cerevisiae*. Replication fork stalling causes Rad6-Rad18 recruitment and monoubiquitylation of PCNA, causing subsequent recruitment of TLS proteins which preferentially bind monoubiquitylated PCNA. Rad5 and the MMS2-Ubc13 complex can catalyze polyubiquitylation of monoubiquitylated PCNA, blocking TLS and activating the error-free damage avoidance pathway. In addition, Ubc9-Siz1 can add SUMOylate PCNA in the same position that Rad6-Rad18 monoubiquitylate it, blocking TLS and damage avoidance and promoting error-prone RAD52-dependent recombination. Reproduced with permission from Watson N B *et al*, Cancer Lett. 2006 Sep 8;241(1):13-22. Copyright 2006 Elsevier Ireland Ltd.

TLS is performed by a relatively new category of accessory DNA polymerases. Polymerase η (Pol η), Pol ι , Pol κ , and REV1 in the Y-family [13] and Pol ζ in the B-family [14,15] are responsible for most TLS in mammalian cells. These proteins have active sites that are larger and more open than those of the high-fidelity replicative DNA polymerases (Pol α , δ , and ϵ), allowing accommodation of and synthesis past DNA templates with large, helix-distorting lesions [16]. This unique ability to synthesize DNA opposite bulky adducts helps cells avoid double strand breaks associated with replication fork stalling, but can also lead to mutagenesis by incorrect base addition. It is important to note that polymerases in the Y-family are expressed in all three kingdoms of life, indicating a critical and evolutionarily conserved role for these proteins [13]. The obviously conflicting roles of these enzymes in both preventing and promoting genetic instability are reflected in the tight cellular control of the TLS pathway (Fig. 1-1). Although extensive *in vitro* studies have given us a better understanding of their role in the cell, much less is known about the function of TLS polymerases in living animals. Limited epidemiological studies have been conducted to associate single nucleotide polymorphisms (SNPs) in TLS genes with cancer risk in humans [17,18]. Knockout mice have been generated for each gene, and carcinogenesis studies are published [19,20] or underway. Importantly, studies in mice and humans have shown that TLS polymerases, particularly Pol η , are involved in immunoglobulin gene hypermutation [21], which is beyond the scope of this dissertation

REV1

REV1 was discovered in budding yeast by the Lawrence group in 1989 as a component of the Pol ζ complex [22]. The catalytic activity of REV1 is limited to

insertion of dCMP across from a template dG [23]. The human homolog was cloned in 1999 and has the same template-dependent dCMP transferase catalytic activity on an undamaged template or an abasic site [24]. One locus used in eukaryotic cells to measure mutation frequency is *HPRT*, a gene involved in the purine salvage pathway. In this forward mutation assay, cells with loss-of-function mutations in *HPRT* are resistant to the drug 6-thioguanine (TG). REV1 is required for carcinogen-induced *HPRT* mutagenesis in human cells [25,26,27], but the catalytic activity appears to be dispensable for the induction of UV-induced mutations [28,29], indicating that this protein probably plays a structural rather than catalytic role in UV mutagenesis.

Cells from mice with a targeted deletion of the BRCA1 C-terminal (BRCT) homology domain of Rev1 (*Rev1^{B/B}*) have a reduced UV-induced mutation frequency at the *Hprt* locus [30]. However, the animals have a paradoxically decreased latency of squamous cell carcinoma (SCC) formation and only marginally reduced p53 mutagenesis in the skin after UV exposure [20]. Despite *Rev1^{B/B}* cells showing a moderate increase in chromatid breaks and exchanges after UV *in vitro* [30], comparative genomic hybridization of UV-induced SCC and normal skin DNA reveals no increase in the frequency of gross genomic alterations in *Rev1^{B/B}* SCC [20]. If point mutations and chromosomal rearrangements are near normal levels in BRCT-deleted *Rev1^{B/B}* mice, what is the reason for accelerated SCC development? Acute UV exposure of these *Rev1*-mutant mice induces enhanced Atr signaling, senescence, and apoptosis in the skin. However, long-term low-dose UV exposure causes a mitogenic response, as evidenced by epidermal hyperplasia, decreased apoptosis, and increased proliferation of CPD-containing keratinocytes [20]. Based on literature reports of the etiological role of IL-6

in carcinogenesis and elevated IL-6 levels in the skin after a single subtoxic UV dose, the authors conclude that error-prone TLS of UV-induced DNA damage is responsible for suppressing the proinflammatory, tumor-promoting effects of UV in the skin. However, more direct immunological studies are needed to confirm that Rev1 suppresses UV-induced inflammation and tumor suppression.

REV1 has also been implicated in TLS across other types of DNA lesions. Benzo[a]pyrene dihydrodiolepoxide (BPDE) is the primary carcinogenic metabolite of B[a]P and causes point mutations in a REV1-dependent manner [27,31]. BPDE-induced *Hprt* mutations are dramatically decreased in primary mouse fibroblasts after ribozyme-mediated *Rev1*-knockdown. When a plasmid expressing this ribozyme is delivered to the lungs of A/J mice by aerosol nebulization, *Rev1* mRNA is reduced by ~5%0 in the bronchial epithelium. This targeted gene therapy causes a ~40% reduction in the lung tumor multiplicity after B[a]P treatment. In addition, only 73% of ribozyme-treated mice develop lung adenomas after B[a]P, compared with 100% penetrance in control animals [32]. This report highlights the potential for interrupting translesion synthesis as a chemoprevention strategy.

Although no human disorder involving *REV1* deficiency is known, there are 16 SNPs in humans that result in nonsynonymous amino acid changes. The F257S SNP, which lies outside of all known functional domains of the protein, has been associated with an increased risk of squamous cell carcinoma of the lung in patients who have ever smoked cigarettes [33]. However, this association remains controversial [34]. The same F257S SNP was associated with decreased risk of cervical cancer, and N373S within the catalytic domain was associated with increased risk of cervical cancer. Both effects were

specific for squamous cell carcinoma and not relevant for adenocarcinoma of the cervix [17]. Although the functional consequences of these polymorphisms are unknown, these studies support a role for REV1 in the formation of multiple internal cancers.

POL η

The study of translesion synthesis in mammals began in 1999 with the discovery of the molecular defect that results in Xeroderma Pigmentosum (XP) variant syndrome. All XP patients have dramatically increased susceptibility to UV-induced skin cancer [35]. Patients in complementation groups A through G are deficient in nucleotide excision repair (NER), the major pathway for removal of helix-distorting lesions, including those induced by UV. However, the XP variant subset of patients has normal NER activity [36,37], yet displays the skin cancer-prone phenotype of NER-deficient patients. The XP variant mystery persisted for nearly three decades. Intensive investigations indicate that after UV-irradiation cells from these patients have difficulty exiting S-phase that is exacerbated by caffeine [38,39]. Further, these cells are extremely hypermutable after UV [40]. In 1999, two groups independently discovered that XP variant patients carry autosomal recessive mutations in *POLH*, the human gene coding for Pol η , and that the enzyme can catalyze error-free DNA synthesis across from a template TT cyclobutane pyrimidine dimer (CPD) [41,42,43]. The dramatic increase in skin cancer risk of XP variant patients could now be explained by the absence of a critical translesion DNA polymerase. UV principally induces photoaddition products between intrastrand adjacent pyrimidines, the most frequent of which are TT CPD. These lesions block progression of the replication fork. Data indicate that helicase activity may continue in spite of the blocked replication complex, resulting in single-stranded DNA

that is rapidly coated with replication protein A (RPA). This appears to attract the ubiquitin ligase RAD18, which has binding sites for the ubiquitin conjugase RAD6, Pol η , and RPA. One target of ubiquitylation is PCNA. Since Pol η has a ubiquitin binding domain, Pol η is now thought to be preferentially attracted to the stalled fork because it is chaperoned directly by RAD18 and binds to the ubiquitylated PCNA (Fig.1) [44]. Data indicate that Pol η then incorporates AA across from TT CPD in the template. In the absence of Pol η , another translesion polymerase, which is potentially error-prone when bypassing these common UV-induced lesions, accesses the damaged template (reviewed in [2,45]). Generation of Pol η -knockout mice shows that the highly homologous mouse Pol η protein functions similarly in UV-induced mutagenesis and carcinogenesis. Pol η -deficient mice develop squamous cell carcinoma with 100% penetrance at a UV fluence that does not cause any tumors in wild-type littermates. In addition, approximately one-third of heterozygous mice develop cancer after UV exposure [19]. This raises the possibility that humans carrying heterozygous mutations in the *POLH* gene may have an increased risk of developing skin cancer. However, this speculation has not been clinically investigated.

There is evidence that XP variant patients develop internal cancers faster than Pol η -proficient individuals [46,47], raising the possibility that Pol η -deficiency is involved in the formation of multiple human cancers caused by DNA damaging agents other than UV. Six SNPs in *POLH* have been found to date that result in nonsynonymous amino acid substitutions, but their functional significance is unknown. There is a single study evaluating the effects on cancer risk of *POLH* polymorphisms. Flanagan and colleagues found no significant changes in coding-region SNPs of *POLH* among 40 basal cell

carcinoma and squamous cell carcinoma patients in a fair-skinned Irish population [48]. It is clear that larger epidemiological studies of *POLH* status are needed to evaluate the effects of *POLH* polymorphisms.

POL ι

DNA polymerase ι (Pol ι) was discovered in 1999 as a novel homolog of Pol η in mammals and is encoded by the human *POLI* gene [49]. *In vitro* studies with purified enzyme indicate error-prone TLS function on almost all substrates examined, perhaps due to the still controversial ability of Pol ι to incorporate incoming nucleotides using Hoogsteen base pairing [50,51]. Exhaustive characterization of the error-prone replication properties of Pol ι has lent credibility to the hypothesis that *Polι* is a candidate gene for the Pulmonary adenoma resistance 2 (*Par2*) locus in mice [52,53,54]. The *Par2* locus was identified in 1996 by chromosomal linkage mapping between BALB/cJ and A/J mouse strains and plays a major role in the relative resistance of BALB mice versus the A/J strain to developing urethane-induced lung adenomas [55]. Wang *et al* identified ten amino acid-substitution polymorphisms between A/J and BALB mice that produce changes in substrate recognition of Pol ι ; while the enzyme from both strains is functional, the isoform expressed in BALB mice may be more accurate on certain undamaged templates [53]. These studies suggest that Pol ι acts to suppress urethane-induced lung adenomas. It has been hypothesized that this activity is due to the augmentation of base excision repair (BER) by Pol ι , because the enzyme has 5' deoxyribose phosphate (dRP) lyase activity and can partially reconstitute the BER-deficiency of Pol β -null cells *in vitro* [56]. It is possible that after urethane-induced DNA damage, which produces 1,*N*⁶-ethenoadenine adducts [57] that are primarily repaired by

BER [58], Pol ι acts in the gap-filling step of lesion repair. If the isoform of Pol ι expressed in A/J mice is more likely to add the incorrect G opposite a template T in the gap-filling step of BER, as was found *in vitro* [53], this could explain the increased incidence of lung adenomas in A/J mice. In support of this hypothesis, nearly all urethane-induced adenomas in mice have a CAA \rightarrow CGA transition in codon 61 of *Kras2* [52]. In addition, 129-derived mouse strains that carry a SNP in codon 27 of *Pol1* resulting in a severely truncated protein [59] display extreme sensitivity to urethane-induced lung adenomas [54]. Despite reports that splice variants of *Pol1* can exclude exon two [53], which contains the premature stop codon in 129 mice, and that brain extracts from 129 mice show Pol ι activity in a complex *in vitro* assay [60], a recent report clearly showed that the isoform of Pol ι missing exon two is catalytically inactive [61]. Thus, 129 mice either express a severely truncated 26 amino acid Pol ι protein, or an isoform lacking exon two which contains two of the three residues that make up the catalytic triad of the active site. In either case, the functional effect is *Pol1* deficiency.

In the absence of Pol ι , it has been hypothesized that another DNA polymerase, such as Pol β , inserts the incorrect base during gap filling in the repair of urethane-induced DNA damage. However, normal mouse Pol ι displays extremely error-prone properties during synthesis opposite all four undamaged template bases *in vitro* [59], making it unlikely to prevent mutations during BER in mice that are Pol ι -competent. Further studies must be completed to determine the tumor suppression mechanism of Pol ι in mouse lung carcinogenesis.

A growing body of evidence suggests that Pol ι is involved in error-prone TLS of UV-induced DNA damage *in vivo*. The heightened UV mutagenesis of Pol η -null (XP

variant) human cells has been attributed to TLS by Pol ι [62]. Loss of the functional *Poli* gene in dermal cells results in a dramatically reduced UV-induced mutation frequency at the *Hprt* locus in both wild-type and Pol η -deficient mice (Fig. 1-2). Remarkably, however, the decreased UV-induced mutagenesis observed due to loss of the error-prone Pol ι from Pol η -deficient mice is associated with *increased* cancer risk after UV exposure (Fig. 1-3) [63]. This result was confirmed and extended by Ohkumo and colleagues who showed that *Poli*^{-/-} mice are more likely to develop aggressive mesenchymal tumors after UV than *Poli*-proficient siblings [64]. These apparently contradictory findings speak to the fact that cancer etiology is more complex than the point mutations scored by the *Hprt* assay, and that one cannot use cell biology alone to accurately predict cancer risk in a TLS model. Indeed, they suggest a tumor suppressor role for Pol ι that could be separate from its role as a TLS polymerase prone to induce single base-substitution mutations. It is also possible that Pol ι is error-free when bypassing a minor UV adduct, or that it is involved in error-free BER of the minimal oxidative damage induced by UVB used in these studies [65], but more detailed experiments must be performed to evaluate these possibilities.

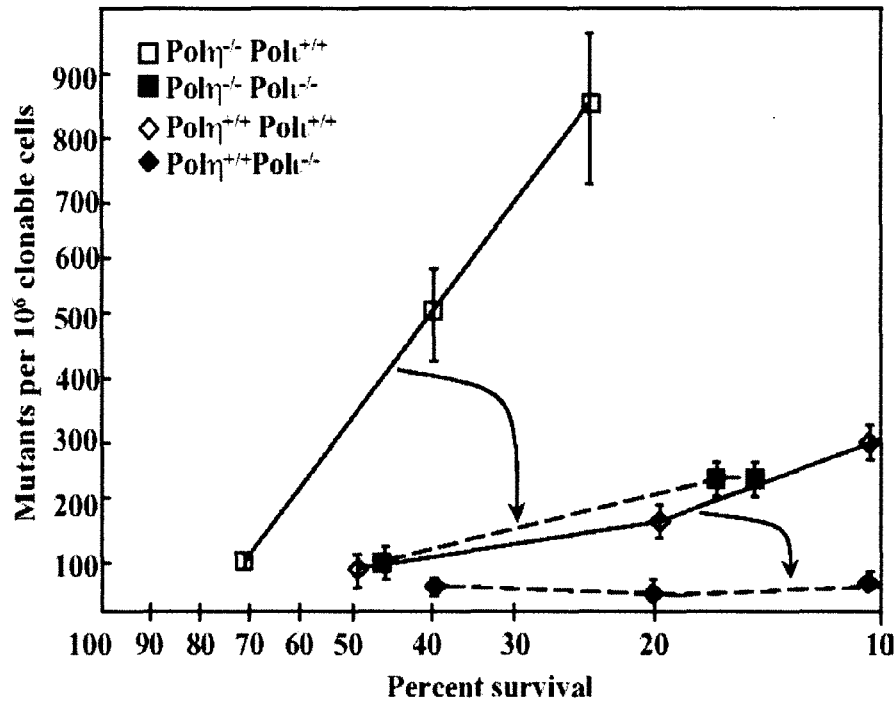


Fig. 1-2. Frequency of 6-thioguanine-resistant (TG^r) clones as a function of survival after UV irradiation. Cells were plated on three 150-mm-diameter dishes at a density of 10^4 cm^{-2} to determine mutant frequency or at cloning density to determine survival. After attachment, plates were irradiated with UV fluences to yield 20–40% survival. The actual survival in the mutagenesis experiments was determined by refeeding the survival plates at one week and staining with crystal violet after two weeks. Percent survival for each UV fluence was corrected for replating and plotted on the x -axis. The corresponding mutant frequency at each survival is plotted on the y -axis. Each point represents the mean of three independent dishes at the indicated survival, ± 1 SD. Mutant frequency at the *Hprt* locus is defined as the number of TG^r clones per million clonable cells. Each data point represents independent experiments in which $2-4 \times 10^6$ surviving cells were selected after UV irradiation and an 8- to 9-day expression period. The data have been

corrected for cloning efficiency on the day of selection, and the spontaneous background mutant frequency (1×10^{-5}) has been subtracted. The arrows indicate the reduction in mutant frequency when *PolI* is disrupted in the Pol η -deficient background (larger arrow) and in the Pol η -proficient background (smaller arrow). Reproduced with permission from Dumstorf C A et al. PNAS 2006;103:18083-18088, Copyright 2006 National Academy of Sciences, USA.

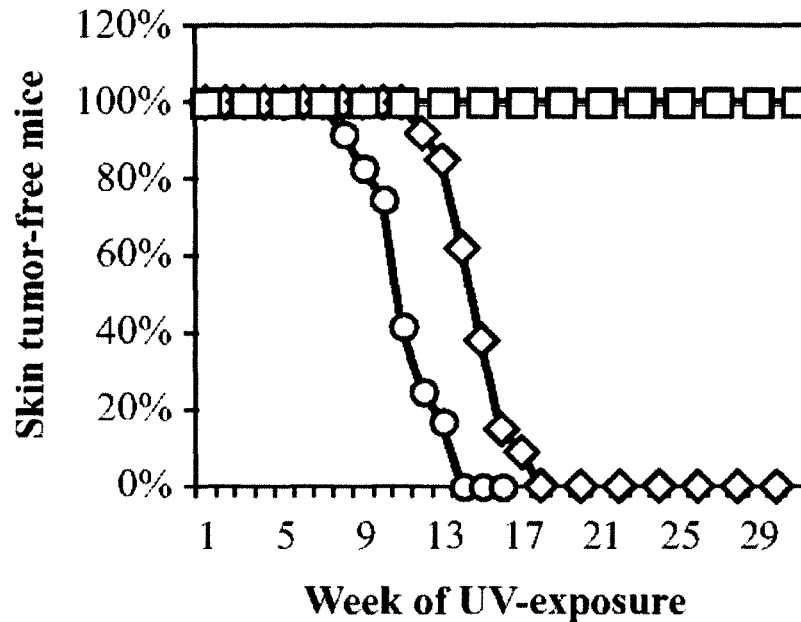


Fig. 1-3. UV light-induced skin cancer in mice. Mice were shaved once per week and irradiated three times per week with 3.75 kJ/m² for 20 weeks or until the first skin tumor arose. Mice were inspected weekly for the development of skin tumors. All 12 homozygous *Polη* knockout mice (open diamonds) developed skin tumors by 18 weeks, while all 12 *Polη*^{-/-} *Polι*^{-/-} mice (open circles) developed skin tumors by 13 weeks. This *Polι*-dependent decrease in tumor latency is highly significant (p<0.0002). No difference was found in the histological analysis of skin tumors among the groups. Reproduced with permission from Dumstorf C A et al. PNAS 2006;103:18083-18088, Copyright 2006 National Academy of Sciences, USA.

The role of Pol ι in the induction of cancer induced by other carcinogens has not been systematically studied to date. It is interesting to note that Newcomb *et al* found that Pol ι -deficient 129 mice are resistant to γ -irradiation-induced thymic lymphoma but sensitive to methylating agent-induced thymic lymphoma [66]. γ -Irradiation induces DNA strand breaks and oxidative damage, and Pol ι is known to protect cells from oxidative stress [67]. It is therefore possible that increased cell death after γ -irradiation protects *Poli*^{-/-} 129 mice from lymphomagenesis. However, Pol ι does not affect the sensitivity of Pol β -null cells to methylating agents [68], so the sensitivity of 129 mice to thymic lymphoma induced in this way is still unexplained.

There is no known human disorder involving deficiency for Pol ι . However, Pol ι is overexpressed in some lung cancer cell lines [69] as well as in primary human gliomas [18]. The T706A SNP was found to increase the risk of adenocarcinoma and squamous cell carcinoma of the lung in persons <61 years of age [33]. However, this association was not confirmed by another independent study [70] and failed to show significance in a meta analysis [71]. Another SNP in human *POLI*, F532S, is associated with prostate cancer patients whose tumors display *TMPRSS2-ERG* fusion with a highly significant odds ratio of 4.6 [72]. The protooncogenic transcription factor *ERG* was identified as the most frequently overexpressed gene in human prostate cancers [73], and fusion with the androgen-responsive serine protease *TMPRSS2* by chromosomal rearrangement was found in >90% of *ERG*-overexpressing cases [74]. Threonine 706 and phenylalanine 532, the two residues altered by these SNPs in Pol ι , are located in the noncanonical ubiquitin-binding motifs UBM2 and UBM1, respectively [75]. These two polymorphisms could therefore affect binding of Pol ι to ubiquitylated PCNA, which is

required for its recruitment to stalled replication forks following DNA damage. In the case of prostate cancer, the F532S variant of Pol ι may promote chromosomal instability by causing replication fork stalling and double-strand break (DSB) formation. DSB formed in this way could promote cellular transformation by causing chromosomal rearrangements that place the protooncogene *ERG* under control of the androgen-responsive promoter elements of *TMPRSS2* and lead to *ERG*-overexpression as is found in many prostate cancers [74]. Evidence supports the suppression of skin and lung cancers by Pol ι in humans and mice, and new studies suggest that other cancers could be affected by this protein, making it a promising candidate for future investigation. This dissertation focuses on the role of Pol ι in cell cycle checkpoint regulation and carcinogenesis after exposure to UV light.

POL κ

The fourth member of the Y-family is DNA polymerase κ . Pol κ performs faithful TLS of BPDE-induced DNA damage *in vitro* by inserting dC opposite a template BPDE-adducted G [76,77,78]. Pol κ is required for recovery from a novel BPDE-induced intra-S phase checkpoint, and the protein relocalizes to stalled replication forks after BPDE-induced DNA damage [79,80]. *Polk*^{-/-} mouse embryonic fibroblasts (MEFs) show persistent S-phase arrest after BPDE exposure, which results in increased DSB formation at stalled replication forks and increased toxicity in cells without functional Pol κ [80]. Avkin and colleagues measured TLS efficiency and fidelity in *Polk*^{-/-} MEFs using a shuttle vector technique. TLS efficiency on a plasmid containing a site-specific BPDE-*N*²-dG adduct is reduced nearly threefold in *Polk*^{-/-} MEFs, and mutagenic TLS is increased from 29% to 50% in knockout cells, supporting a role for Pol κ in the efficient

and error-free bypass of BPDE DNA damage [81]. siRNA-mediated *POLK*-knockdown also reduces the efficiency of TLS past BPDE-*N*²-dG in human U2OS cells [82]. This body of evidence suggests that Pol κ could have an important role in cancers caused by bulky chemical carcinogens like BPDE. Pol κ has also recently been linked to nucleotide excision repair. *Polk*^{-/-} MEFs have reduced levels of NER of UV damage, including reduced repair synthesis and removal of 6-4 photoproducts after UV. Both of these phenotypes are largely corrected by expressing wild-type Pol κ , but not a catalytically inactive mutant [83]. Pol κ carries out NER repair synthesis and is recruited to sites of NER through its interaction with XRCC1 and ubiquitylated PCNA [84]. These remarkable studies highlight the ability of TLS polymerases to function in multiple cellular pathways and the likelihood that *Polk* plays an important role in preventing DNA damage-induced carcinogenesis. While *Polk*-knockout mice have been generated [85,86] and show increased spontaneous mutagenesis in kidney, liver, and lung [87], no cancer studies have yet been reported using these models.

Pol κ is overexpressed in ~70% of non-small cell lung cancers (NSCLC) examined [88], and this overexpression correlates with mutation status of *TP53* [69] which is itself an indicator of poor prognosis [89]. In addition, *POLK* promoter activity is increased in *TP53*^{-/-} cells, and p53 protein suppresses *POLK* promoter activity *in vitro*. These reports suggest that Pol κ overexpression in NSCLC could be secondary to loss of functional p53, but the correlation between these two events must be investigated to rule out an etiological role for Pol κ in lung cancer. Much stronger epidemiological evidence shows that Pol κ is overexpressed in gliomas. Multivariate analysis indicates that Pol κ overexpression is an independent prognostic factor for the assessment of glioma patient

outcomes (Fig. 1-4) [18]. Although the potential role of Pol κ in the etiology of brain tumors is unclear, Pol κ is clearly a candidate for investigation of cancer risk and chemoprevention of multiple tumor types.

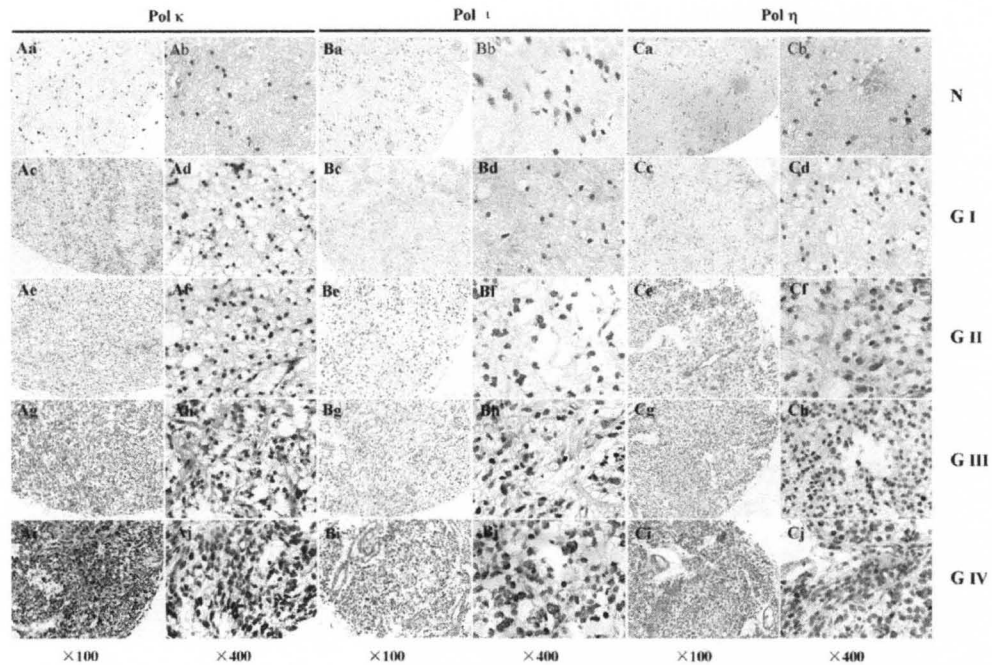


Fig. 1-4. Immunohistochemical analysis of Pol κ , Pol ι , and Pol η expression in primary glioma tissues (G) and normal brain tissues (N). Paraffin-embedded tissue microarrays comprising 104 primary glioma specimens from WHO grades I-IV were stained for Pol κ , Pol ι , or Pol η . Representative images of Pol κ , Pol ι , and Pol η expression: Aa, Ab, Ba, Bb, Ca, and Cb, normal brain tissue; Ac, Ad, Bc, Bd, Cc, and Cd, pilocytic astrocytoma (WHO grade I); Ae, Af, Be, Bf, Ce, and Cf, diffuse astrocytoma (WHO grade II); Ag, Ah, Bg, Bh, Cg, and Ch, anaplastic astrocytomas (WHO grade III); Ai, Aj, Bi, Bj, Ci, and Cj, glioblastoma multiforme (WHO grade IV); magnification: X100 (Aa, Ac, Ae, Ag, Ai, Ba, Bc, Be, Bg, Bi, Ca, Cc, Ce, Cg, and Ci) and X400 (Ab, Ad, Af, Ah, Aj, Bb, Bd, Bf, Bh, Bj, Cb, Cd, Cf, Ch, and Cj). Reproduced with permission from Wang et al. *NEURO ONCOL.* 2010; 12(7): 679-686; by permission of the Society for Neuro-Oncology.

Copyright 2010 Society for Neuro-Oncology.

POL ζ

The human homolog of yeast DNA Polymerase ζ is required for mutagenesis by UV, BPDE, and other carcinogens [14,90]. Pol ζ belongs to the B-family of DNA polymerases and contains a large catalytic subunit encoded by the *REV3* gene in humans [14] along with the much smaller regulatory protein REV7 [91]. Early investigations in *Saccharomyces cerevisiae* showed that *rev3* mutant strains have reduced rates of spontaneous mutation [92], indicating that Pol ζ is involved in the mutagenic processing of spontaneous and UV-induced mutations. Studies in mammalian cells indicate Pol ζ has a role in both repair of double strand breaks and base substitution mutagenesis, the latter likely involving extension of mispaired primer termini after initial TLS by another polymerase [93,94]. Pol ζ is the only TLS polymerase required for development, and complete *Rev3*-knockout results in mitotic catastrophe and lethality at mouse embryonic day 10.5 [95,96,97]. However, conditional *Rev3*-knockout mice have been generated and are viable and fertile. While *Rev3*-deficiency alone is insufficient to promote cancer formation, conditional *Rev3* knockout accelerates the spontaneous formation of lymphoma in *Trp53*^{-/-} mice. In humans, *REV3* gene expression is reduced by two-fold in 40 of 74 (54%) colon carcinomas compared to matched normal tissue [98]. However, normal expression is found in much smaller sample sets of gastric, colon, lung, and renal cancers [99] and the gene is not mutated in primary tumors or cell lines from breast and colon cancers [91]. The expression levels of *REV3* in human cancers, particularly colon carcinoma, must be revisited using larger sample sizes to draw firm conclusions about the correlation of gene expression and cancer progression. No studies are published

investigating the 25 nonsynonymous SNPS in human *REV3*, but the possibility exists that functional changes in human Pol ζ could alter the risk of cancer formation.

NUCLEOTIDE EXCISION REPAIR

Translesion synthesis is a mutagenic process that leaves intact lesions in DNA. Most lesions which initiate TLS are removed from the genome by nucleotide excision repair (NER), a process by which damaged bases such as CPD are enzymatically removed as a part of an oligonucleotide fragment (comprehensive review in [100] (Fig 1-5). NER has two branches; global genomic-NER (GG-NER) describes the repair of damage from transcriptionally silent areas of the genome, while transcription-coupled NER (TC-NER) is dependent on the stalling of RNA polymerase II. The two branches of NER differ in the mode of damage recognition. All lesions recognized by NER cause local disturbances in the helical structure of DNA; this disturbance is recognized by the XPC:RAD23B complex in GG-NER to initiate binding of the complex to the lesion site in the DNA [101,102]. XPC acts to recruit TFIIH, a multi-subunit complex [103,104]. The next step in GG-NER is the formation of the preincision complex, which requires recruitment of the scaffolding protein XPA, the endonuclease XPG, and the ssDNA-binding protein RPA [105]. XPD and XPB are ATP-dependent helicases contained in the TFIIH complex confer single-strand character on a ~30 nucleotide region surrounding the lesion [106]. The damaged lesion is pinpointed during formation of the preincision complex, which allows XPG to be positioned and to cleave the damaged DNA strand 3' of the lesion. The ERCC1-XPF complex is then recruited to excise the oligonucleotide fragment by cleaving the damaged strand 5' of the lesion [107]. Repair synthesis then fills the resulting single-strand DNA gap, and this step is performed by one of the

replicative B-family polymerases, Pol δ [108] or Pol ϵ [109], or by Pol κ as previously discussed [84]. Finally, the patch is sealed by a DNA ligase [110].

TC-NER differs from GG-NER in the manner of lesion recognition, and was discovered based on the observation that UV-induced CPD are removed from the highly transcribed *DHFR* gene approximately 50-fold faster than a nearby untranscribed region of the genome [111]. Stalling of RNA polymerase II causes recruitment of the SWI/SNF ATP-dependent chromatin remodeling complex CSB/RAD26 and rewinding of the transcription bubble [112]. This promotes dissociation of the RNA polymerase and identification of the lesion in the DNA template, at which point RPA, XPA, and TFIIH are recruited to the lesion site to form the preincision complex, as in GG-NER.

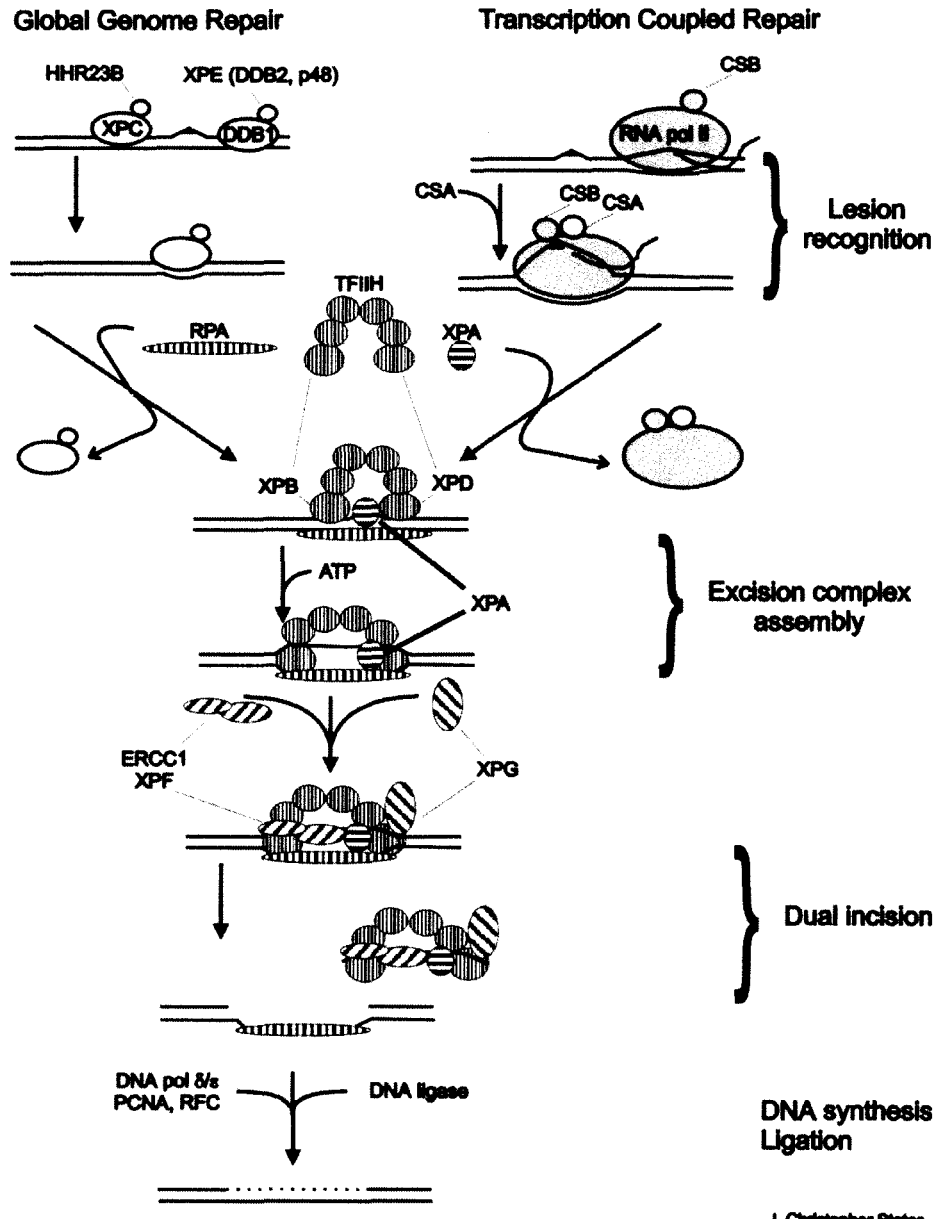


Fig. 1-5. Nucleotide excision repair (NER). Transcription coupled NER and global genomic NER differ in the mechanism of lesion recognition, but share common excision and repair synthesis proteins. Illustration kindly provided by Dr. J. Christopher States, University of Louisville.

XPA-deficient cells have no residual NER activity [113], and *XPA* humans and mice have dramatically increased risk of UV-induced skin cancer [35,114]. *XPA* cells are hypermutable due to deficiency in both TC-NER and GG-NER subpathways of excision repair. *Xpa*^{-/-} mice are used in UV carcinogenesis studies described in this dissertation due to the advanced timeline of cancer development in these animals.

CELL CYCLE CHECKPOINTS

Precise regulation of cell cycle progression is critical for maintenance of genomic integrity for actively dividing cells. Cell cycle progression was originally proposed to have a fixed timeline, but this theory was disproved when γ -irradiation caused cell cycle arrest proportional to the amount of DNA damage induced [115]. Eukaryotic cells display G1/S, G2/M, intra-S, mitotic spindle, and postreplication checkpoints after various types of DNA damage; the G2/M and intra-S phase checkpoints are most relevant to this dissertation.

Progression from G2 to M phase is regulated by the cyclin dependent kinase CDK1, and DNA damage-induced arrest regulates the activity of CDK1 through a series of phosphorylation events (Fig. 1-6). G2-arrest is maintained by the inhibitory phosphorylation of CDK1 on Tyr15, catalyzed by the kinase WEE1 [116,117]. CDK1 is dephosphorylated at Tyr15 and activated to promote G2 \rightarrow M progression by the dual-specificity phosphatase CDC25. CDC25C is regulated by sequestration in the cytoplasm by 14-3-3 proteins. CHK1 kinase-mediated phosphorylation of Ser216 on CDC25C in the nucleus promotes binding of 14-3-3 and nuclear export [118,119]. Polo-like kinase 1 (PLK1) is a master regulator of the G2/M checkpoint. PLK1 phosphorylates cyclin B at

Ser133 and Ser147 and promotes further activation of the CDC2/cyclin B complex to promote mitotic entry [120,121]. WEE1 kinase is regulated by destabilizing phosphorylation by PLK1 and CDC2 [122]. MYT1 is another kinase responsible for inhibitory Tyr15 and Thr14 phosphorylation of CDC2, and MYT1 is hyperphosphorylated and deactivated by PLK1. PLK1 also phosphorylates CDC25C in the nuclear export signal to prevent its nuclear export in a 14-3-3-independent manner [123].

The intra-S phase checkpoint is a p53-independent mechanism of arresting DNA synthesis upon DNA damage. γ -irradiation-induced DNA damage activates the sensor kinase ATM, which in turn activates the effector kinase CHK2. Activated CHK2 then phosphorylates CDC25A at Ser123 to promote the proteasomal degradation of CDC25A. Degradation of CDC25A, the regulatory phosphatase, for the G1/S checkpoint leads to sustained inhibitory phosphorylation of CDK2 at Tyr15 and Thr14 and persistent S-phase arrest [124,125]. Translesion synthesis proteins are known to regulate the intra-S phase checkpoint. While UV most strongly activates the p53-dependent G1/S checkpoint in normal cells, XP variant cells show a strong intra-S phase checkpoint [38,39]. While new origins of replication fire at expected rates, replication fork progression is blocked at sites of UV-induced DNA damage. The absence of Pol η , the evolutionarily conserved TLS polymerase for bypassing UV-induced DNA damage, prevents resolution of stalled replication forks and leads to activation of the ATR/CHK1 pathway [126]. BPDE also induces an intra-S phase checkpoint [79,127], that is dependent upon the Y-family Pol κ . A deficiency in this polymerase results in failure to recover from BPDE-induced S-phase arrest and causes double strand breaks, likely due to collapse of stalled replication forks

[80]. These studies show that TLS polymerase can directly impact cell cycle checkpoints via their role in stabilizing stalled replication forks

CONCLUSIONS

The importance of translesion DNA synthesis in preventing human cancer is well understood from the example of XP variant, in which patients lacking the Y-family DNA polymerase η are prone to develop UV-induced skin cancers due to an extremely hypermutable phenotype. However, we understand very little about how the other polymerases involved in TLS affect human health and cancer risk. Recently developed mouse models have so far provided conflicting results; ribozyme-mediated knockdown of total Rev1 and removal of the BRCT domain both result in reduced mutagenesis by BPDE or UV, respectively. As expected, when *Rev1* mRNA is knocked down using the same ribozyme delivered to the lungs of mice, multiplicity of B[a]P-induced lung adenomas decreases [32]. In contrast, Rev1 BRCT-null mice develop UV-induced squamous cell carcinomas *faster* than wild-type controls [20]. In a similarly paradoxical finding, mice lacking both Pol η and Pol ι have decreased UV-induced mutations in their dermal fibroblasts and accelerated development of squamous cell carcinoma after UV treatment compared to Pol ι -proficient animals [63]. While it is understood that the mutations induced by these polymerases are etiological in many environmentally-induced cancers, it is clear from these studies that simply blocking TLS is not sufficient to reduce cancer risk, and in fact may cause an acceleration of carcinogenesis. One potential explanation for these apparently contradictory findings is that TLS polymerases have pleiotropic functions; DNA damage tolerance is the classic role, but they are also involved in cell cycle checkpoint regulation [80], NER [84], and somatic hypermutation [21]. Data presented in this dissertation indicate that Pol ι is involved in regulating the G2/M checkpoint after UV-induced DNA damage. These results suggest a novel role for

Pol ι and could explain the apparent tumor suppressor activity of Pol ι seen in multiple studies [63,64,66]

CHAPTER II

CELL CYCLE CHECKPOINT REGULATION

INTRODUCTION

Translesion synthesis (TLS) is the direct synthesis of DNA across from a damaged template and is performed by the Y-family of DNA polymerases [2]. These specialized enzymes (Pol η , ι , κ , and REV1 in higher eukaryotes) are recruited to stalled replication forks due to blockage of the replicative DNA polymerases, Pol δ and Pol ϵ , at sites of DNA damage. Mammalian cells use TLS instead of more accurate damage bypass mechanisms as much as 50% of the time to bypass replication-blocking lesions [10,11,12]. The frequency of TLS combined with its highly mutagenic potential make it a critical target of study for cancer chemoprevention. Pol η catalyzes accurate TLS of the most common CPD [41,42] and is defective in xeroderma pigmentosum (XP) variant syndrome [43,128]. XP variant patients have extremely high risk of UV-induced skin cancer because their cells are extremely hypermutable upon UV exposure [40]. Pol ι catalyzes inaccurate, error-prone TLS of UV-induced DNA damage [129] and is at least partially responsible for the high frequency of UV-induced mutations in XP variant cells [62,130]. We previously found that mouse cells lacking functional Pol ι have reduced mutation frequencies after UV irradiation, but the loss of this error-prone DNA polymerase accelerates tumorigenesis in Pol η -deficient mice [63]. Accelerated tumorigenesis in

Polη^{-/-} Polι^{-/-} mice has been confirmed [64] and suggests that Pol ι could participate in UV-induced carcinogenesis outside of its role in TLS.

In addition to participation in DNA synthesis, Y-family polymerases are known to regulate cell cycle progression. The first known example was the pronounced intra-S phase arrest observed in XP variant cells after UV irradiation [38,39]. Cells lacking Polη fire new origins of replication, but elongation of nascent strands is blocked due to unresolved replication fork stalling. Polκ has also been shown to regulate a distinct intra-S phase checkpoint. After treatment with benzo[a]pyrene dihydrodiol epoxide (BPDE), *Polκ^{-/-}* MEFs fail to complete S phase at the rate of wild-type cells and display elevated activation of ATM and Chk1 [80]. Other reports have shown that *S. cerevisiae* Rev1 protein levels are ~50-fold higher in G2/M phase than in G1 [131], and that disruption of the BRCT domain of Rev1 in mouse cells causes G2 arrest after UV treatment [30]. These studies together suggest that Y-family DNA polymerases can affect cell cycle checkpoints after treatment with genotoxic agents. The experiments in this chapter were designed to address the hypothesis that Pol ι regulates cell cycle progression after UV-induced DNA damage.

Materials and Methods

Cells and cell culture

Primary murine fibroblasts from *Polη^{-/-}* and *Polι^{-/-}* mice were a generous gift from Raju Kucherlapati (Harvard University) and were prepared as described previously [63] with slight modifications. A piece of ear tissue was rinsed thoroughly in ethanol, then sterile PBS, then finely minced in a 10 cm cell culture dish using two scalpels. The minced tissue was allowed to sit for 10 minutes in a laminar flow hood with the dish lid cracked for ~15 min to allow the tissue to adhere to the dish. Media was then gently added to the dish to cover the surface of the tissue. Media consisted of MEM- α (Cambrex Bioscience, Walkersville, MD) supplemented with 10% FBS (HyClone, Logan, UT), 2 mM glutamine, nonessential amino acids (Mediatech, Herndon, VA), penicillin (100 units/ml), and streptomycin (100 g/ml). Minced tissue was placed incubated for up to three weeks under normoxic conditions at 37°C / 5% CO₂ / 21% O₂ and refed weekly. Once cells reached confluence, tissue pieces were aspirated off and cells were designated “passage zero” and split to a 15 cm dish. After passage zero was reached, all primary mouse cells were incubated under hypoxic conditions (5% CO₂ / 2% O₂) based on a previous report that these cells have increased population doublings and time to senescence under hypoxia [132]. For UV treatments, UV_{254nm} flux was measured using a radiometer (model IL 1700; International Light, Peabody, MA). The average fluence was ~0.5 J/m²/s. Media was aspirated and cells were washed twice with PBS exposure to 4, 8, or 16 J/m². SV40-transformed human fibroblasts (GM0637) were cultured in DMEM (Cambrex Bioscience, Walkersville, MD) supplemented with 10% FBS (HyClone, Logan, UT), 2 mM glutamine, penicillin (100 units/ml), and streptomycin (100 g/ml).

mRNA expression

Total mRNA was isolated from cell culture plates on ice using the miRNeasy kit (Qiagen, Valencia, CA), amplified, and resultant cDNA was transcribed using the GeneChip® IVT Labeling Kit for hybridization on Affymetrix MOE 430_2.0 arrays using a GeneChip® Scanner 3000 7G. A two-way ANOVA including interaction was used to detect transcripts with significant interactions between cell line and treatment. An overall F-test was used to determine which transcripts had at least one significant effect using the SAS software package. An FDR cut-off of 0.1 was used for multiple testing correction, followed by a cut-off for interaction p-value of 0.05 to produce a list of transcripts with a statistically significant interaction effect. This interaction list was filtered to include only transcripts with relative fold changes of >1.5 or <-1.5 in either cell line. Statistical analyses were performed in collaboration with the Bioinformatics, Biostatistics, and Computational Biology core facility at the Center for Environmental Genomics and Integrated Biology at UofL.

microRNA expression

cDNA was generated and labeled, hybridized to microarrays, and scanned by LC Sciences (Dallas, TX). Total RNA was isolated using the miRNeasy kit (Qiagen, Valencia, CA) and enriched for transcripts <300nt using size fractionation after which these transcripts were 3' extended with poly(A) polymerase and fluorescently labeled with either Cy3 or Cy5. Hybridization of one Cy3- and one Cy5-labeled sample per chip was followed by detection and quantification of fluorescence and as the Cy3/Cy5 ratio. Microarrays were designed by LC Sciences and included redundant probes to detect all

miRNA transcripts listed in Sanger miRBase 10.1. Data were analyzed by background subtraction and LOWESS normalization, and a p-value cut-off of 0.05 was applied for the t-test.

RT-qPCR

Confirmation of mRNA and microRNA expression was performed by amplifying target transcripts using specific primers and probes and a 7900HT Fast Real-Time PCR System from Applied Biosystems (Foster City, CA). The $\Delta\Delta C_T$ method was used to measure target mRNA or microRNA expression relative to *GAPDH* or *snoRNA202*, respectively.

microRNA target prediction:

Individual microRNAs determined to have significant expression changes after UV treatment ($p < 0.05$ by a t-test) were used as search terms for the miRanda microRNA target prediction algorithm [133,134]. The list of predicted microRNA targets for each genotype were intersected with the list of UV-responsive mRNAs to produce a list of filtered microRNA targets for each genotype.

Global pathway analysis

Three lists of mRNAs were analyzed using Ingenuity Pathway Analysis (Ingenuity systems): interaction mRNA, *Pol η ^{-/-} Pol η ^{+/+}* filtered microRNA targets, and *Pol η ^{-/-} Pol η ^{-/-}* filtered microRNA targets.

Immunoblots

For immunoblots, cell lysates were prepared from trypsinized cell pellets with 10 mM tris base pH 7.4, 1 mM EDTA, 0.1% SDS, 180 μ g/ml phenylmethanesulfonylfluoride).

Twenty μg whole cell lysate was separated on a 4-15% SDS-PAGE gel and transferred to a PVDF membrane via electroblot using Towbin's transfer buffer (25 mM tris base pH 8.3, 192 mM glycine, 20% methanol, 0.02% sodium dodecyl sulfate), and analyzed with the following antibodies: Wee1 (Millipore, 1:500), cyclin B1 (BD Pharmingen, 1:1000), Cdk1 (Millipore 1:1000), cyclin E (Abcam, 1:500), phospho-histone H3 (Cell Signal, 1:1000), and β -actin (Sigma, 1:10,000). All antibodies were diluted in 5% nonfat dry milk and incubated overnight at 4°C.

Cell cycle analysis

Cells were pulse labeled for 30 min with 10 μM BrdU (BD Pharmingen, San Diego, CA), washed twice with PBS, and immediately UV irradiated. At 0, 6, 12, 18, 24, and 30 hours after UV, cells were trypsinized and collected for FACS analysis. Samples were double-stained for BrdU and 7-aminoactinomycin D (7AAD) using the FITC BrdU Flow Kit (BD Pharmingen, San Diego, CA) following the manufacturer's instructions. FACS analysis was performed on a FACScan flow cytometer (BD Biosciences, San Jose, CA). Results were analyzed using FlowJo software.

Direct nuclear counting

Asynchronous cells were plated at $10^4 / \text{cm}^2$ and stained with giemsa the following day. Stained cells were analyzed under 40X magnification. Two hundred cells per well were counted for each genotype with three wells in total counted per experiment per genotype. Three independent experiments were performed and results were analyzed using a single factor ANOVA. Individual comparisons were made using the student's t-test.

RESULTS

Polymerase iota deficiency alters the DNA damage response after UV treatment at the transcriptional level

To determine the effect of *Poli*-deficiency on the UV DNA damage response, primary ear fibroblasts from *Polη^{-/-} Poli^{+/+}* and *Polη^{-/-} Poli^{-/-}* mice were irradiated with 4 J/m² UV, a dose which results in ~30% survival [63]. Total RNA was harvested 24 hours later and global microarrays were performed to analyze mRNA and microRNA expression profiles. There were 6,397 and 5,207 UV-responsive mRNAs in *Polη^{-/-} Poli^{+/+}* and *Polη^{-/-} Poli^{-/-}* cells, respectively. These transcripts all had fold changes >1.5 or <-1.5 with $p < 0.05$ and $q < 0.1$. To statistically differentiate between these large lists of UV-responsive mRNAs and identify the transcriptional effect of *Poli*-knockout on the UV DNA damage response, the interaction term was included in the two-way ANOVA analysis of UV treatment and genotype effect. In this statistical test, a significant interaction term indicates that the UV-induced fold change of a particular mRNA was different between the two cells trains. This analysis identified 484 mRNAs, termed the “Interaction mRNA” (Fig. 2-1), with a significant interaction between *Polη^{-/-} Poli^{+/+}* and *Polη^{-/-} Poli^{-/-}* cells after UV treatment ($p < 0.05$, $q < 0.1$, fold change >1.5 or <-1.5).

UV-responsive miRNAs are shown in Fig. 2-2. Nine microRNAs were identified in *Polη^{-/-} Poli^{+/+}* cells and 11 microRNAs in *Polη^{-/-} Poli^{-/-}* cells with significant fold changes after UV treatment ($p < 0.05$). Remarkably, the lists of UV-responsive microRNAs were mutually exclusive. To confirm the microarray results, two mRNAs

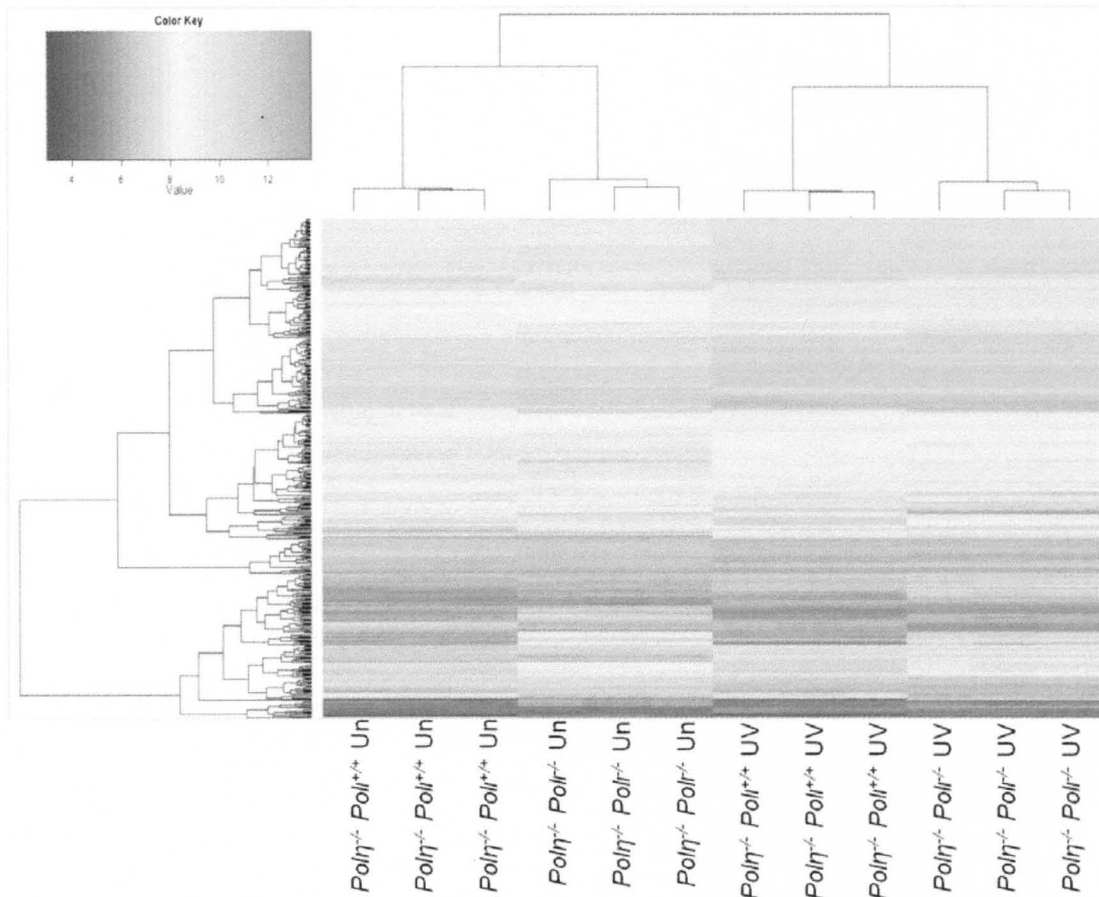


Fig. 2-1. UV-induced mRNA expression changes in $Pol\eta^{-/-} Pol\iota^{+/+}$ and $Pol\eta^{-/-} Pol\iota^{-/-}$ cells. Treatment with ultraviolet radiation altered expression of 6,397 genes in $Pol\eta^{-/-} Pol\iota^{+/+}$ cells and 5,207 genes in $Pol\eta^{-/-} Pol\iota^{-/-}$ cells ($p < 0.05$, $q < 0.1$, and $-1.5 > \text{fold change} > 1.5$ in either genotype). A list of 484 transcripts showed a significant interaction effect with $p < 0.05$ and $q < 0.1$. Results are from three replicate dishes from a single biological experiment. The color key indicates normalized signal intensity values.

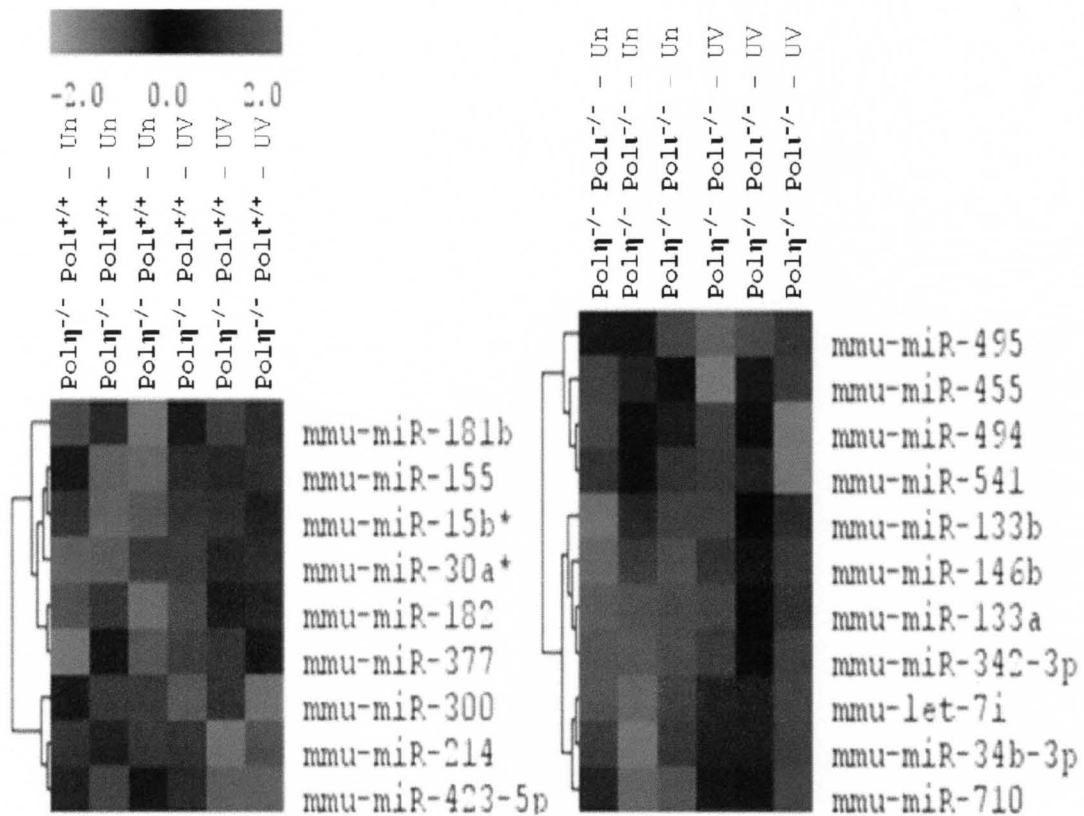


Fig. 2-2. UV- induced microRNA expression changes in *Polη*^{-/-} *Polt*^{+/+} and *Polη*^{-/-} *Polt*^{-/-} cells. A t-test identified 9 microRNA in *Polη*^{-/-} *Polt*^{+/+} cells and 11 microRNA in *Polη*^{-/-} *Polt*^{-/-} cells that showed significantly altered expression after UV treatment ($p < 0.05$). The two lists were mutually exclusive. Results are from three replicate dishes from a single biological experiment.

and two microRNAs were chosen at random from the lists of significantly altered transcripts for RT-qPCR confirmation. As shown in Figure 2-3, microarray results for mRNA and microRNA were reproducible with the exception of *Ptprv* increased in *Polη^{-/-} Poli^{+/+}* cells which could not be confirmed. We also found using RT-qPCR that miR-214 was slightly but significantly decreased in *Polη^{-/-} Poli^{-/-}* cells, which was not found using the microarray platform.

Bioinformatics analysis indicates that Poli-deficiency alters the PLK pathway for mitotic entry and exit

In order to combine mRNA and microRNA expression data, a bioinformatics approach was used to identify the cellular pathway(s) affected by *Poli*-deficiency after UV treatment. Figure 2-4 shows a schematic representation of the analyses performed. The miRanda microRNA target prediction algorithm was used to computationally predict mRNA targets of the 9 and 11 UV-responsive microRNAs in *Polη^{-/-} Poli^{+/+}* and *Polη^{-/-} Poli^{-/-}* cells, respectively. This analysis yielded 8,519 predicted microRNA targets in *Polη^{-/-} Poli^{+/+}* cells and 6,360 predicted targets in *Polη^{-/-} Poli^{-/-}* cells. To reduce the total size and increase the biological relevance of the predicted microRNA targets dataset, the list of predicted microRNA targets for each genotype was then intersected with the list of UV-responsive mRNAs identified in the two-way ANOVA. In *Polη^{-/-} Poli^{+/+}* cells, this final filtered microRNA targets list contained 1,529 mRNAs, while 1,339 filtered microRNA targets remained in *Polη^{-/-} Poli^{-/-}* cells.

Three lists of mRNAs were analyzed for global pathway enrichment using Ingenuity Pathway Analysis (IPA). The 484 interaction mRNAs, 1,529 filtered *Polη^{-/-}*

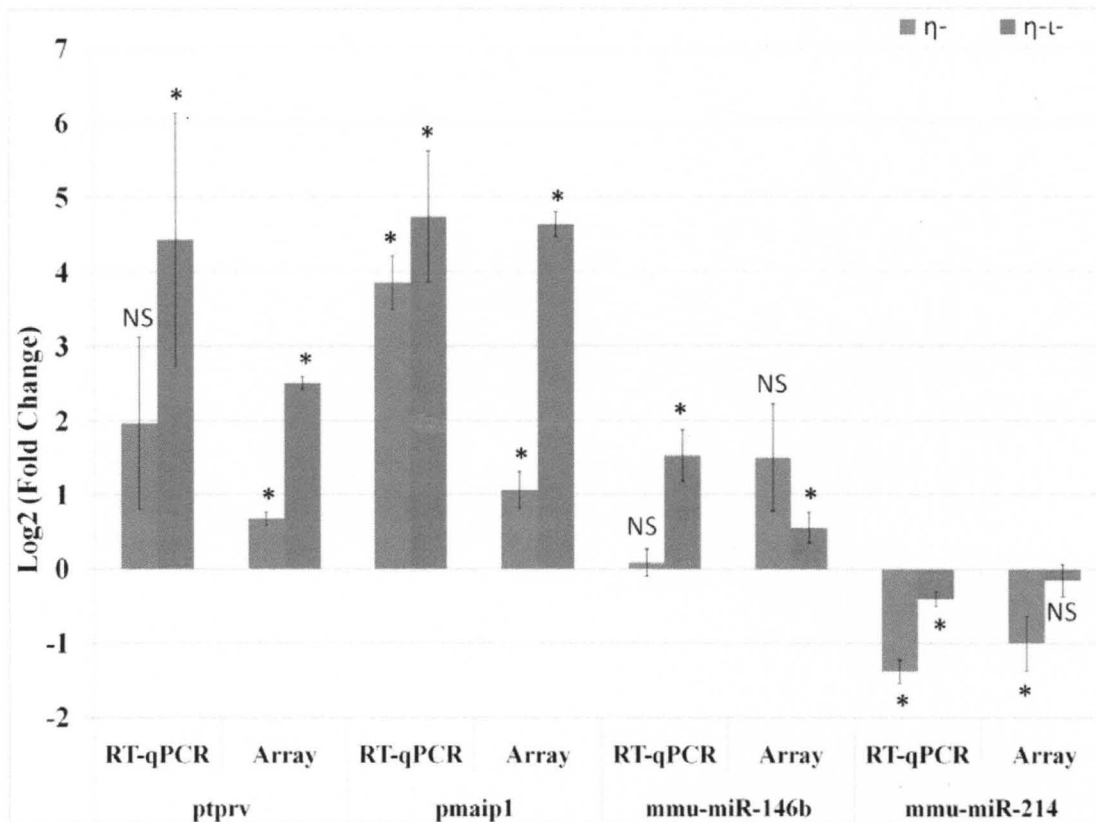


Fig. 2-3. Confirmation of microarrays by RT-qPCR. UV-induced gene expression changes were validated using RT-qPCR for four transcripts. A significant decrease was measured for miR-214 in *Pol $\eta^{-/-}$ Pol $\iota^{-/-}$* cells using qRT-PCR that was not identified using the microarray platform. Results are from four replicates from two independent experiments. $p < 0.05$, NS = not significant. Error bars, standard deviation.

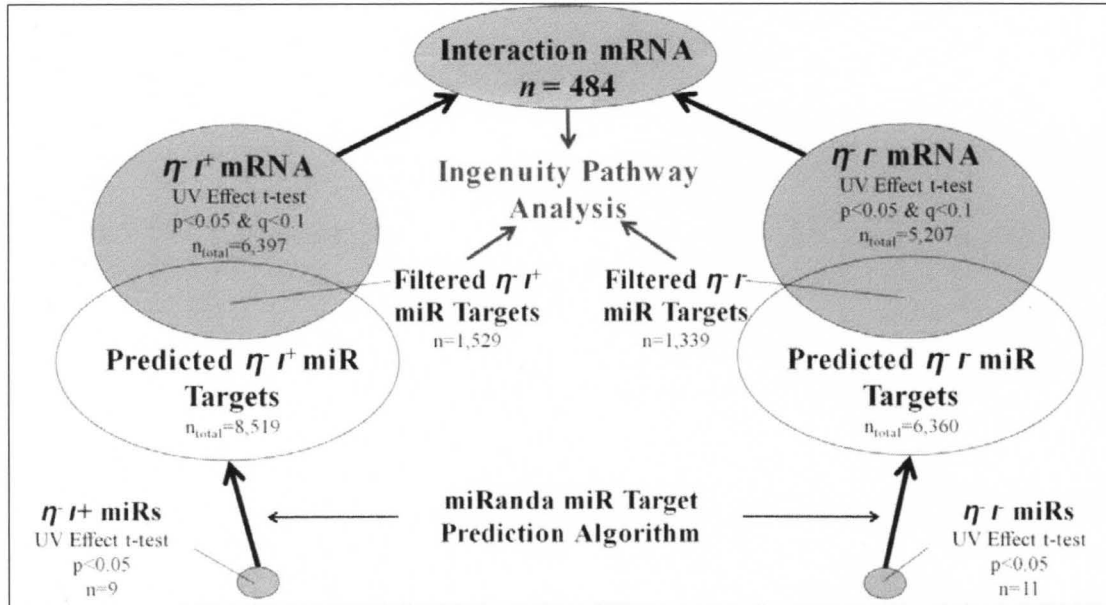


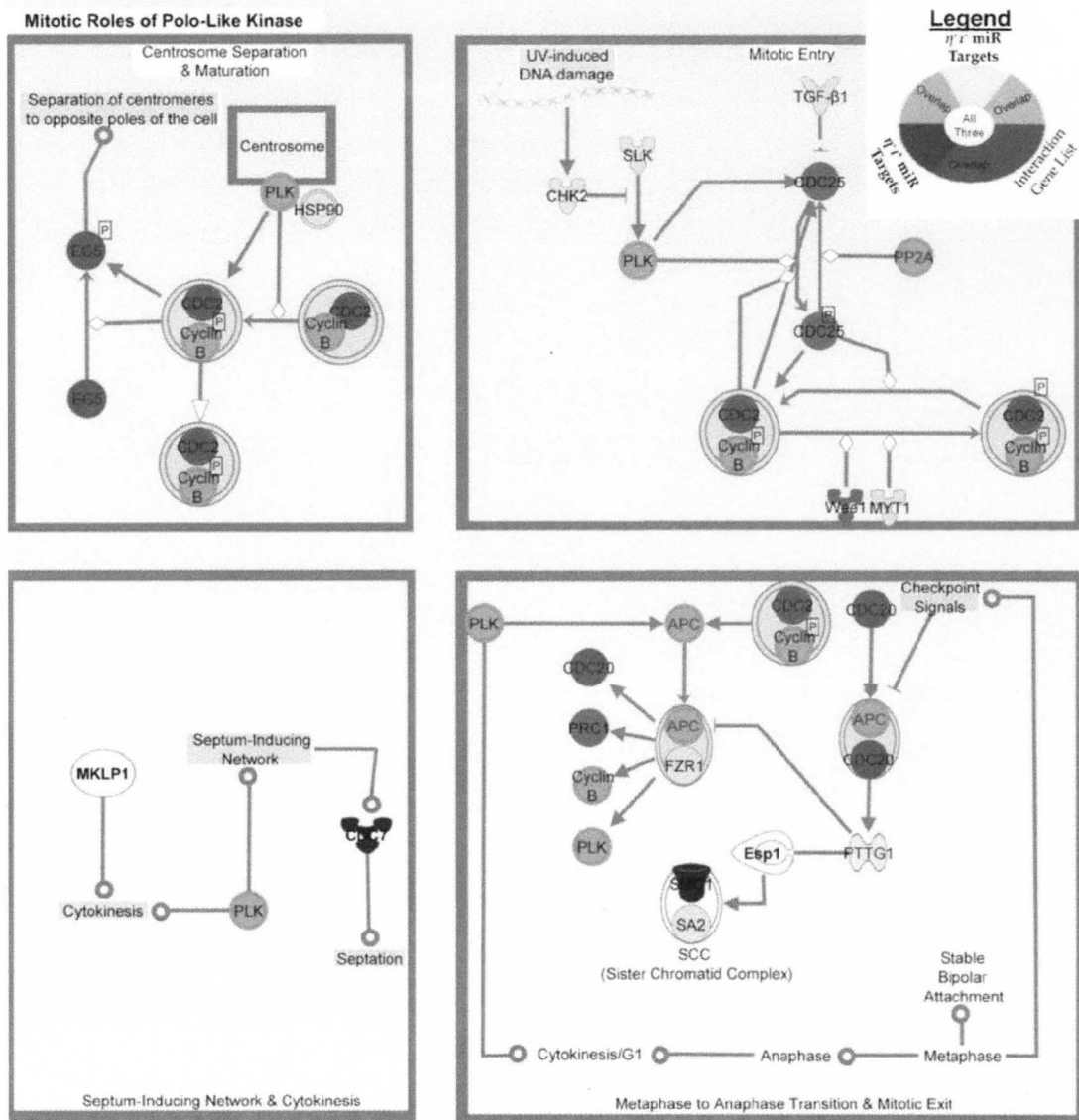
Fig. 2-4. Combining mRNA and microRNA expression datasets. Venn diagram representing biostatistical and bioinformatics analyses of mRNA and microRNA datasets. Shaded ovals represent experimentally obtained datasets, unshaded ovals represent computationally determined datasets. A two-way ANOVA featuring the interaction term was used to generate the interaction mRNA list (see Figure 1). The miRanda target prediction algorithm was used to predict all mRNA targets of UV-responsive miRNA's in both cell strains. To reduce the size and increase the biological relevance of the microRNA targets list, the predicted targets list was intersected with the UV effect t-test list. The resulting filtered microRNA targets lists totaled 1,529 in *Polη^{-/-}* *Poli^{+/+}* cells and 1,339 in *Polη^{-/-}* *Poli^{-/-}* cells.

Poli^{+/+} microRNA targets, and 1,339 filtered *Polη*^{-/-} *Poli*^{-/-} microRNA targets lists were all analyzed using IPA and the results are presented in Fig. 2-5. The only canonical pathway that was significantly enriched in all three lists was the PLK signaling pathway for mitotic entry and exit. Of the 62 molecules that IPA lists in the pathway, the interaction mRNA list contained 12/62 (p = 1.17E-9), the *Polη*^{-/-} *Poli*^{+/+} filtered microRNA targets list contained 10/62 (p = 1.48E-2), and the *Polη*^{-/-} *Poli*^{-/-} filtered microRNA targets list contained 10/62 (p = 2.19E-3).

To more closely examine gene expression patterns in the PLK signaling pathway for mitotic entry and exit, all genes listed in this pathway by IPA were downloaded and analyzed in our mRNA dataset for expression patterns. Of the 70 genes listed by IPA in the pathway, 31 were significantly altered in both *Polη*^{-/-} *Poli*^{+/+} and *Polη*^{-/-} *Poli*^{-/-} cells (p < 0.05, q < 0.1, and -1.5 > fold change > 1.5); the lists were not identical. Fig. 2-6 shows the log₂(fold change) ratios for all of the 37 genes that were altered in either genotype. Twenty-seven of 37 (73%) genes were increased in one or both genotypes; of these, 23 (85%) showed greater increase in *Polη*^{-/-} *Poli*^{+/+} cells.

Loss of Pol 1 relieves a strong mitotic checkpoint in Polη^{-/-} cells after UV treatment.

In order to validate the bioinformatics analysis indicating altered mitotic checkpoint activity with *Poli*-deficiency, cells were treated with 4 J/m² UV and analyzed for protein expression at 24 hours by western blot. Fig. 2-7 shows that in *Polη*^{-/-} *Poli*^{+/+} cells, UV caused a modest increase in the G2/M marker cyclin B1. In contrast, cyclin B1 levels were reduced after UV in *Polη*^{-/-} *Poli*^{-/-} cells. The kinase WEE1 was stable at 24



© 2009 Ingenuity Systems, Inc. All rights reserved.

Fig. 2-5. Polo-like kinase signaling pathway is enriched in gene lists analyzed. The interaction mRNA list, filtered *Polη^{-/-} Poli^{+/+}* microRNA targets, and filtered *Polη^{-/-} Poli^{-/-}* microRNA targets were analyzed using Ingenuity Pathway Analysis for global pathway enrichment. Polo-like kinase signaling for mitotic entry and exit was the only pathway that was enriched and shared among all three lists. Twelve of the 62

molecules in the pathway were present on the interaction mRNA list ($p=1.17E-09$), along with 10 of 62 molecules on the filtered *Pol η ^{-/-} Pol ι ^{+/+}* microRNA targets list ($p=1.48E-02$), and 10 of 62 molecules on the filtered *Pol η ^{-/-} Pol ι ^{-/-}* microRNA Targets ($p= 2.19E-03$, 10/62 molecules).

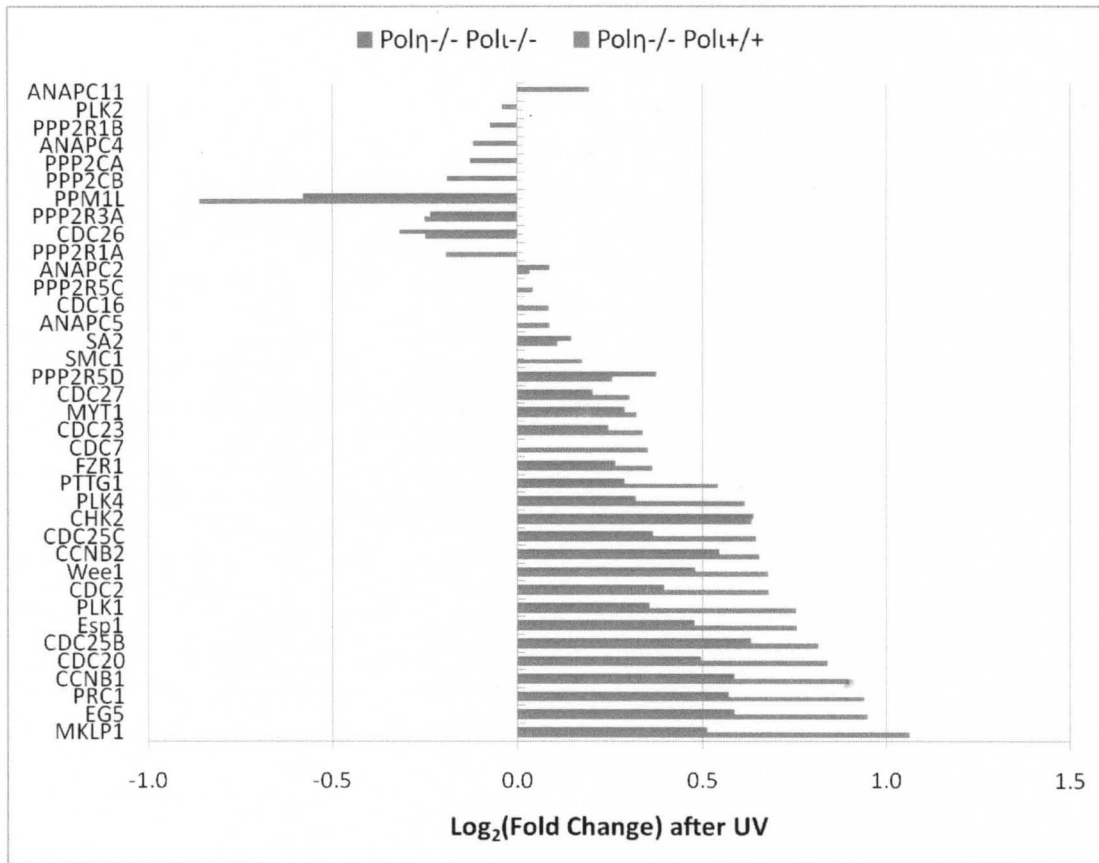


Fig. 2-6. mRNA expression changes of PLK signaling pathway members 24 hours after UV. Cells were treated as in Fig 2-1. Thirty-seven of 70 genes in the canonical PLK signaling pathway for G2/M checkpoint regulation were significantly altered ($p < 0.05$, $q < 0.1$, and fold change $> |1.5|$ in either genotype). Where the blue or red histogram bar is omitted for a gene, that gene was not significantly altered in the respective phenotype.

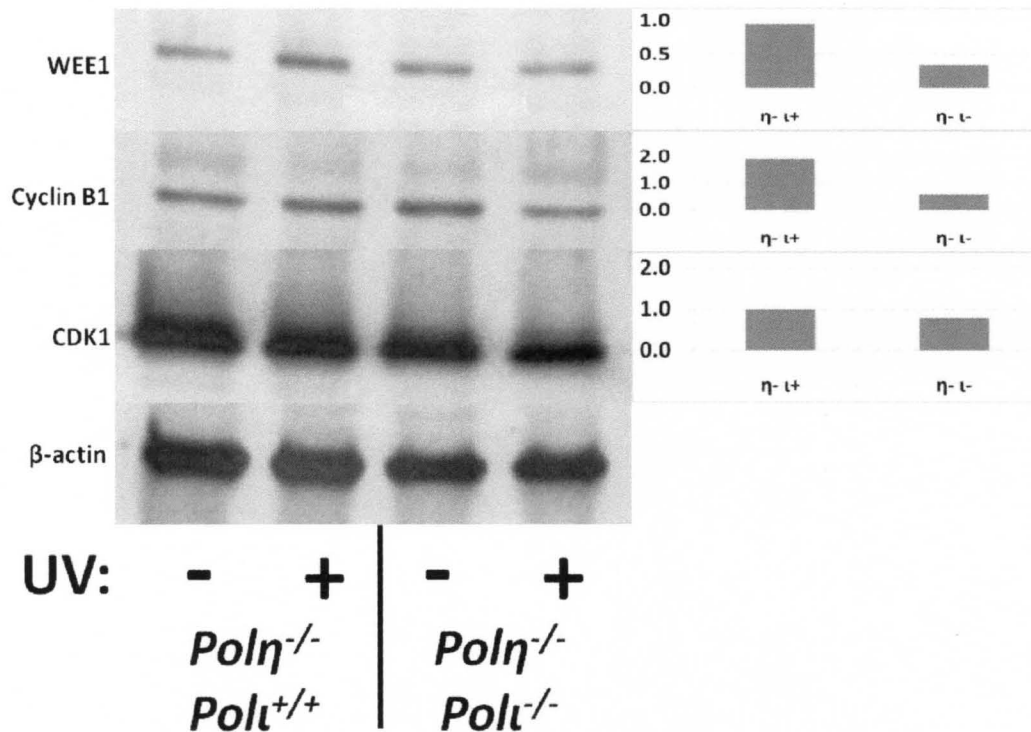


Fig. 2-7. Alterations in G2/M checkpoint pathway proteins after UV. Twenty four hours after treatment with 4 J/m² UVC, *Polη^{-/-} Polι^{+/+}* cells displayed a nearly two-fold increase in cyclin B1 (quantification shown on right). This protein was reduced by a factor of two in *Polη^{-/-} Polι^{-/-}* double knockout cells at the same time point. WEE1 levels were stable in *Polη^{-/-} Polι^{+/+}* cells but modestly reduced in *Polη^{-/-} Polι^{-/-}* cells. Levels of CDK1 were essentially unchanged in both genotypes after UV treatment. Densitometric quantitation shown on the right. Results are from a single experiment.

hours in *Polη^{-/-} Poli^{+/+}* cells but was reduced ~4-fold in *Polη^{-/-} Poli^{-/-}* cells. CDK1 levels were unchanged in both genotypes examined.

To expand the scope of our analysis, cell cycle markers for G2/M and G1/S arrest were analyzed by western blot in all four genotypes. Fig. 2-8 shows that in *Polη^{-/-} Poli^{+/+}* cells, UV caused a strong increase in the mitotic marker histone H3 phospho-Ser10 (phospho-H3). In contrast, phospho-H3 levels were reduced after UV in *Polη^{-/-} Poli^{-/-}* cells. Levels of phospho-H3 were unchanged in wild type and *Polη^{+/+} Poli^{-/-}* cells. Cyclin E, which is expressed at the G1/S transition, was strongly reduced after UV in wild type and *Polη^{-/-} Poli^{+/+}* cells, while *Polη^{-/-} Poli^{-/-}* showed a strong increase in cyclin E levels. *Polη^{+/+} Poli^{-/-}* cells showed no change in cyclin E at the UV dose used.

Figure 2-9 shows bivariate FACS analysis of cell cycle progression in all four genotypes after bromodeoxyuridine BrdU labeling and treatment with equitoxic UV doses. All cells were pulse labeled with BrdU for 30 minutes to label actively the replicating population. Immediately after pulse labeling, cells were UV treated. Wild type and *Polη^{+/+} Poli^{-/-}* cells were treated with 8 J/m² while *Polη^{-/-} Poli^{+/+}* and *Polη^{-/-} Poli^{-/-}* cells were treated with 4 J/m², doses that result in ~37% clonogenic survival [63]. To examine the behavior of cells in S phase at the time of UV treatment, the BrdU(+) population was gated and analyzed for cell cycle progression. After 18 hours, ~20% of BrdU(+) wild-type cells had completed S, G2, and M phases and were arrested in G1 phase. In contrast, only ~10% of BrdU(+) *Polη^{+/+} Poli^{-/-}* cells completed the first division at 18 hrs, and these numbers were unchanged at 30 hours. Both wild type and *Polη^{+/+} Poli^{-/-}* cells displayed functional G1/S checkpoints as indicated by the absence of cells entering S phase after UV treatment. In *Polη^{-/-} Poli^{+/+}* cells, the BrdU(+) population

showed delayed S-phase progression; the G1 population was 6% at 18 hours and 12% at 30 hours. BrdU(-) *Polη*^{-/-} *Poli*^{+/+} cells did not arrest at the G1/S border but progressed into a very slow S phase and accumulated in G2/M. BrdU(-) cells in G1 phase were 31%, 18%, and 13% of total cells at 0, 18, and 30 hours, respectively. BrdU(+) *Polη*^{-/-} *Poli*^{-/-} cells were 7% G1 at 18 hours and 2% G1 at 30 hours. Double knockout cells showed an increase in the number of polyploid cells which peaked at 18 hours and was reduced at 30 hours. Accumulation of polyploid cells was most pronounced in *Polη*^{-/-} *Poli*^{-/-} cells, reaching 40% of total cells at 18 hours, versus ~20% in *Polη*^{-/-} *Poli*^{+/+} and ~10% in wild type.

To further investigate the apparent increased ploidy of *Poli*^{-/-} cells even before UV treatment, all four genotypes of cells were stained with giemsa during asynchronous exponential growth and nuclei were counted. The percentage of binucleated cells is shown in Fig. 2-10. Loss of Pol ι , both from the wild type and *Polη*^{-/-} backgrounds, resulted in a strong and significant increase in the number of binucleated cells. The percentages of binucleated cells were 1.1%, 5.6%, 2.0%, and 4.9% in wild type, *Poli*^{-/-}, *Polη*^{-/-}, and double knockout cells, respectively. The difference between wild type and *Polη*^{-/-} was also statistically significant, indicating that loss of Pol η also causes a slight increase in the number of binucleated cells. We also examined the percentage of binucleated cells in SV40-transformed human diploid fibroblasts (GM0637). The GM0637 cell line displayed a low level of binucleated cells, two-fold lower than *Polη*^{-/-} cells and approximately five-fold lower than *Poli*^{-/-} and double knockout murine cells.

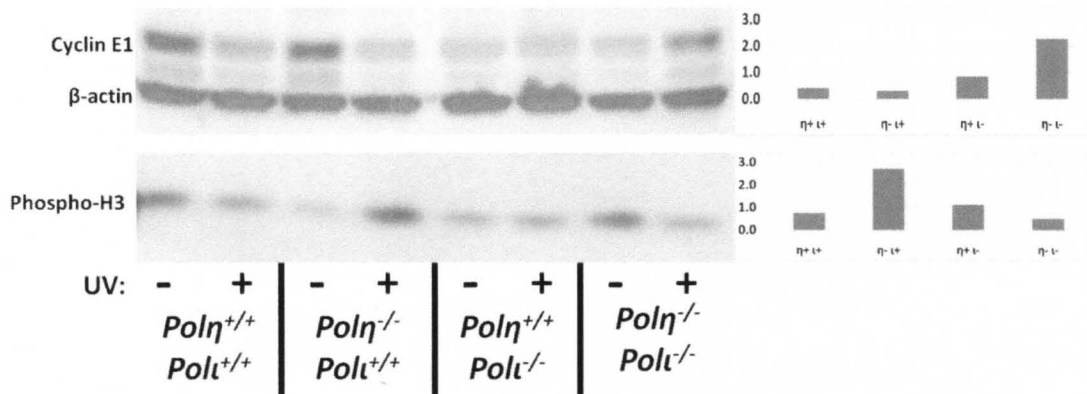


Fig. 2-8. UV-induced accumulation of mitotic markers is reversed by *Polt*-knockout. Twenty four hours after treatment with 4 J/m² UVC, *Polη*^{-/-} *Polt*^{+/+} cells showed accumulation of phospho-serine 10 histone H3 (phospho-H3, quantification on right). This marker was reduced more than two-fold in *Polη*^{-/-} *Polt*^{-/-} double knockout cells at the same time point, but remained essentially unchanged in wild-type and *Polη*^{+/+} *Polt*^{-/-} cells. The G1/S marker cyclin E was reduced in wild type and *Polη*^{-/-} *Polt*^{+/+} cells, while *Polη*^{-/-} *Polt*^{-/-} cells show increased cyclin E levels 24 hours after UV treatment. No change in cyclin E was observed in *Polη*^{+/+} *Polt*^{-/-} cells.

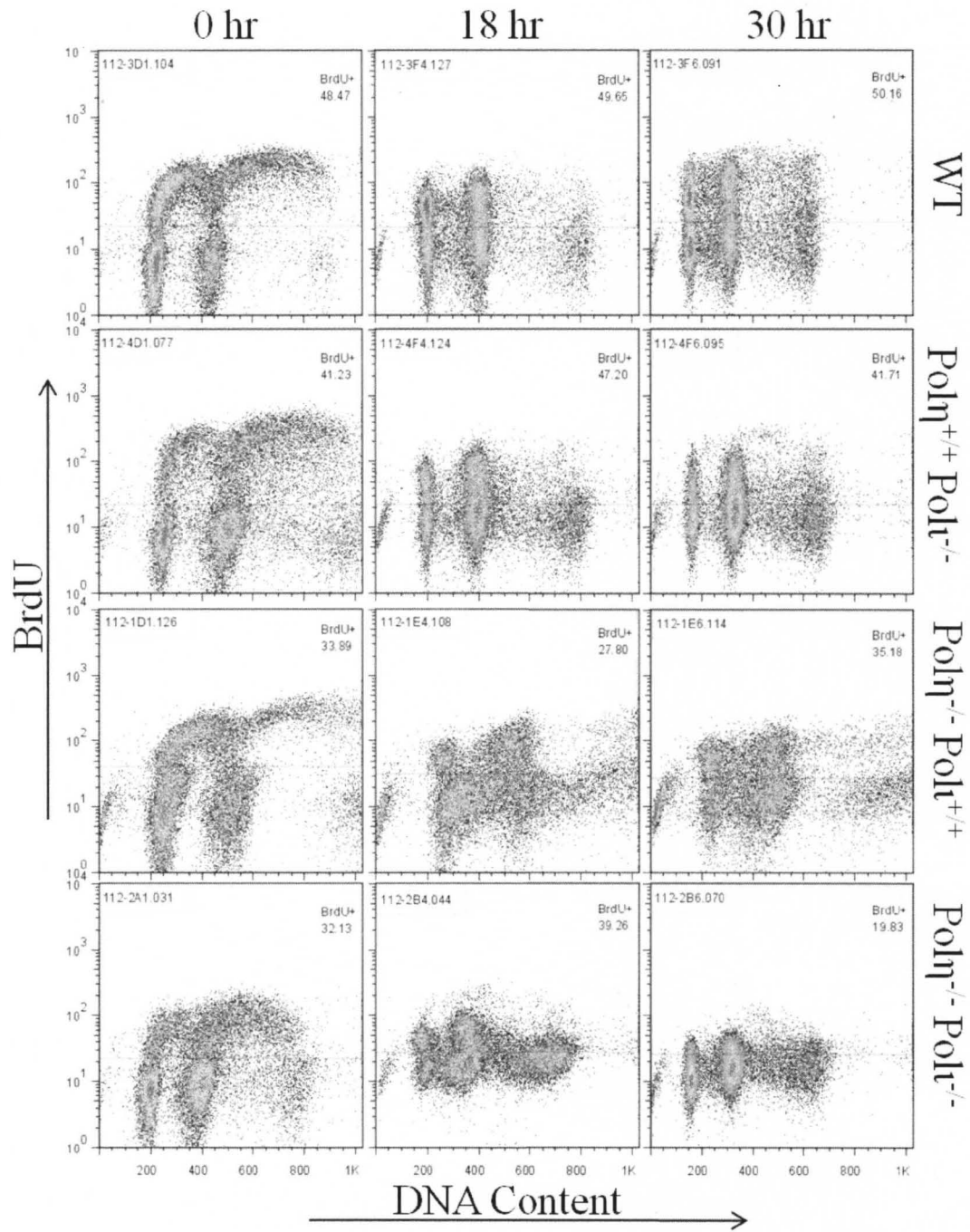


Fig. 2-9. *Pol*-deficient cells display polyploidy after UV treatment. Wild type, $Pol\eta^{-/-}$ $Pol\iota^{+/+}$, $Pol\eta^{+/+} Pol\iota^{-/-}$, and $Pol\eta^{-/-} Pol\iota^{-/-}$ fibroblasts were pulse labeled with BrdU for 30 minutes immediately before UV treatment. Cells were irradiated with equitoxic UV

doses (8 J/m² for wild type and *Polη*^{+/+} *Poli*^{-/-}; 4J/m² for *Polη*^{-/-} *Poli*^{+/+}, *Polη*^{-/-} *Poli*^{-/-}) and collected at the indicated time points for BrdU/7AAD multiparametric FACS analysis. All cells showed active DNA synthesis of haploid populations as well as of polyploid populations (>4n DNA content). After 18 hours, ~20% of BrdU(+) wild-type cells had completed S, G2, and M phases and were arrested in G1 phase. Only ~10% of BrdU(+) *Polη*^{+/+} *Poli*^{-/-} cells completed the first division at 18 hrs, and these numbers were unchanged at 30 hours. BrdU(+) *Polη*^{-/-} *Poli*^{+/+} cells showed delayed S-phase progression; the G1 population was 6% at 18 hours and 12% at 30 hours. BrdU(+) *Polη*^{-/-} *Poli*^{-/-} cells were 7% G1 at 18 hours and 2% G1 at 30 hours. Double knockout cells showed an increase in the number of polyploid cells which peaked at 18 hours and was reduced at 30 hours.

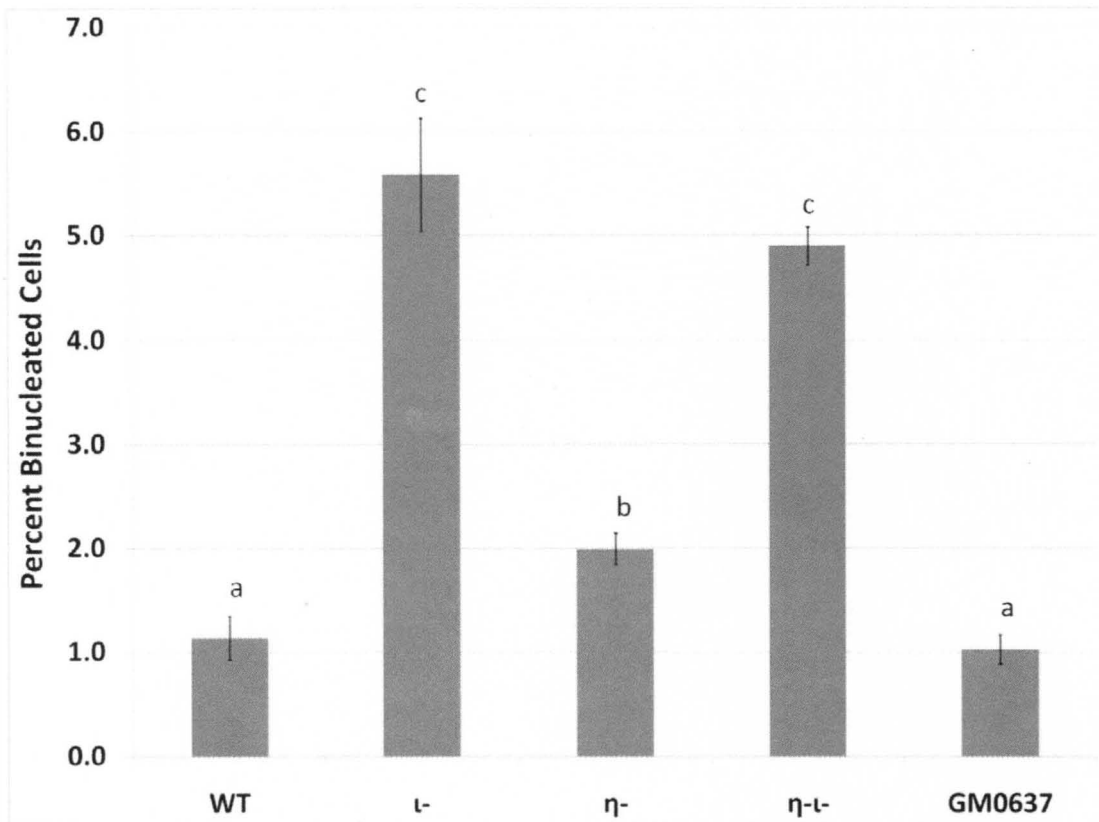


Fig. 2-10. *PolI*-deficient cells display a failure in cytokinesis. Primary mouse fibroblasts (wild type, *PolI*^{-/-}, *Polη*^{-/-}, double knockout) and SV40-transformed human fibroblasts (GM0637) were trypsinized during asynchronous growth and replated at 10⁴ cm⁻². The following day the cells were stained with giemsa and scored on the basis mono- or binucleated status. Averages represent three independent experiments. Histogram bars with different letters are significantly different (p<0.05). Error bars, SEM.

Discussion

Despite the fact that multiple reports have characterized Pol η as a mutagenic TLS polymerase in the bypass of UV-induced DNA damage [62,63,129], *Pol η* -deficiency has been found by two independent groups to decrease the latency of UV-induced carcinogenesis in *Pol η ^{-/-}* mice [63,64]. These remarkable findings suggest that *Pol η* could play a novel role in the cellular response to UV-induced DNA damage, and to investigate this possibility gene expression changes were examined after UV irradiation in *Pol η ^{-/-}* *Pol η ^{+/+}* and *Pol η ^{-/-} Pol η ^{-/-}* primary murine ear fibroblasts. UV treatment caused significant expression changes of thousands of mRNAs in both genotypes, and pathway analysis indicated that these genes are in expected pathways including p53 and apoptotic signaling. To more specifically identify the effect of *Pol η* -deficiency, the two-way ANOVA used to analyze the mRNA expression data included the interaction term. This statistical test was chosen to parse out the common effects of UV treatment on both genotypes in order to identify the ways in which each cell type responds differently to UV treatment. The 484 mRNAs with a significant interaction term (the “Interaction mRNA”) represent the mRNA expression signature of *Pol η* and can be exploited to determine which cellular pathways are perturbed after UV treatment by the loss of *Pol η* .

UV irradiation was also found to affect microRNA expression, and this was also directly impacted by *Pol η* -deficiency. Nine and 11 microRNAs were identified in *Pol η ^{-/-}* *Pol η ^{+/+}* and *Pol η ^{-/-} Pol η ^{-/-}* cells, respectively, as having significant UV-induced changes. These two lists of microRNAs were mutually exclusive, indicating a complete divergence of the microRNA response to UV-induced DNA damage concomitant with *Pol η* -deficiency. UV-responsive microRNA have been identified in mammalian cells [135]

and linked to the DNA damage response [136]. However, our list of UV-responsive microRNA shows little overlap with previously published reports. Since the cells used in this study are derived from nonisogenic mice as described [63] ($Pol\eta^{-/-} Pol\iota^{+/+}$ = C58Bl/6; $Pol\eta^{-/-} Pol\iota^{-/-}$ = hybrid C57Bl/6 X 129 X B6 background from an F2 generation backcross), we chose to use high stringency statistical cutoffs and multiple methods of analysis for the expression data. The nonisogenic nature of the cell strains used does raise the possibility that the gene expression results we obtained are actually attributable to strain differences rather than to loss of Pol ι . It is for this reason we used strict statistical cutoffs followed by biological validation of the microarray results.

Fig. 2-4 illustrates how mRNA and microRNA expression datasets were analyzed using statistical and bioinformatics tools to formulate lists of mRNAs that represent the “signature” of *Pol* ι in the UV DNA damage response. These lists of mRNAs can then be analyzed for pathway enrichment to identify novel candidate pathways modulated by *Pol* ι after UV. As described, the Interaction mRNA list was derived directly from mRNA microarray data using a two-way ANOVA. The interaction term was utilized in this ANOVA to remove the common gene expression patterns of UV-response between the genotypes. In order to have a significant interaction term, a particular mRNA must show different fold changes after UV between the two genotypes; thus, the interaction test is one way to distinguish unique gene expression patterns due to the loss of *Pol* ι . To analyze the microRNA expression data for pathway enrichment, the miRanda target prediction algorithm was used to generate putative mRNA target lists for the UV-responsive microRNAs from each genotype [133,134]. Target predictions from miRanda are based on partial or complete complementarity of the microRNA with the 3' UTR of

the target mRNA. Importantly, because of the computational nature of the target prediction method used, several hundred mRNAs were returned as putative targets of each UV-responsive microRNA. This generated very large lists of predicted microRNA targets which were expected to contain a high percentage of false positives due to inaccurate algorithm predictions, estimated to be as high as 34% [133]. For each genotype, the list of predicted microRNA targets was intersected with the list of UV-responsive mRNAs to generate the list of “Filtered microRNA Targets.” This method of filtering the predicted microRNA targets list was used to reduce list size and eliminate false positives. All mRNAs included on the final list of Filtered microRNA Targets in each genotype met two criteria; first, each mRNA was predicted to be the target of at least one UV-responsive microRNA from that genotype, and second, each mRNA was itself significantly altered by UV treatment. This final filtering step reduced by ~5-fold the number of microRNA targets for each genotype to 1,529 in *Polη^{-/-} Poli^{+/+}* cells and 1,339 in *Polη^{-/-} Poli^{-/-}* cells.

Ingenuity Pathway Analysis (IPA) was used to analyze three lists of mRNAs: Interaction mRNA, Filtered *Polη^{-/-} Poli^{+/+}* microRNA Targets, and Filtered *Polη^{-/-} Poli^{-/-}* microRNA Targets. These three lists were taken to represent the signature of *Poli* in the UV DNA damage response, and global pathway analysis revealed the enrichment of only one canonical pathway shared among the three datasets. The PLK signaling pathway for mitotic entry and exit was significantly enriched in all three mRNA lists analyzed, indicating that deficiency in *Poli* alters cellular responses to UV damage through this pathway.

To validate the dysregulation of the G2/M checkpoint after *Polι* loss, cell cycle markers were analyzed by immunoblotting. Accumulation of phospho-H3 and cyclin B1 24 hours after 4 J/m² UV indicates that *Polι*^{-/-} *Polι*^{+/+} cells accumulate in G2/M in response to UV-induced DNA damage (Fig. 2-7 and 2-8). Apparent activation of this checkpoint coincides with a reduction in levels of the G1/S marker, cyclin E, as expected. The UV-induced accumulation of mitotic markers was reversed in *Polι*^{-/-} *Polι*^{-/-} cells, providing evidence that expression of *Polι* is required for activation of the G2/M checkpoint seen in *Polι*^{-/-} *Polι*^{+/+} cells. Cyclin E expression was increased in double knockouts 24 hours after treatment, indicating that cells accumulated at the G1/S boundary. While WEE1 levels were stable in *Polι*^{-/-} *Polι*^{+/+} cells, double knockouts showed a strong reduction in WEE1 after UV treatment. WEE1 phosphorylates and inactivates CDK1 and is a target of PLK1 for phosphorylation and subsequent degradation. Reduced levels of WEE1 in *Polι*^{-/-} *Polι*^{-/-} cells could indicate increased PLK1 activity, supporting our finding that the PLK1 pathway is dysregulated by *Polι* deficiency. Cyclin E levels were reduced after UV in wild type cells, but stable in *Polι*^{+/+} *Polι*^{-/-} cells. This change in the response of the G1/S marker could be explained if *Polι*^{+/+} *Polι*^{-/-} underwent endoreduplication and did not divide in order to arrest at G1/S, as our hypothesis would predict.

To specifically address cell cycle kinetic changes after UV treatment, we examined 7AAD staining of BrdU-labeled cells. In order to label the S phase population of all four genotypes immediately before UV treatment, all cells were incubated with BrdU for 30 minutes and then treated with equitoxic UV doses (Fig. 2-9). This experimental design allows one to gate the BrdU(+) population of cells, those that were

in S phase immediately before UV treatment, and follow that population over time to examine S and G2/M exit. Conversely, one can also follow the BrdU(-) population to examine rates of entry into S phase after UV. All four genotypes displayed appreciable replication of polyploid cells, indicating the presence of a stable population of cells with DNA content $>4n$. BrdU(+) $Pol\eta^{+/+} Poli^{-/-}$ cells exited mitosis more slowly than wild type cells; at 18 hours only 10% of $Pol\eta^{+/+} Poli^{-/-}$ cells had completed the first cell cycle compared to 20% of wild type cells. Both genotypes displayed a functional G1/S checkpoint as indicated by the lack of BrdU(-) G1 cell migration into S phase. The finding that *Poli*-deficiency causes G2/M accumulation in wild-type cells conflicts with our previous findings that loss of *Poli* causes alleviation of the mitotic checkpoint in $Pol\eta^{-/-}$ cells (Fig. 2-9).

There was significant intra-S phase arrest in $Pol\eta^{-/-} Poli^{+/+}$ cells as expected; BrdU(+) G1 peaked at 12% 30 hours after UV treatment. In addition, these cells did not arrest at G1/S but instead proceeded into a very slow S phase and arrested in the G2/M compartment. BrdU(-) $Pol\eta^{-/-} Poli^{+/+}$ cells decreased from 31% to 13% of total cells over 30 hours, indicating a mitotic block which prevented division of these BrdU(-) cells. Strong intra-S phase arrest in this genotype was expected [38,39], but the accumulation of cells in the G2/M compartment at this late time point is a novel finding to our knowledge. BrdU(-) $Pol\eta^{-/-} Poli^{-/-}$ cells displayed a normal G1/S checkpoint and did not proceed *en masse* into S phase as the $Pol\eta^{-/-} Poli^{+/+}$ cells had done, indicating that loss of both polymerases reactivates the G1/S checkpoint. BrdU(+) $Pol\eta^{-/-} Poli^{-/-}$ cells did not divide and return to G1, but instead underwent endoreduplication. Levels of polyploid cells were highest in the double knockouts, and peaked at 40% 18 hours after UV

treatment. This finding supports our hypothesis that Pol ι modulates the mitotic checkpoint and our previous data that loss of *Pol ι* relieves a mitotic checkpoint.

Our FACS analysis indicated that a mitotic checkpoint was not activated in *Pol ι ^{-/-}* cells, allowing them to complete mitosis without dividing and enter a tetraploid state. To directly support this hypothesis, we stained asynchronous cultures of cells with giemsa and counted mono- and binucleated cells (Fig. 2-10). We found that loss of Pol ι increased the percentage of binucleated cells by more than two fold. These data support our hypothesis that Pol ι is involved in activation of the mitotic checkpoint, and in its absence checkpoint failure leads to the accumulation of endoreduplicated cells. We did not see a slight but significant increase in the percentage of binucleated cells in the *Pol η ^{-/-}* genotype. We did not find evidence of increased tetraploidy in Pol η -deficient cells via FACS analysis; nevertheless, direct analysis of the nuclei indicates that Pol η could also play a role in regulating the mitotic checkpoint

The phenotype of increased tetraploidy we observed in *Pol ι ^{-/-}* mouse fibroblasts is relevant to human cells, particularly to transformation by simian virus 40. Typically, human cells are not permissive of a tetraploid state; anything that induces tetraploidy causes death of the cell population via a p53-dependent postmitotic checkpoint [137]. However, SV40 infection blocks the activity of p53 and promotes the gradual accumulation of a tetraploid population very similar to that seen in Pol ι -deficient cells [138]. This is an important finding as it indicates that Pol ι deficiency could be an unidentified human health concern.

Results presented in this chapter support the hypothesis that Pol ι regulates the mitotic checkpoint, though the exact nature of the regulation appears to depend upon the cells' ability to tolerate UV-induced DNA damage. Our gene expression analyses were done using *Pol η ^{-/-}* cells, which lack the major TLS polymerase for accurate bypass of UV damage and rely on Pol ι to complete mutagenic TLS and, in theory, prevent DSB and genetic instability. Our results indicated that loss of *Pol ι* promotes endoreduplication, allowing mitotic completion and blocking cytokinesis. This finding was supported by cell cycle kinetics, which showed that *Pol η ^{-/-} Pol ι ^{+/+}* cells in S phase at the time of UV treatment slowly complete S and G2 and divide. Loss of *Pol ι* causes cells to bypass division and endoreduplicate, indicating they have bypassed the spindle assembly checkpoint in M phase and entered a tetraploid state. In wild type cells replicating DNA during UV treatment, loss of *Pol ι* causes a reduced rate of division after UV. This is likely caused by an activated mitotic checkpoint in *Pol η ^{+/+} Pol ι ^{-/-}* cells, in contrast to our findings in *Pol η ^{-/-}* cells. This difference in response is likely due to the major role in UV DNA damage tolerance played by Pol η ; in the presence of Pol η , Pol ι plays only a minor catalytic role in TLS at the replication fork. In the absence of Pol η (XP variant), cells rely on Pol ι to perform TLS across from UV lesions. It is possible that Pol ι is required to signal G2 arrest for postreplication repair, when TLS is performed in G2 phase after semiconservative DNA synthesis has left single-strand gaps in DNA across from lesions. Loss of Pol ι could fail to trigger this checkpoint and allow a cell with numerous ssDNA gaps to proceed through G2 and M phases and undergo recombination or endoreduplication.

CHAPTER III

UV CARCINOGENESIS

INTRODUCTION

Ultraviolet radiation (UV) is the most ubiquitous environmental carcinogen and is clearly linked to the etiology of skin cancer in humans [139]. The UV spectrum is divided into low-energy UVA (320-400 nm), mid-range UVB (295-320 nm), and high-energy UVC (100-295 nm). Wavelengths below 300 nm are completely filtered out by ozone in the atmosphere between 10 and 50 km above the earth's surface, along with a large portion of the UVB component of solar radiation [140](Fig 3-1). While only 10% of the UV radiation reaching the earth's surface is UVB, this component is still the major cause of sunburn and skin cancer. UV wavelengths of ~295 nm (UVB) are ~10,000-fold more potent in causing cancer than those >340 nm (UVA) [141](Fig 3-2). UV exposure acts as a complete carcinogen; the DNA damage induced by higher energy UVB rays causes mutations in protooncogenes and tumor suppressors [139,142], and long-term exposure causes immunosuppression and tumor promotion [143]. Human exposure levels are typically measured in terms of the minimal erythema dose (MED) for the skin type being exposed. For a person with skin type I ("always burns, never tans"), the MED is 200 J/m². Over the Fourth of July weekend in 2010, maximum UV fluxes achieved, measured in the range of 300-400 nm, were 24

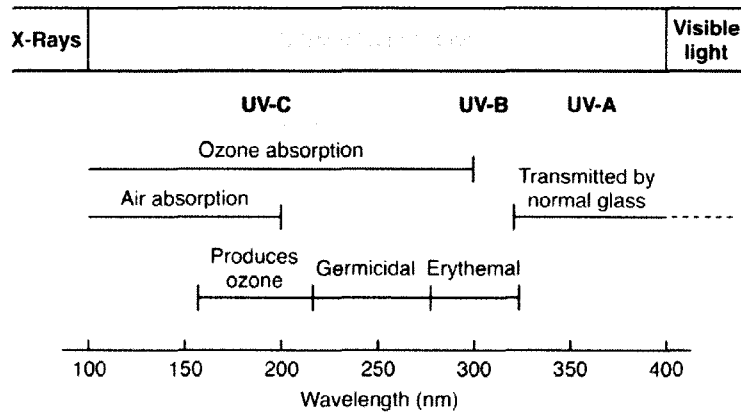


Fig. 3-1. UV spectrum and effects on terrestrial absorption. UVC and some UVB wavelengths are filtered by ozone in the atmosphere. UVB is primarily responsible for UV-induced cancer, while UVA is primarily responsible for photoaging. Adapted with permission from Fiedberg et al [100].

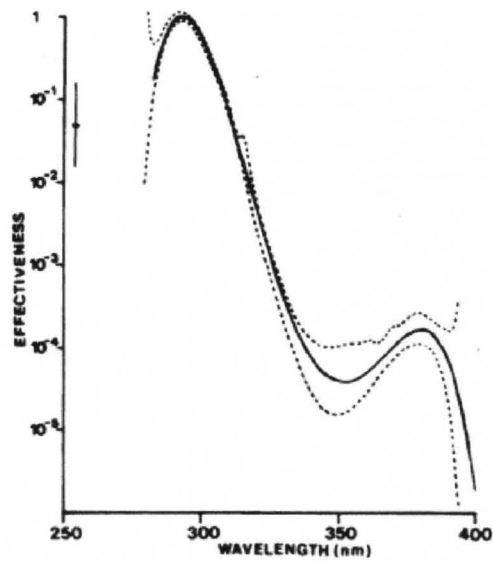


Fig. 3-2. Skin Cancer Utrecht-Philadelphia (SCUP) action spectrum for hairless albino mice. Data were collected from 14 UV sources and about 1100 mice to generate an action spectrum for the induction of skin cancer by UV light in mice. Adapted from de Gruijl, Cancer Res 1993 [141] with permission.

$J/m^2 \cdot \text{min}$ in Waimea, Hawaii, $18 J/m^2 \cdot \text{min}$ in Homestead, Florida, and $15 J/m^2 \cdot \text{min}$ in West Lafayette, Indiana [144]. At these levels of exposure, it would take as little as eight minutes for sun damage to occur to unprotected skin of type I. *In vivo* studies of photocarcinogenesis utilize suberythemal doses of UV to avoid the massive stimulation of the immune system triggered by the sunburn response. In this dissertation, the daily doses of $50 J/m^2$ UVB were approximately 20-fold lower than the MED of the animals being treated.

It is important to note that most studies of cells in culture, including those in this dissertation, make use of high-energy UVC lamps with emission peaks at 254 nm due to the high efficiency of absorption of DNA (260 nm absorption peak). Despite the fact that this exposure is not physiologically relevant, 254 nm UVC radiation is highly specific for inducing DNA damage and is therefore an ideal genotoxicant for DNA repair studies. In addition, the true environmental carcinogen UVB also induces 6-4 photoproducts and CPDs in the same relative frequency as UVC, although with less efficiency [65,145]. Evidence also shows that UVC can generate the oxidate damage that is the hallmark of UVA exposure and thought to lead to the phenomenon of skin ageing, although with a different frequency [146]. Thus, while treating cells in culture with UVC is not physiologically relevant, this genotoxicant is chosen as a precision tool to induce almost exclusively damage to the DNA, and results obtained from these studies must be considered in that context.

NONMELANOMA SKIN CANCER

Skin cancer is divided into two basic categories: melanoma and nonmelanoma skin cancer (NMSC). NMSC is the most prevalent cancer in the world and is further divided into basal cell carcinoma and squamous cell carcinoma (SCC). More than six million cases of nonmelanoma skin cancer were diagnosed in the US in 2006, and the number of cases continues to rise annually [147,148]. Up to one-fifth of seventy-year-olds have had at least one NMSC diagnosis [149]. Despite the low mortality of the disease, it still poses a significant public health burden due to the number of affected individuals. Direct costs attributable to NMSC treatment in the US were nearly \$1.5 billion in 2004 and are primarily made up by office visits for outpatient surgeries [150].

Pol ι is implicated in error-prone TLS of UV-induced DNA damage *in vivo*. While Pol η -deficient mice develop cancer rapidly due to high UV-induced mutation frequencies, loss of Pol ι causes both a reduction in cancer latency and mutation frequency [62,63,64]. This remarkable finding indicates that Pol ι could have a role outside of TLS, but the conclusion is limited due to the fact that the phenotype was only observed with concurrent deletion of Pol η . The studies in this chapter were designed to address the hypothesis that Pol ι deficiency decreases UV-induced tumor latency.

Materials and Methods

Mouse Model

All animal studies were approved by the Institutional Animal Care and Use Committee at the University of Louisville. *Poli*^{-/-} 129/SvJ mice [59] were purchased from Jackson Laboratories (Bar Harbor, Maine), and *Polη*^{-/-} mice [19] were a gift from Raju Kucherlapati (Harvard University). SKH1/hairless *Xpa*^{-/-} mice [151] were a gift from Harry van Steeg (Leiden University Medical Centre). *Polη*^{-/-} and *Poli*^{-/-} 129/SvJ mice were each backcrossed for seven generations with SKH1/hairless *Xpa*^{-/-} mice. Resultant isogenic genotypes were *Xpa*^{-/-} *Polη*^{+/+} *Poli*^{+/+} controls, *Xpa*^{-/-} *Polη*^{-/-} *Poli*^{+/+}, and *Xpa*^{-/-} *Polη*^{+/+} *Poli*^{-/-}.

UV Irradiation

Mice were irradiated with a bank of two UVM-225D bulbs with peak emission at 302 nm (UVP, Upland CA). UV flux was measured using an IL1700 radiometer with a UVB-1 sensor fitted with a W1 diffuser (International Light, Peabody, Massachusetts). The sensor measures the output at 313 nm. Mice were irradiated with 50 J/m² five days per week for 12 weeks and monitored for tumor growth twice weekly. This dose is well below the MED of ~1,000 J/m². Animals were euthanized 20 weeks after the start of UV or when one tumor reached >10% of body mass. The animals were photographed and skin tumors were dissected, formalin fixed, paraffin embedded, and sectioned for histological analysis.

RESULTS

Xpa^{-/-} mice developed tumors with 100% penetrance and short latency, with all mice bearing one tumor by 15 weeks after UV treatment started (Fig. 3-3). *Xpa*^{-/-} *Polη*^{-/-} mice developed cancer faster than Pol η-proficient controls, with all mice bearing at least one tumor by 12 weeks (p < 0.01). *Xpa*^{-/-} *Poli*^{-/-} mice all had one tumor by 13.6 weeks, a reduction in tumor latency that trended towards significance (p = 0.057). This is the first time that loss of Pol ι as the only TLS polymerase has been shown to reduce UV-induced tumor latency.

Histopathological analysis revealed no distinct differences among genotypes of mice (n = 10 tumors per genotype, Fig. 3-4). All tumors analyzed were SCC. We did not observe the highly aggressive spindle cell tumors in *Poli*^{-/-} mice reported by others [64]. Our finding of only SCC in all genotypes is consistent with the work of Dumstorf *et al* [63].

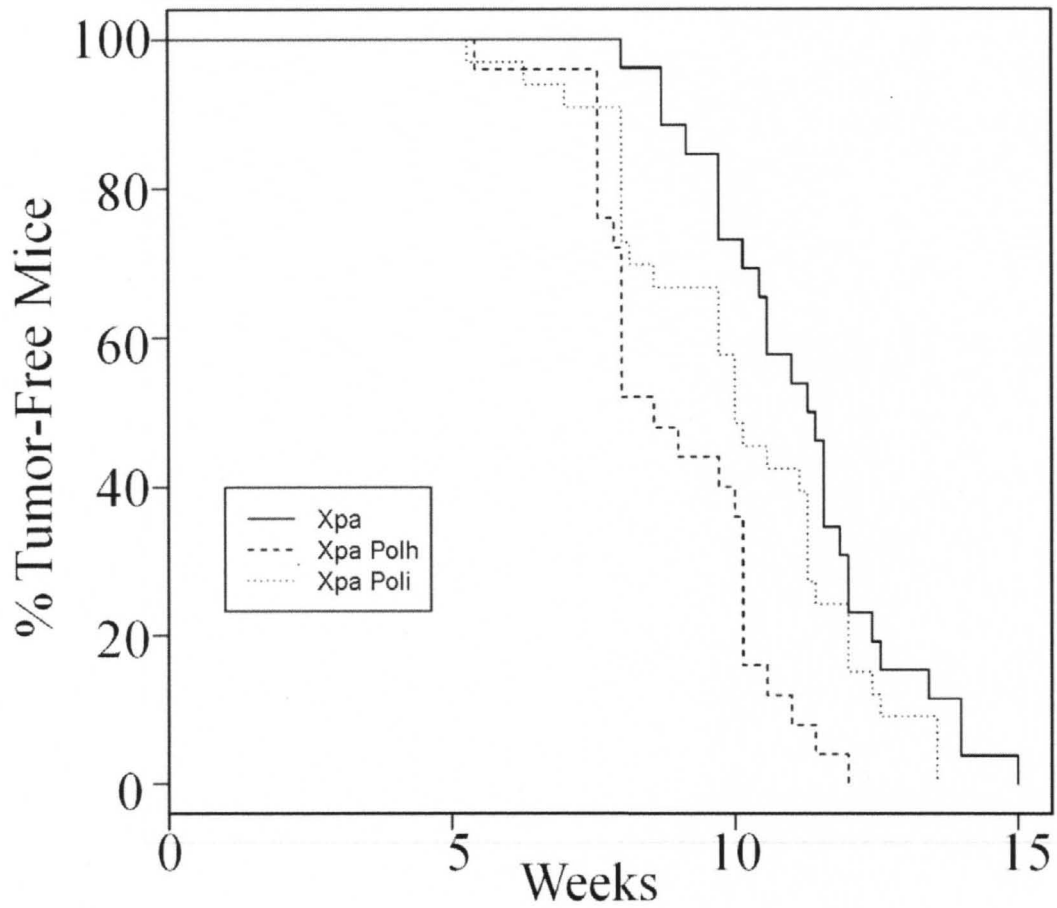


Fig. 3-3. UV-induced carcinogenesis in $Xpa^{-/-}$ mice. Kaplan-Meier plot induced by 12 weeks of treatment with 50 J/m^2 five days per week. Survival is defined as the fraction of tumor-free mice. $n = 26$ ($Xpa^{-/-}$), 25 ($Xpa^{-/-} Polh^{-/-}$), and 33 ($Xpa^{-/-} Poli^{-/-}$). Overall (3 group) $p = .0002$. $Xpa^{-/-} Poli^{-/-}$ vs. $Xpa^{-/-}$: $p = .057$. $Xpa^{-/-} Poli^{-/-}$ vs. $Xpa^{-/-} Polh^{-/-}$: $p = .026$. $Xpa^{-/-} Polh^{-/-}$ vs. $Xpa^{-/-}$: $p = .008$.

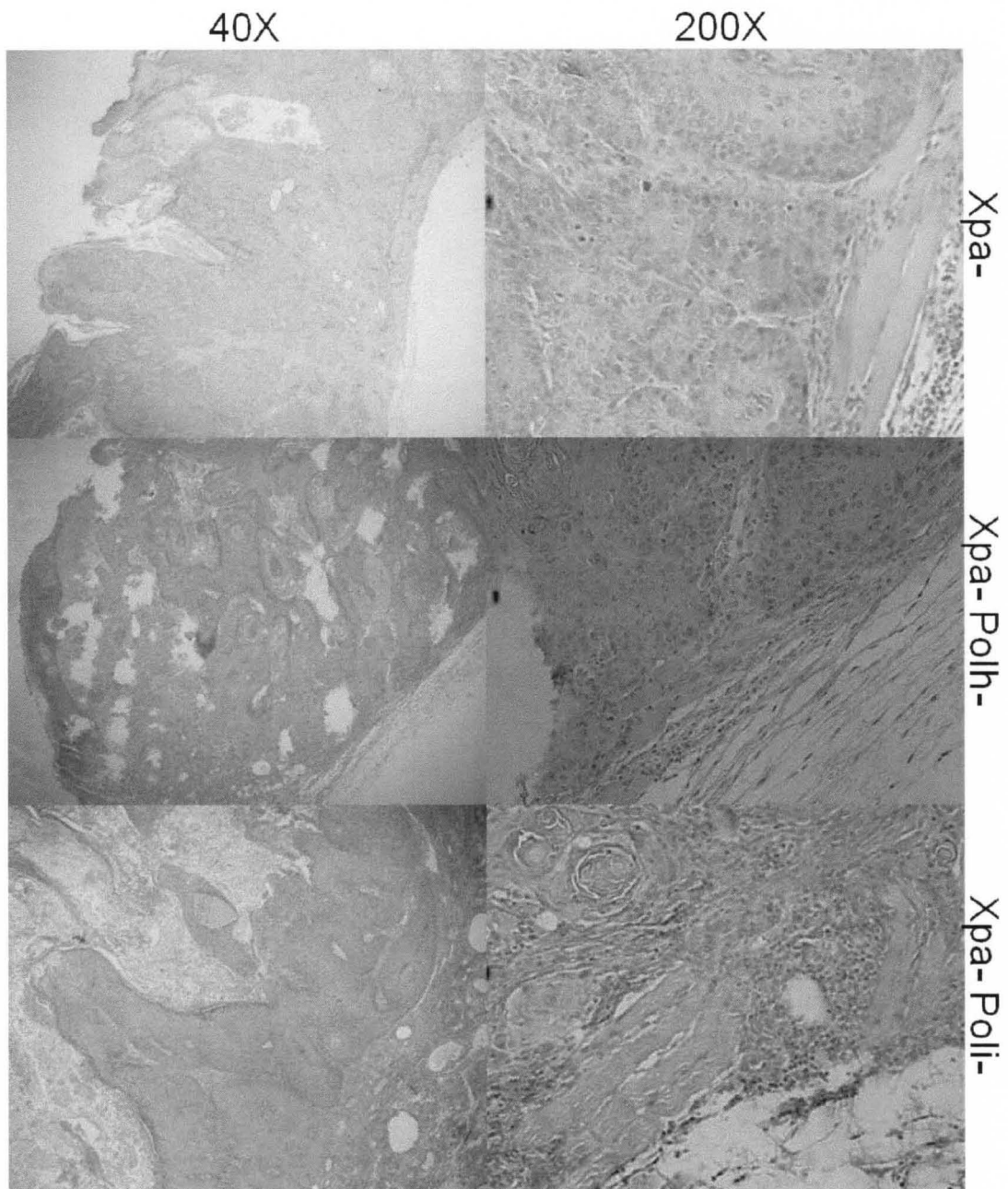


Fig. 3-4. Histopathology of squamous cell carcinoma in *Xpa*^{-/-} mice. Ten tumors from each genotype were sectioned and stained with H&E for blinded pathological analysis. All tumors were locally invasive squamous cell carcinoma.

DISCUSSION

It is well known that loss of Pol η results in dramatically reduced UV-induced skin cancer latency in humans [35] and mice [19]. Pol η appears to be evolutionarily conserved [13] to perform accurate bypass of UV-induced DNA damage [41,42,43,128], but much less is known about the effect of the error-prone Pol ι in animals. We have demonstrated that loss of Pol ι causes a trend toward decreased tumor latency (Fig 2-3). This was an intermediate phenotype compared to the *Pol η ^{-/-}* mice. These studies support our hypothesis that Pol ι suppresses formation of UV-induced skin cancer. This hypothesis was based on the previous finding that *Pol η ^{-/-} Pol ι ^{-/-}* double knockout mice develop tumors faster than *Pol η ^{-/-} Pol ι ^{+/+}* mice, despite reduced UV-induced mutation frequencies in *Pol η ^{-/-}* cells [63].

The reason we did not find a significant difference between *Xpa^{-/-}* and *Xpa^{-/-} Pol ι ^{-/-}* mice is possibly due to the small effect sizes that result from the *Xpa^{-/-}* background. C57Bl/6 mice are resistant to UV-induced skin cancer, and wild type animals usually do not develop tumors even after months of chronic UV exposure [19]. It is for this reason that previous studies could not assess the effect of *Pol ι ^{-/-}* on UV carcinogenesis; neither wild-type nor *Pol ι ^{-/-}* mice developed tumors [63]. We backcrossed *Pol η ^{-/-}* and *Pol ι ^{-/-}* into the SKH1/hairless *Xpa^{-/-}* background, which is highly susceptible to UV-induced SCC [151]. As a result, the difference in tumor latency between the control and experimental groups is very small. It is also possible that the severe phenotype of complete NER-deficiency in the *Xpa^{-/-}* controls partially masks the phenotype of Pol ι knockout. Using *Xpa*-wild type mice, which develop tumors after approximately 20 weeks of chronic UV treatment, as controls could increase the effect size of *Pol ι ^{-/-}* knockout and the

significance of the difference between groups. It is also possible that we did not have significant numbers of mice per group to detect a significant difference. We did perform a power analysis in collaboration with the Statistical Consulting Center at the University of Louisville School of Medicine, estimating an effect size based on previous data from our lab [63]. We determined that a sample size of 28 mice per group would provide 80% power for pairwise two-sided log rank test to detect differences in tumor latency at a significance of 0.05. Based on the smaller effect sizes in this study and the fact that our control and $Xpa^{-/-} Pol\eta^{-/-}$ group were under-populated, it is possible that increasing the number of mice in these groups, or all three groups would bring the p-value below 0.05.

Our histopathological analysis indicated that $Pol\eta^{-/-}$ and $Poli^{-/-}$ mice develop the same locally invasive SCC as $Xpa^{-/-}$ control mice. This finding is in agreement with a previous report from Dumstorf *et al* [63], but conflicts with the findings of aggressive spindle cell tumors in $Poli^{-/-}$ mice found by Ohkumo *et al* [64]. One possible explanation of the discrepancy among findings of tumor pathology in these studies is the background of the mice used; Ohkumo *et al* used isogenic $Pol\eta^{-/-}$ and $Poli^{-/-}$ mice in a C57Bl/6 background [64], and mice in this study were isogenic in the SKH1/hairless $Xpa^{-/-}$ background. Dumstorf *et al* used mixed backgrounds for carcinogenesis studies. Wild type and $Pol\eta^{-/-}$ mice were C57Bl/6, and $Poli^{-/-}$ mice were 129 background. Double knockout mice were in a hybrid C57Bl/6 X 129 X B6 background from an F2 generation backcross [63]. The spindle cell tumors were only observed in $Poli^{-/-}$ mice [64], which were in a C57Bl/6 background in that study. The fact that $Poli^{-/-}$ mice are in different backgrounds in both this study and in Dumstorf *et al* is a confounding factor in comparing the results of these three carcinogenesis studies.

We also carefully examined all tumors for the presence of multinucleated cells. Based on our findings of increased binucleated cells in the *Poli*^{-/-} genotype (Fig. 2-10), we expected that tumors from *Xpa*^{-/-} *Poli*^{-/-} mice would exhibit binucleated cells. The fact that we did not find evidence of binucleated cells or multinucleated tumor giant cells could be a result of the long period of time between tumor initiation and histopathological analysis (as long as 15 weeks for *Xpa*^{-/-} *Polη*^{-/-} and *Xpa*^{-/-} *Poli*^{-/-} mice). Also, our studies in Chapter II were also based on primary fibroblasts in culture, whereas the tumors analyzed in this study are epithelial in origin. It is possible that the Pol ι has a cell-type specific role in regulating cytokinesis; however, we also analyzed fibroblasts in the basement membrane below the tumors and found no evidence of binucleated or multinucleated cells. Another possible explanation is the strain of the mice used, since cells used in Chapter II were isolated from the mixed background mice described in Dumstorf *et al* [63]. Strain differences are a confounding factor when comparing the cell culture studies that showed impaired cytokinesis in *Poli*^{-/-} cells and *in vivo* studies with isogenic SKH1/hairless *Xpa*^{-/-} mice which did not confirm these findings. More direct studies are needed to address the role of Pol ι in regulating cytokinesis in live animals, but this study does support our hypothesis that Pol ι suppresses UV-induced carcinogenesis by showing a trend towards decreased tumor latency in *Poli*^{-/-} mice.

CHAPTER IV

BPDE MUTAGENESIS

INTRODUCTION

Mutagenesis is a recognized cornerstone of every form of human cancer [152] dating back to the discovery of aneuploidy in cancer cells [153]. According to the modern somatic mutation hypothesis of cancer, a cell must undergo several independent genetic and epigenetic events that together confer properties associated with the malignant phenotype. These include acquisition of infinite lifespan, resistance to apoptotic signals, growth factor independence, resistance to antigrowth signals, angiogenesis, and tissue invasion [1]. Acknowledgment of the critical role of mutations in carcinogenesis opens the possibility of chemoprevention using antimutator strategies. Although recent advances have elucidated key details of the pathways underlying mutagenesis, there exist critical gaps in our knowledge of the fundamental mechanisms by which DNA is mutated during carcinogenesis. In this thesis, we will investigate how environmental carcinogens permanently alter the sequence of DNA in order to cause cancer.

Benzo[a]pyrene (B[a]P) is also a well-studied skin carcinogen. It is clear that anti-benzo[a]pyrene-7,8-diol-9,10-epoxide (BPDE), a metabolic derivative of B[a]P, is the ultimate carcinogen [154,155]. BPDE formation proceeds through the action of

CYP450, microsomal epoxide hydratase, and repeated CYP450 oxidation (reviewed in [156]). Carcinogenic activity of B[a]P is primarily due to *in vivo* binding of the ultimate carcinogen to DNA to form bulky adducts [155]. As analyzed by ³²P-postlabeling, stable BPDE-N2-dG adducts constitute over 98% of adducts formed in mouse skin treated with anti-BPDE [157]. However, other reports indicate that multiple other adducts are formed by B[a]P in mouse skin and may be at a higher frequency than 2% [158,159]. These adducts are normally recognized and repaired by enzymes in the NER pathway. Purified Pol η and Pol ι perform well-characterized error-prone bypass of BPDE lesions *in vitro* [77], but this chapter is designed to address the hypothesis that these enzymes are involved in mutagenic bypass of BPDE-induced DNA lesions in living cells.

METHODS

Cell culture

Polη knockout mice were recently generated by our collaborators in a C57Bl/6 hybrid background [19]. To generate *polη*^{-/-}*polι*^{-/-} double knockouts, these animals were bred with 129/Ola mice, which have been shown to carry a nonsense mutation in *polι* resulting in a protein truncated at Ser-27 [59]. Primary fibroblasts have been isolated from these mice and used for mutagenesis studies in our laboratory [63], and these cells were used in this Chapter. Mouse fibroblasts were grown in monolayer cultures using α -MEM supplemented with non-essential amino acids, penicillin-streptomycin and 10% fetal bovine serum. They were maintained in exponential growth. We routinely grow primary murine cells in a 3% O₂/5% CO₂/92% N₂ atmosphere [132].

Hprt mutagenesis

For genotoxicant treatment, cells were plated at 1×10^4 cm⁻². The culture media was removed and cells were washed twice with sterile phosphate-buffered saline (PBS, pH 7.4). Serum-free media was added to the cells along with each chemical carcinogen for a period of one hour. We used 150 nM BPDE for survival and mutagenesis studies. After one hour of treatment, the culture media was aspirated followed by two washes in PBS. For cytotoxicity, cells were trypsinized and counted, then replated at cloning density (the exact number depends on the expected survival). After two weeks, plates were stained with 1% crystal violet and counted. For mutagenesis, cells were maintained in exponential growth for eight days after treatment, after which we trypsinized, counted, and selected 1×10^6 cells with 20 μ M 6-thioguanine at a density of 3000 cm⁻². After 2

weeks of selection, we isolated individual TG^r clones, trypsinized, and resuspended them in RNase-free PBS. The technique for amplifying the hprt gene was performed as described [160] with modifications routine in our laboratory [90]. Briefly, TGr colonies were pelleted at 4°C and the PBS removed. The cells were directly lysed and cDNA generated using a cDNA cocktail. After incubation at 37°C for 1 h amplification was performed using a Taq polymerase cocktail and two outer primers. The 5' primer is from position -47 to -28 relative to the start codon (GGC TTC CTC CTC AGA CCG CT). The 3' primer is from position 790 to 771 (ACA TCA ACA GGA CTC CTC GT). Reamplification using an inner primer set (5', from -27 to -8, TTT TGC CGC GAG CCG ACC GG and 3', from 770 to 751, ATT TGC AGA TTC AAC TTG CG) will follow. The PCR products were sequenced with each of the inner primers using an ABI 370 automated DNA sequencer and dRhodamine dye terminator chemistry.

RESULTS

Fig. 4-1 shows clonogenic survival of wild type, $Pol\eta^{-/-} Pol\iota^{+/+}$, $Pol\eta^{+/+} Pol\iota^{-/-}$, and $Pol\eta^{-/-} Pol\iota^{-/-}$ cells treated with 150 nM BPDE. There were no differences in BPDE-induced cytotoxicity. *Hprt*-induced mutation frequencies are shown in Fig. 4-2. Loss of Pol η or Pol ι alone reduced mutation frequencies by ~80%; double knockout cells displayed mutation frequencies similar to those of the single knockouts. Mutation frequencies were 191, 34, 44, and 56 TG^r mutants per 10⁶ clonable cells in wild type, $Pol\eta^{-/-}$, $Pol\iota^{-/-}$, and double knockout cells, respectively. These data support our hypothesis that Pol ι participates in error-prone TLS of BPDE-induced lesions, probably in coordination with Pol η due to the similar phenotype of the Pol η -knockout and the fact that the double knockout cells have the same mutation frequency. Table 4-1 summarizes *Hprt* sequencing data from TG^r clones. These data indicate that the polymerase responsible for making mutations opposite the bulky BPDE-DNA lesion in both wild type and $Pol\eta^{-/-}$ cells has a similar mutation spectrum. The percentage of frequent UV-induced mutations such as C→T transitions and G→T transversions were very similar between genotypes despite the dramatic reduction in the mutation frequency in $Pol\eta^{-/-}$ cells. However, tandem mutations (10.5%) were only found in the wild type cells, and small deletions (5.6%) were only found in $Pol\eta^{-/-}$ cells. The number of TG^r clones analyzed was insufficient for statistical analysis. Due to consistently low replating efficiency, insufficient clones could be isolated from $Pol\eta^{+/+} Pol\iota^{-/-}$ and $Pol\eta^{-/-} Pol\iota^{-/-}$ cells for analysis.

Table 4-2 lists the mutant *Hprt* sequences from TG^r clones. Specific analysis of the sequence data reveals similar distribution of mutations throughout the *Hprt* gene. We

did find that the only mutations arising from adducts in the transcribed strand were in wild type cells (3 of 19).

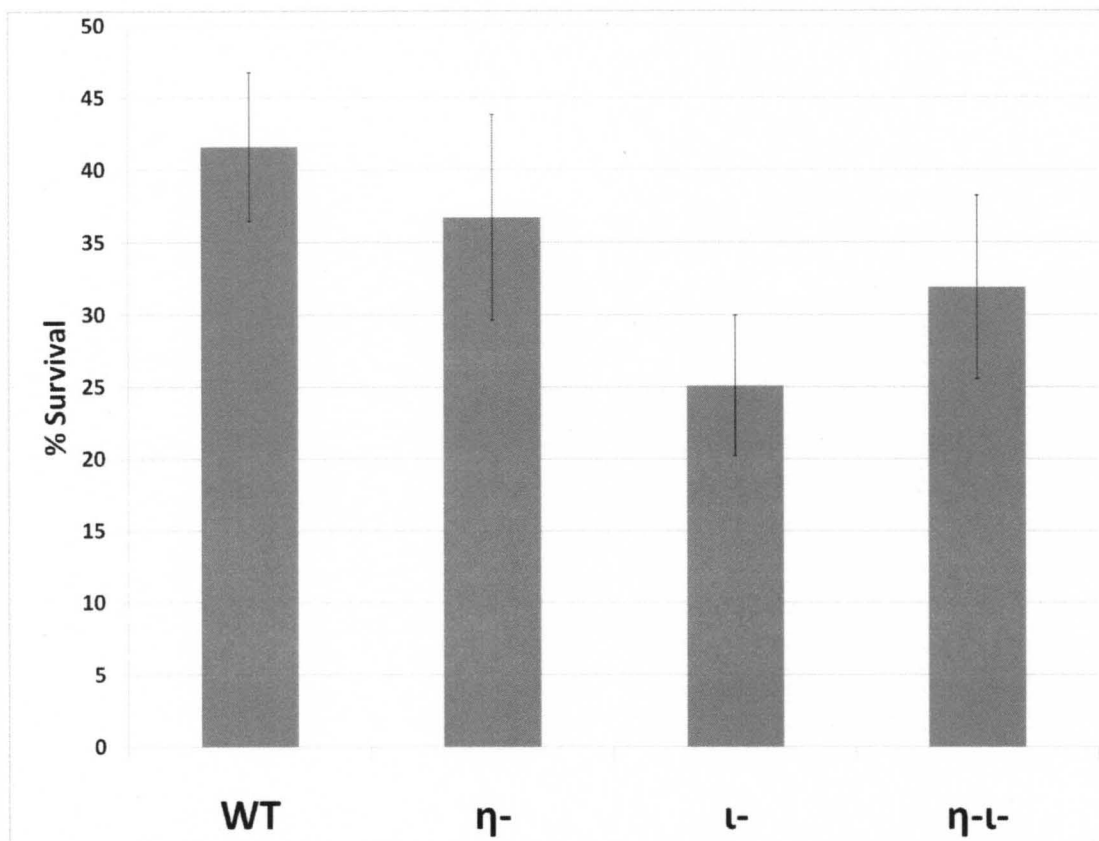


Fig. 4-1. Loss of Pol η or Pol ι does not affect BPDE-induced cytotoxicity. Primary dermal fibroblasts isolated from mice of the indicated genotypes were treated with 150 nM BPDE at 10^4 cm^{-2} and immediately replated at cloning density. Cells were refed after seven days and stained with crystal violet after 14 days to determine clonogenic survival. There were no significant differences in clonogenic survival among the genotypes. Average survivals were calculated based on results from at least four independent experiments. Error bars, SEM.

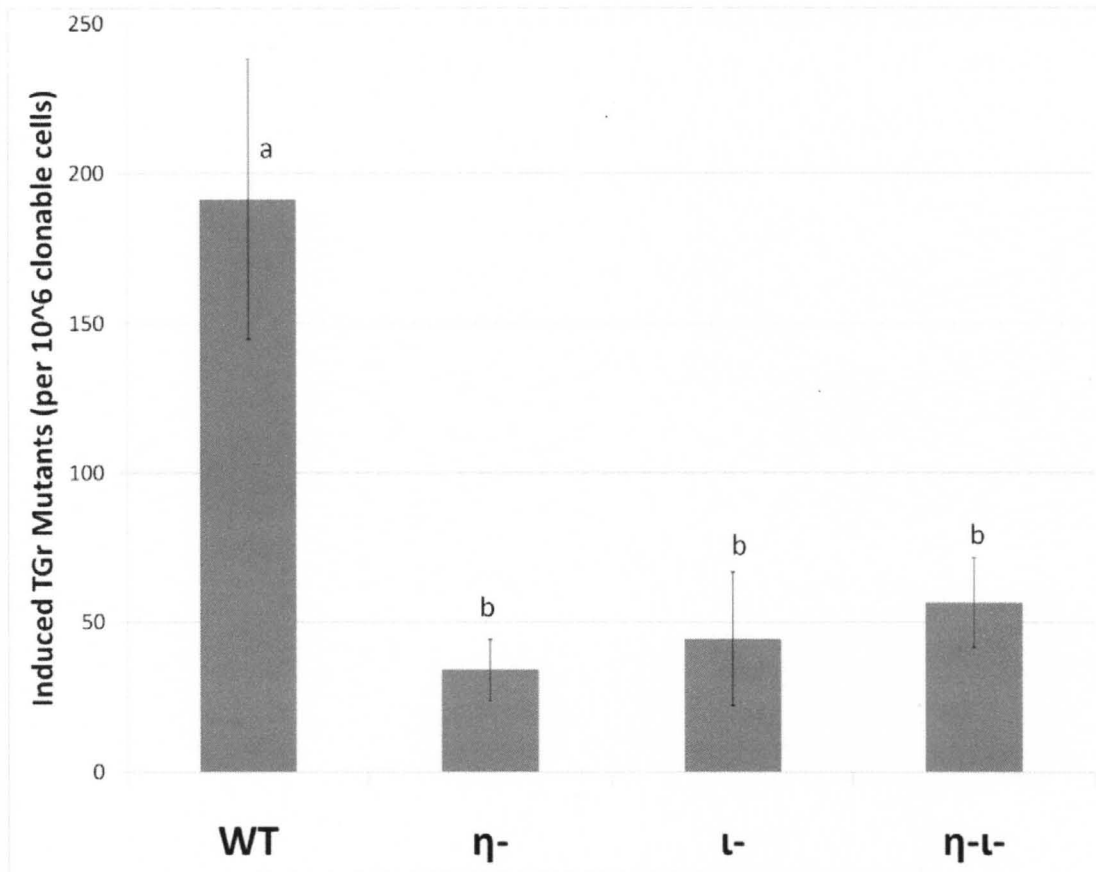


Fig. 4-2. Loss of Pol η or Pol ι dramatically reduces BPDE-induced mutagenesis. Primary dermal fibroblasts isolated from mice of the indicated genotypes were treated with 150 nM BPDE at 10^4 cm^{-2} . After eight days of exponential growth, cells were replated in 40 μM 6-thioguanine and grown for two weeks. Thioguanine-resistant clones were stained with crystal violet. There Averages represent at least three independent experiements. Histogram bars with different letters are significantly different ($p < 0.05$). Error bars, SEM.

Mutation Type	Wild Type		Pol η ^{-/-}	
	Independent Clones	Percent of Total	Independent Clones	Percent of Total
Transitions	4	21.1	5	27.8
A•T → G•C	1	5.3	2	11.1
G•C → A•T	3	15.8	3	16.7
Transversions	13	68.4	12	66.7
A•T → C•G	2	10.5	0	0.0
A•T → T•A	1	5.3	0	0.0
G•C → T•A	10	52.6	11	61.1
G•C → C•G	0	0.0	1	5.6
Tandem	2	10.5	0	0.0
Small Deletion	0	0.0	1	5.6
Total	19	100.0	18	100.0

Table 4-1. Summary of BPDE-induced mutations. Isolation and sequencing of *Hprt* cDNA from thioguanine-resistant clones indicated that the mutation spectrum of BPDE is similar in both wild type and *Pol η ^{-/-}* cells. Tandem mutations were only seen in the wild type cells (10.5%), while only one deletion mutation was seen in the *Pol η ^{-/-}* cells (5.6%).

<i>Wild Type</i>				<i>Polη^{-/-}</i>			
Sample	Mutation Type	Nucleotide	Strand	Sample	Mutation Type	Nucleotide	Strand
35-0-1	A>C	449	T	48a-24	A>G	155	NT
35d-4	A>C	449	T	C1	A>G	497	NT
68-32	A>G	491	T	48a-28	G Deletion	337	NT
83-2	A>T	1	NT	48a-26	G>A	197	NT
68-13	G>A	27	NT	A1	G>A	209	NT
68-7	G>A	617	NT	48a-10	G>A	27	NT
68-14	G>A	617	NT	48-1A-6	G>C	566	NT
35d-2	G>T	197	NT	48a-19	G>T	119	NT
68-3	G>T	197	NT	H1	G>T	123	NT
68-2	G>T	230	NT	C	G>T	129	NT
68-6	G>T	419	NT	48-1A-1	G>T	208	NT
68-19	G>T	563	NT	48a-14	G>T	208	NT
68-35	G>T	569	NT	B1	G>T	212	NT
68-33	G>T	601	NT	48a-25	G>T	3	NT
68-9	G>T	617	NT	G1	G>T	398	NT
68-15	G>T	624	NT	48-1B-3	G>T	420	NT
83-18	G>T	88	NT	H	G>T	569	NT
68-26	CG>>GT	612-3	NT	48a-33	G>T	88	NT
68-25	GG>>CC	418-9	NT				

Table 4-2. *Hprt* mutant sequences. Isolation and sequencing of individual thioguanine-resistant clones after BPDE treatment revealed that the mutation spectrum in wild type (n=19 unique mutations) and *Pol η ^{-/-} Pol ι ^{+/+}* cells (n=18 unique mutations) both consisted primarily of G>T transversions originating from BPDE lesions on the nontranscribed strand. The nucleotide column lists the base pair position of the mutation relative to the *Hprt* cDNA.

DISCUSSION

Purified Pol ι has been characterized in the error-prone bypass of BPDE lesions [77], but the cellular role of this enzyme in bypassing bulky adducts induced by environmental carcinogens remains unclear. As a first step towards extending our UV studies to carcinogenesis by B[a]P, we first characterized the cellular role of Pol ι after treatment with the active metabolite BPDE. Using primary ear fibroblasts from *Pol η ^{-/-}* and *Poli^{-/-}* mice, we discovered that loss of either enzyme reduced the mutation frequency induced by 150 nM BPDE by approximately 80%. The mutation frequency in the double knockout cells was indistinguishable from either single knockout, indicating that Pol η and Pol ι are epistatic in the bypass of BPDE lesions. In the absence of either Pol η or Pol ι , it is likely that Pol κ performs bypass of BPDE DNA damage. Purified Pol κ bypasses BPDE lesions in an accurate manner [76,77,161], and experiments in *Pol κ ^{-/-}* mouse embryonic fibroblasts show elevated BPDE-induced mutation frequency in the absence of this enzyme [81]. The faithful nature of Pol κ BPDE lesion-bypass could explain the low mutation frequency in *Pol η ^{-/-}* and *Poli^{-/-}* cells.

The mechanism of bypass involving both Pol η and Pol ι is possibly a two-step model of TLS [161] where both enzymes are a part of the molecular complex required for efficient bypass synthesis. Following this model, Pol η would perform direct lesion bypass synthesis, frequently making errors [77]. Pol κ or ζ could perform the extension step and leave a suitable DNA template for the continuation of normal replication. It is unlikely that Pol ι is involved in the direct bypass of BPDE due to the fact that the purified protein is blocked by this adduct [77]. Pol ι has also never been characterized as an extender in a two-polymerase model, so it is likely that Pol ι is not involved in the

extension step of BPDE bypass. Since Pol ι is not likely to be directly involved in BPDE bypass synthesis and yet its absence still results in reduced mutation frequency, we hypothesize that this protein is a necessary component of the TLS complex. Without Pol ι , the multisubunit complex necessary for the proposed two-step bypass of BPDE could become unstable, allowing the direct bypass synthesis by the secondary Y-family Pol κ . The relative fidelity of Pol κ on the BPDE lesion template would explain the reduced mutation frequency in our *Pol η ^{-/-}* and *Pol ι ^{-/-}* cells.

It is important to note that Y-family polymerases are recruited to stalled replication forks by protein-protein interactions. Y-family polymerases all have novel ubiquitin binding regions which mediate their preferential binding to monoubiquitylated PCNA [75], a post-translational modification that is made by the Rad6/Rad18 complex after replication fork stalling. This interaction with monoubiquitylated PCNA appears to be critical to the initiation of TLS. It has also been shown that Rad18 directly shuttles Pol η to the site of replication forks stalled at UV-induced DNA damage [44]. This interaction is mediated by the preferential interaction of Pol η with phosphorylated Rad18 [162]. The demonstrated central role of protein-protein interactions in promoting functional TLS indicates that the proposed model of BPDE bypass requiring both Pol η and Pol ι for the stability of a multiprotein complex is plausible.

Another explanation for the very low mutation frequency in cells lacking Pol η and/or Pol ι is that BPDE lesions are tolerated using template switching, an error-free method of damage avoidance where the nascent DNA strand is used as an undamaged homologous template. Replacing mutagenic TLS with error-free template switching could also account for the reduced mutation frequency in *Pol η ^{-/-}* and *Pol ι ^{-/-}* cells. This

method of damage avoidance is likely to increase at least slightly in our knockout cells if our hypothesis of an unstable TLS complex is true, as even accurate TLS by Pol κ would require association with such a multiprotein complex to function.

Despite the fact that the number of TG^r clones isolated was too small for statistical analysis, we can draw some conclusions about the nature of the mutation spectrum of the active Y-family polymerase in each genotype examined. Wild type and *Pol η ^{-/-} Pol ι ^{+/+}* cells showed mutation spectra that were very similar. This suggests that Pol η either does not directly catalyze TLS across from BPDE lesions, or another polymerase takes over TLS in its place with the same mutation spectrum. If Pol η is not directly involved in the lesion bypass step, the most likely enzyme to perform this function would be Rev1. Evidence in yeast indicates that Rev1 is required with Pol η and Pol κ for mutagenic BPDE bypass [31]; it is therefore possible that both Pol η and Pol ι are necessary for the formation of a TLS complex, and that loss of either enzyme results in a disruption in this predominant mutagenic bypass pathway. There was a trend towards increased tandem mutations in wild type cells (% of total) versus small deletions in *Pol η ^{-/-}* cells, which could indicate a change in the active bypass polymerase. This slight change in mutation spectrum could suggest that Pol η is the active bypass polymerase in wild type cells and displays relatively high processivity on the BPDE lesion template, rarely adding two incorrect bases rather than one. In *Pol η ^{-/-}* cells, Rev1 could perform mutagenic lesion bypass, preferentially skipping a base a causing a deletion and giving rise to the shifted mutation spectrum.

While we were able to isolate and sequence approximately equal numbers of TG^r clones from wild type and *Pol η ^{-/-}* cells, we repeatedly encountered low replating

efficiencies in the thioguanine selection of *Polι*^{-/-} and *Polη*^{-/-} *Polι*^{-/-} cells. We optimized the TG dose and selection time in an attempt to make the clones more easily visible for isolation, but the small number of TG^r clones we were able to isolate did not yield cDNA of sufficient quality for PCR amplification of the *Hprt* gene.

In conclusion, we have shown that Pol η and Pol ι participate in mutagenic translesion synthesis past BPDE-induced DNA damage. These two enzymes likely participate in the same mutagenic bypass pathway, such that loss of either Pol η or Pol ι disrupts mutagenic TLS and allows for a more faithful damage tolerance mechanism, likely TLS by Pol κ or template switching. This is the first indication that Pol ι is involved in the cellular response to BPDE; it also represents the first step in applying our findings from studies of Pol ι in a UV model to the effects of BPDE.

CHAPTER V

CONCLUSIONS AND FUTURE DIRECTIONS

The role of Y-family polymerases is expanding rapidly to include somatic hypermutation [21], nucleotide excision repair synthesis [83], and cell cycle checkpoint function [80]. Despite great advances in our understanding of the roles of these enzymes in mammalian systems, the cellular role of Pol ι remains unknown. The purified protein has been characterized in the inaccurate bypass of numerous damaged DNA templates [77,163,164,165]. It is also known that Pol ι is responsible for the high UV-induced mutation frequency in XP variant patients who lack Pol η [62].

Studies in this dissertation were designed to investigate the potential role of Pol ι outside TLS. Our hypothesis that Pol ι could have a role in regulating other cellular functions was based on a previous report [63] that *Poli*^{-/-} have reduced UV-induced mutations in their cells, but the mice develop cancer more quickly. We have evidence, discussed in Chapter II, suggesting that the disparity between mutation frequency and tumor latency is due to the regulation of the mitotic spindle checkpoint by Pol ι . This finding is unexpected and novel, and bears further investigation; important questions remain about the mechanism of checkpoint regulation by Pol ι . Our initial findings should first be replicated in another cell type, preferably human. Then the function of the spindle assembly checkpoint could be directly analyzed after genetic manipulation of the cells; *Poli* or *Rad18* knockdown could be used as specific and general TLS inhibitors,

and cytochalasin B or aurora B kinase inhibitors could be used to block cells at cytokinesis. Fluorescent tagged recombinant Pol ι could be expressed in synchronized cells for the examination of Pol ι at the kinetochore. The purpose of these proposed studies is to determine the exact nature of the regulation of the mitotic checkpoint by Pol ι . Plosky *et al* reported that ~30% of *Poli* clones in a yeast two hybrid screen were found to interact with clones encoding ubiquitin precursor proteins [166]. Therefore, it is possible that ubiquitin signaling could play a role in the activity of Pol ι in mitotic checkpoint regulation. It is also interesting to note that Pol η -deficiency caused a slight but significant increase in the percentage of binucleated cells. Future studies should investigate whether Pol η also plays a role in the regulation of the mitotic checkpoint, and whether this regulation involves the entire Y family of polymerases or is linked to TLS.

We found in Chapter III that loss of Pol ι in an isogenic, cancer prone background caused a trend towards reduced cancer latency in mice. It is possible that the *Xpa*-deficiency of this model rendered the effect sizes too small for statistical differences between groups to be realized with the sample sizes used. Therefore, we propose future studies using isogenic *Xpa*^{+/+} mice to increase the latency of the control group and therefore increase the effect sizes of the experimental groups. Future studies should also include at least 30 mice per genotype in order to be sufficiently powered to detect differences among groups. One major question raised in Chapter III is why we did not see multinucleated cells in *Xpa*^{-/-} *Poli*^{-/-} mice. Future studies should investigate tissues of *Poli*^{-/-} mice in multiple strains in order to determine if background differences play a role in the observed discrepancy between our cell culture and *in vivo* data.

In Chapter IV we analyzed the role of Pol ι and Pol η in BPDE mutagenesis. We propose that these studies serve as the foundation for future work into Pol ι -mediated regulation of BPDE-induced checkpoints. It is known that Pol κ is required for escape from an intra-S phase checkpoint induced by BPDE [80], but future studies on Pol ι should focus on activation of the mitotic checkpoint. It is feasible that Pol ι is active in the regulation of cytokinesis in more conditions than UV-induced DNA damage. It would therefore be of interest to examine whether BPDE activates the mitotic checkpoint in wild type cells, which has not been studied, and whether loss of Pol ι alters this activity.

In conclusion, we have found a novel role for the Y-family DNA polymerase ι in activating the mitotic spindle assembly checkpoint after UV-induced DNA damage. In the absence of Pol ι , cells proceed through mitosis but do not undergo cytokinesis and give rise to a tetraploid population. This is one possible explanation of the observed tumor suppressor function of *PolI* in previous studies [63,64]. In Pol ι -deficient-mice, we found a strong trend towards decreased latency of UV-induced tumors. Finally, we found that Pol ι is involved in mutagenic TLS of BPDE-induced DNA damage. These studies support Pol ι as an important candidate for future investigation and a potentially and as yet unrecognized regulator of mitotic progression.

REFERENCES

1. Hanahan D, Weinberg RA (2000) The Hallmarks of Cancer. *Cell* 100: 57-70.
2. Waters LS, Minesinger BK, Wiltrott ME, D'Souza S, Woodruff RV, et al. (2009) Eukaryotic Translesion Polymerases and Their Roles and Regulation in DNA Damage Tolerance. *Microbiology and Molecular Biology Reviews* 73: 134-154.
3. Branzei D, Seki M, Enomoto T (2004) Rad18/Rad5/Mms2-mediated polyubiquitination of PCNA is implicated in replication completion during replication stress. *Genes to Cells* 9: 1031-1042.
4. Motegi A, Liaw H-J, Lee K-Y, Roest HP, Maas A, et al. (2008) Polyubiquitination of proliferating cell nuclear antigen by HLTF and SHPRH prevents genomic instability from stalled replication forks. *Proceedings of the National Academy of Sciences* 105: 12411-12416.
5. Motegi A, Sood R, Moinova H, Markowitz SD, Liu PP, et al. (2006) Human SHPRH suppresses genomic instability through proliferating cell nuclear antigen polyubiquitination. *The Journal of Cell Biology* 175: 703-708.
6. Unk I, Hajdú I, Fátyol K, Hurwitz J, Yoon J-H, et al. (2008) Human HLTF functions as a ubiquitin ligase for proliferating cell nuclear antigen polyubiquitination. *Proceedings of the National Academy of Sciences* 105: 3768-3773.
7. Unk I, Hajdú I, Fátyol K, Szakál B, Blastyák A, et al. (2006) Human SHPRH is a ubiquitin ligase for Mms2-Ubc13-dependent polyubiquitylation of proliferating

- cell nuclear antigen. Proceedings of the National Academy of Sciences 103: 18107-18112.
8. Hoegge C, Pfander B, Moldovan GL, Pyrowolakis G, Jentsch S (2002) RAD6-dependent DNA repair is linked to modification of PCNA by ubiquitin and SUMO. Nature 419: 135-141.
 9. Baynton K, Bresson-Roy A, Fuchs RP (1998) Analysis of damage tolerance pathways in *Saccharomyces cerevisiae*: a requirement for Rev3 DNA polymerase in translesion synthesis. Molecular and Cellular Biology 18: 960-966.
 10. Adar S, Izhar L, Hendel A, Geacintov N, Livneh Z (2009) Repair of gaps opposite lesions by homologous recombination in mammalian cells. Nucleic Acids Research: gkp632.
 11. Vasquez KM, Marburger K, Intody Z, Wilson JH (2001) Manipulating the mammalian genome by homologous recombination. Proceedings of the National Academy of Sciences 98: 8403-8410.
 12. Shulman MJ, Collins C, Connor A, Read LR, Baker MD (1995) Interchromosomal recombination is suppressed in mammalian somatic cells. EMBO Journal 14: 4102-4107.
 13. Ohmori H, Friedberg EC, Fuchs RP, Goodman MF, Hanaoka F, et al. (2001) The Y-family of DNA polymerases. Molecular Cell 8: 7-8.
 14. Gibbs PE, McGregor WG, Maher VM, Nisson P, Lawrence CW (1998) A human homolog of the *Saccharomyces cerevisiae* REV3 gene, which encodes the catalytic subunit of DNA polymerase zeta. Proceedings of the National Academy of Sciences 95: 6876-6880.

15. Lin W, Wu X, Wang Z (1999) A full-length cDNA of hREV3 is predicted to encode DNA polymerase zeta for damage-induced mutagenesis in humans. *Mutation Research* 433: 89-98.
16. McCulloch SD, Kunkel TA (2008) The fidelity of DNA synthesis by eukaryotic replicative and translesion synthesis polymerases. *Cell Research* 18: 148-161.
17. He X, Ye F, Zhang J, Cheng Q, Shen J, et al. (2008) REV1 genetic variants associated with the risk of cervical carcinoma. *European Journal of Epidemiology* 23: 403-409.
18. Wang H, Wu W, Wang HW, Wang S, Chen Y, et al. (2010) Analysis of specialized DNA polymerases expression in human gliomas: association with prognostic significance. *Neuro-Oncology* 12: 679-686.
19. Lin Q, Clark AB, McCulloch SD, Yuan T, Bronson RT, et al. (2006) Increased Susceptibility to UV-Induced Skin Carcinogenesis in Polymerase {eta}-deficient Mice. *Cancer Research* 66: 87-94.
20. Tsaalbi-Shtylik A, Verspuy JWA, Jansen JG, Rebel H, Carlee LM, et al. (2009) Error-prone translesion replication of damaged DNA suppresses skin carcinogenesis by controlling inflammatory hyperplasia. *Proceedings of the National Academy of Sciences* 106: 21836-21841.
21. Zeng X, Winter DB, Kasmer C, Kraemer KH, Lehmann AR, et al. (2001) DNA polymerase eta is an A-T mutator in somatic hypermutation of immunoglobulin variable genes. *Nature Immunology* 2: 537-541.

22. Larimer FW, Perry JR, Hardigree AA (1989) The REV1 gene of *Saccharomyces cerevisiae*: isolation, sequence, and functional analysis. *The Journal of Bacteriology* 171: 230-237.
23. Nelson JR, Lawrence CW, Hinkle DC (1996) Deoxycytidyl transferase activity of yeast REV1 protein. *Nature* 382: 729-731.
24. Diaz M, Velez J, Singh M, Cerny J, Flajnik MF (1999) Mutational pattern of the nurse shark antigen receptor gene (NAR) is similar to that of mammalian Ig genes and to spontaneous mutations in evolution: the translesion synthesis model of somatic hypermutation. *International Immunology* 11: 825-833.
25. Gibbs PE, Wang XD, Li Z, McManus TP, McGregor WG, et al. (2000) The function of the human homolog of *Saccharomyces cerevisiae* REV1 is required for mutagenesis induced by UV light. *Proceedings of the National Academy of Sciences* 97: 4186-4191.
26. Clark DR, Zacharias W, Panaitescu L, McGregor WG (2003) Ribozyme-mediated REV1 inhibition reduces the frequency of UV-induced mutations in the human HPRT gene. *Nucleic Acids Research* 31: 4981-4988.
27. Mukhopadhyay S, Clark DR, Watson NB, Zacharias W, McGregor WG (2004) REV1 accumulates in DNA damage-induced nuclear foci in human cells and is implicated in mutagenesis by benzo [a]pyrenediolepoxide. *Nucleic Acids Research* 32: 5820-5826.
28. Lawrence CW, Gibbs PE, Murante RS, Wang XD, Li Z, et al. (2000) Roles of DNA polymerase zeta and Rev1 protein in eukaryotic mutagenesis and translesion replication. *Cold Spring Harbor Symposia on Quantitative Biology* 65: 61-69.

29. Ross AL, Simpson LJ, Sale JE (2005) Vertebrate DNA damage tolerance requires the C-terminus but not BRCT or transferase domains of REV1. *Nucleic Acids Research* 33: 1280-1289.
30. Jansen JG, Tsaalbi-Shtylik A, Langerak P, Calléja F, Meijers CM, et al. (2005) The BRCT domain of mammalian Rev1 is involved in regulating DNA translesion synthesis. *Nucleic Acids Research* 33: 356-365.
31. Zhao B, Wang J, Geacintov NE, Wang Z (2006) Poleta, Polzeta and Rev1 together are required for G to T transversion mutations induced by the (+)- and (-)-trans-anti-BPDE-N2-dG DNA adducts in yeast cells. *Nucleic Acids Research* 34: 417-425.
32. Dumstorf CA, Mukhopadhyay S, Krishnan E, Haribabu B, McGregor WG (2009) REV1 Is Implicated in the Development of Carcinogen-Induced Lung Cancer. *Molecular Cancer Research* 7: 247-254.
33. Sakiyama T, Kohno T, Mimaki S, Ohta T, Yanagitani N, et al. (2005) Association of amino acid substitution polymorphisms in DNA repair genes TP53, POLI, REV1 and LIG4 with lung cancer risk. *International Journal of Cancer* 114: 730-737.
34. Young RP, Hopkins RJ, Hay BA, Epton MJ, Mills GD, et al. (2009) A gene-based risk score for lung cancer susceptibility in smokers and ex-smokers. *Postgraduate Medical Journal* 85: 515-524.
35. Kraemer KH, Slor H (1985) Xeroderma pigmentosum. *Clinics in Dermatology* 3: 33-69.

36. Cleaver JE (1972) XERODERMA PIGMENTOSUM: VARIANTS WITH NORMAL DNA REPAIR AND NORMAL SENSITIVITY TO ULTRAVIOLET LIGHT. *Journal of Investigative Dermatology* 58: 124-128.
37. Tung BS, McGregor WG, Wang YC, Maher VM, McCormick JJ (1996) Comparison of the rate of excision of major UV photoproducts in the strands of the human HPRT gene of normal and xeroderma pigmentosum variant cells. *Mutation Research* 362: 65-74.
38. Lehmann AR, Kirk-Bell S, Arlett CF, Paterson MC, Lohman PH, et al. (1975) Xeroderma pigmentosum cells with normal levels of excision repair have a defect in DNA synthesis after UV-irradiation. *Proceedings of the National Academy of Sciences of the United States of America* 72: 219-223.
39. Boyer JC, Kaufmann WK, Brylawski BP, Cordeiro-Stone M (1990) Defective postreplication repair in xeroderma pigmentosum variant fibroblasts. *Cancer Research* 50: 2593-2598.
40. Maher VM, Ouellette LM, Curren RD, McCormick JJ (1976) Frequency of ultraviolet light-induced mutations is higher in xeroderma pigmentosum variant cells than in normal human cells. *Nature* 261: 593-595.
41. Masutani C, Araki M, Yamada A, Kusumoto R, Nogimori T, et al. (1999) Xeroderma pigmentosum variant (XP-V) correcting protein from HeLa cells has a thymine dimer bypass DNA polymerase activity. *EMBO Journal* 18: 3491-3501.
42. Johnson RE, Prakash S, Prakash L (1999) Efficient bypass of a thymine-thymine dimer by yeast DNA polymerase, Poleta. *Science* 283: 1001-1004.

43. Masutani C, Kusumoto R, Yamada A, Dohmae N, Yokoi M, et al. (1999) The XPV (xeroderma pigmentosum variant) gene encodes human DNA polymerase eta. *Nature* 399: 700-704.
44. Watanabe K, Tateishi S, Kawasuji M, Tsurimoto T, Inoue H, et al. (2004) Rad18 guides pol [eta] to replication stalling sites through physical interaction and PCNA monoubiquitination. *EMBO Journal* 23: 3886-3896.
45. Guo C, Kosarek-Stancel J, Tang TS, Friedberg E (2009) Y-family DNA polymerases in mammalian cells. *Cellular and Molecular Life Sciences* 66: 2363-2381.
46. Kuwamoto K, Miyauchi-Hashimoto H, Isei T, Horio T (1999) Xeroderma pigmentosum variant associated with multiple cancers. *Photodermatology, Photoimmunology & Photomedicine* 15: 127-132.
47. Kraemer KH, Lee MM, Scotto J (1984) DNA repair protects against cutaneous and internal neoplasia: evidence from xeroderma pigmentosum. *Carcinogenesis* 5: 511-514.
48. Flanagan AM, Rafferty G, O'Neill A, Rynne L, Kelly J, et al. (2007) The human POLH gene is not mutated, and is expressed in a cohort of patients with basal or squamous cell carcinoma of the skin. *International Journal of Molecular Medicine* 19: 589-596.
49. McDonald JP, Ropic-Otrin V, Epstein JA, Broughton BC, Wang X, et al. (1999) Novel human and mouse homologs of *Saccharomyces cerevisiae* DNA polymerase eta. *Genomics* 60: 20-30.

50. Nair DT, Johnson RE, Prakash S, Prakash L, Aggarwal AK (2004) Replication by human DNA polymerase- [iota] occurs by Hoogsteen base-pairing. *Nature* 430: 377-380.
51. Wang J (2005) DNA polymerases: Hoogsteen base-pairing in DNA replication? *Nature* 437: E6-E7.
52. Lee GH, Nishimori H, Sasaki Y, Matsushita H, Kitagawa T, et al. (2003) Analysis of lung tumorigenesis in chimeric mice indicates the Pulmonary adenoma resistance 2 (Par2) locus to operate in the tumor-initiation stage in a cell-autonomous manner: detection of polymorphisms in the Poli gene as a candidate for Par2. *Oncogene* 22: 2374-2382.
53. Wang M, Devereux TR, Vikis HG, McCulloch SD, Holliday W, et al. (2004) Pol {iota} Is a Candidate for the Mouse Pulmonary Adenoma Resistance 2 Locus, a Major Modifier of Chemically Induced Lung Neoplasia. *Cancer Research* 64: 1924-1931.
54. Lee GH, Matsushita H (2005) Genetic linkage between Politoa deficiency and increased susceptibility to lung tumors in mice. *Cancer Science* 96: 256-259.
55. Obata M, Nishimori H, Ogawa K, Lee GH (1996) Identification of the Par2 (Pulmonary adenoma resistance) locus on mouse chromosome 18, a major genetic determinant for lung carcinogen resistance in BALB/cByJ mice. *Oncogene* 13: 1599-1604.
56. Bebenek K, Tissier A, Frank EG, McDonald JP, Prasad R, et al. (2001) 5'-Deoxyribose phosphate lyase activity of human DNA polymerase iota in vitro. *Science* 291: 2156-2159.

57. Fernando RC, Nair J, Barbin A, Miller JA, Bartsch H (1996) Detection of 1,N6-ethenodeoxyadenosine and 3,N4-ethenodeoxycytidine by immunoaffinity/³²P-post-labelling in liver and lung DNA of mice treated with ethylcarbamate (urethane) or its metabolites. *Carcinogenesis* 17: 1711-1718.
58. Choudhury S, Adhikari S, Cheema A, Roy R (2008) Evidence of complete cellular repair of 1,N6-ethenoadenine, a mutagenic and potential damage for human cancer, revealed by a novel method. *Molecular and Cellular Biochemistry* 313: 19-28.
59. McDonald JP, Frank EG, Plosky BS, Rogozin IB, Masutani C, et al. (2003) 129-derived strains of mice are deficient in DNA polymerase iota and have normal immunoglobulin hypermutation. *The Journal of Experimental Medicine* 198: 635-643.
60. Gening LV, Makarova AV, Malashenko AM, Tarantul VZ (2006) A false note of DNA polymerase iota in the choir of genome caretakers in mammals. *Biochemistry (00062979)* 71: 155-159.
61. Makarova AV, Grabow C, Gening LV, Tarantul VZ, Tahirov TH, et al. (2011) Inaccurate DNA Synthesis in Cell Extracts of Yeast Producing Active Human DNA Polymerase Iota. *PLoS ONE* 6: e16612.
62. Wang Y, Woodgate R, McManus TP, Mead S, McCormick JJ, et al. (2007) Evidence that in Xeroderma Pigmentosum Variant Cells, which Lack DNA Polymerase {eta}, DNA Polymerase {iota} Causes the Very High Frequency and Unique Spectrum of UV-Induced Mutations. *Cancer Research* 67: 3018-3026.

63. Dumstorf CA, Clark AB, Lin Q, Kissling GE, Yuan T, et al. (2006) Participation of mouse DNA polymerase iota in strand-biased mutagenic bypass of UV photoproducts and suppression of skin cancer. *Proceedings of the National Academy of Sciences* 103: 18083-18088.
64. Ohkumo T, Kondo Y, Yokoi M, Tsukamoto T, Yamada A, et al. (2006) UV-B radiation induces epithelial tumors in mice lacking DNA polymerase eta and mesenchymal tumors in mice deficient for DNA polymerase iota. *Molecular and Cellular Biology* 26: 7696-7706.
65. Mitchell DL, Jen J, Cleaver JE (1991) Relative induction of cyclobutane dimers and cytosine photohydrates in DNA irradiated in vitro and in vivo with ultraviolet-C and ultraviolet-B light. *Photochemistry and Photobiology* 54: 741-746.
66. Newcomb EW, Diamond LE, Sloan SR, Corominas M, Guerrero I, et al. (1989) Radiation and chemical activation of ras oncogenes in different mouse strains. *Environmental Health Perspectives* 81:33-7.: 33-37.
67. Petta TB, Nakajima S, Zlatanou A, Despras E, Couve-Privat S, et al. (2008) Human DNA polymerase iota protects cells against oxidative stress. *EMBO Journal* 27: 2883-2895.
68. Poltoratsky V, Horton JK, Prasad R, Beard WA, Woodgate R, et al. (2008) Negligible impact of pol [iota] expression on the alkylation sensitivity of pol [beta]-deficient mouse fibroblast cells. *DNA Repair* 7: 830-833.
69. Wang Y, Seimiya M, Kawamura K, Yu L, Ogi T, et al. (2004) Elevated expression of DNA polymerase kappa in human lung cancer is associated with p53 inactivation:

- Negative regulation of POLK promoter activity by p53. *International Journal of Oncology* 25: 161-165.
70. Zienolddiny S, Campa D, Lind H, Ryberg D, Skaug V, et al. (2006) Polymorphisms of DNA repair genes and risk of non-small cell lung cancer. *Carcinogenesis* 27: 560-567.
71. Vineis P, Manuguerra M, Kavvoura FK, Guarrera S, Allione A, et al. (2009) A Field Synopsis on Low-Penetrance Variants in DNA Repair Genes and Cancer Susceptibility. *Journal of the National Cancer Institute* 101: 24-36.
72. Luedeke M, Linnert CM, Hofer MD, Surowy HM, Rinckleb AE, et al. (2009) Predisposition for TMPRSS2-ERG Fusion in Prostate Cancer by Variants in DNA Repair Genes. *Cancer Epidemiology Biomarkers & Prevention* 18: 3030-3035.
73. Petrovics G, Liu A, Shaheduzzaman S, Furusato B, Sun C, et al. (2005) Frequent overexpression of ETS-related gene-1 (ERG1) in prostate cancer transcriptome. *Oncogene* 24: 3847-3852.
74. Tomlins SA, Rhodes DR, Perner S, Dhanasekaran SM, Mehra R, et al. (2005) Recurrent Fusion of TMPRSS2 and ETS Transcription Factor Genes in Prostate Cancer. *Science* 310: 644-648.
75. Bienko M, Green CM, Crosetto N, Rudolf F, Zapart G, et al. (2005) Ubiquitin-Binding Domains in Y-Family Polymerases Regulate Translesion Synthesis. *Science* 310: 1821-1824.
76. Suzuki N, Ohashi E, Kolbanovskiy A, Geacintov NE, Grollman AP, et al. (2002) Translesion synthesis by human DNA polymerase kappa on a DNA template containing a single stereoisomer of dG-(+)- or dG-(-)-anti-N(2)-BPDE (7,8-

- dihydroxy-anti-9,10-epoxy-7,8,9,10-tetrahydrobenzo [a]pyrene). *Biochemistry* 41: 6100-6106.
77. Rechkoblit O, Zhang Y, Guo D, Wang Z, Amin S, et al. (2002) trans-Lesion synthesis past bulky benzo [a]pyrene diol epoxide N2-dG and N6-dA lesions catalyzed by DNA bypass polymerases. *Journal of Biological Chemistry* 277: 30488-30494.
78. Zhang Y, Wu X, Guo D, Rechkoblit O, Wang Z (2002) Activities of human DNA polymerase [kappa] in response to the major benzo [a]pyrene DNA adduct: error-free lesion bypass and extension synthesis from opposite the lesion. *DNA Repair* 1: 559-569.
79. Guo N, Faller DV, Vaziri C (2002) Carcinogen-induced S-phase arrest is Chk1 mediated and caffeine sensitive. *Cell Growth & Differentiation* 13: 77-86.
80. Bi X, Slater DM, Ohmori H, Vaziri C (2005) DNA polymerase kappa is specifically required for recovery from the benzo [a]pyrene-dihydrodiol epoxide (BPDE)-induced S-phase checkpoint. *The Journal of Biological Chemistry* 280: 22343-22355.
81. Avkin S, Goldsmith M, Velasco-Miguel S, Geacintov N, Friedberg EC, et al. (2004) Quantitative analysis of translesion DNA synthesis across a benzo [a]pyrene-guanine adduct in mammalian cells: the role of DNA polymerase kappa 2. *Journal of Biological Chemistry* 279: 53298-53305.
82. Shachar S, Ziv O, Avkin S, Adar S, Wittschieben J, et al. (2009) Two-polymerase mechanisms dictate error-free and error-prone translesion DNA synthesis in mammals. *EMBO Journal* 28: 383-393.

83. Ogi T, Lehmann AR (2006) The Y-family DNA polymerase kappa (pol kappa) functions in mammalian nucleotide-excision repair. *Nature Cell Biol* 8: 640-642.
84. Ogi T, Limsirichaikul S, Overmeer RM, Volker M, Takenaka K, et al. (2010) Three DNA polymerases, recruited by different mechanisms, carry out NER repair synthesis in human cells. *Molecular Cell* 37: 714-727.
85. Schenten D, Gerlach VL, Guo C, Velasco-Miguel S, Hladik CL, et al. (2002) DNA polymerase kappa deficiency does not affect somatic hypermutation in mice. *European Journal of Immunology* 32: 3152-3160.
86. Shimizu T, Shinkai Y, Ogi T, Ohmori H, Azuma T (2003) The absence of DNA polymerase kappa does not affect somatic hypermutation of the mouse immunoglobulin heavy chain gene 2. *Immunology Letters* 86: 265-270.
87. Stancel JNK, McDaniel LD, Velasco S, Richardson J, Guo C, et al. (2009) Polk mutant mice have a spontaneous mutator phenotype. *DNA Repair* 8: 1355-1362.
88. O-Wang J, Kawamura K, Tada Y, Ohmori H, Kimura H, et al. (2001) DNA Polymerase {kappa}, Implicated in Spontaneous and DNA Damage-induced Mutagenesis, Is Overexpressed in Lung Cancer. *Cancer Research* 61: 5366-5369.
89. Skaug V, Ryberg D, Arab EHK, Stangeland L, Myking AO, et al. (2000) p53 Mutations in Defined Structural and Functional Domains Are Related to Poor Clinical Outcome in Non-Small Cell Lung Cancer Patients. *Clinical Cancer Research* 6: 1031-1037.
90. Diaz M, Watson NB, Turkington G, Verkoczy LK, Klinman NR, et al. (2003) Decreased frequency and highly aberrant spectrum of ultraviolet-induced

- mutations in the *hprt* gene of mouse fibroblasts expressing antisense RNA to DNA polymerase zeta. *Molecular Cancer Research* 1: 836-847.
91. Murakumo Y, Roth T, Ishii H, Rasio D, Numata S, et al. (2000) A human REV7 homolog that interacts with the polymerase zeta catalytic subunit hREV3 and the spindle assembly checkpoint protein hMAD2. *Journal of Biological Chemistry* 275: 4391-4397.
92. Quah S-K, von Borstel RC, Hastings PJ (1980) THE ORIGIN OF SPONTANEOUS MUTATION IN *SACCHAROMYCES CEREVISIAE*. *Genetics* 96: 819-839.
93. Van Sloun PP, Varlet I, Sonneveld E, Boei JJ, Romeijn RJ, et al. (2002) Involvement of mouse Rev3 in tolerance of endogenous and exogenous DNA damage. *Molecular and Cellular Biology* 22: 2159-2169.
94. Wittschieben JP, Reshmi SC, Gollin SM, Wood RD (2006) Loss of DNA Polymerase {zeta} Causes Chromosomal Instability in Mammalian Cells. *Cancer Research* 66: 134-142.
95. Bemark M, Khamlichi AA, Davies SL, Neuberger MS (2000) Disruption of mouse polymerase zeta (Rev3) leads to embryonic lethality and impairs blastocyst development in vitro. *Current Biology* 10: 1213-1216.
96. Wittschieben J, Shivji MK, Lalani E, Jacobs MA, Marini F, et al. (2000) Disruption of the developmentally regulated Rev3l gene causes embryonic lethality. *Current Biology* 10: 1217-1220.
97. Esposito G, Godin I, Klein U, Yaspo ML, Cumano A, et al. (2000) Disruption of the Rev3l-encoded catalytic subunit of polymerase [zeta] in mice results in early embryonic lethality. *Current Biology* 10: 1221-1224.

98. Brondello JM, Pillaire MJ, Rodriguez C, Gourraud PA, Selves J, et al. (2008) Novel evidences for a tumor suppressor role of Rev3, the catalytic subunit of Pol [zeta]. *Oncogene*.
99. Kawamura K, Wang J, Bahar R, Koshikawa N, Shishikura T, et al. (2001) The error-prone DNA polymerase zeta catalytic subunit (Rev3) gene is ubiquitously expressed in normal and malignant human tissues. *International Journal of Oncology* 18: 97-103.
100. Friedberg EC (2006) DNA repair and mutagenesis. Washington, D.C.: ASM Press. xxix, 1118 p. p.
101. Batty D, Ropic'-Otrin V, Levine AS, Wood RD (2000) Stable binding of human XPC complex to irradiated DNA confers strong discrimination for damaged sites. *Journal of Molecular Biology* 300: 275-290.
102. Mocquet V, Kropachev K, Kolbanovskiy M, Kolbanovskiy A, Tapias A, et al. (2007) The human DNA repair factor XPC-HR23B distinguishes stereoisomeric benzo [a]pyrenyl-DNA lesions. *EMBO Journal* 26: 2923-2932.
103. Araujo SJ, Nigg EA, Wood RD (2001) Strong functional interactions of TFIIH with XPC and XPG in human DNA nucleotide excision repair, without a preassembled repairsome. *Molecular and Cellular Biology* 21: 2281-2291.
104. Li RY, Calsou P, Jones CJ, Salles B (1998) Interactions of the transcription/DNA repair factor TFIIH and XP repair proteins with DNA lesions in a cell-free repair assay. *Journal of Molecular Biology* 281: 211-218.

105. Evans E, Moggs JG, Hwang JR, Egly JM, Wood RD (1997) Mechanism of open complex and dual incision formation by human nucleotide excision repair factors. *EMBO Journal* 16: 6559-6573.
106. Evans E, Fellows J, Coffey A, Wood RD (1997) Open complex formation around a lesion during nucleotide excision repair provides a structure for cleavage by human XPG protein. *EMBO Journal* 16: 625-638.
107. Moggs JG, Yarema KJ, Essigmann JM, Wood RD (1996) Analysis of incision sites produced by human cell extracts and purified proteins during nucleotide excision repair of a 1,3-intrastrand d(GpTpG)-cisplatin adduct. *Journal of Biological Chemistry* 271: 7177-7186.
108. Budd ME, Campbell JL (1997) The roles of the eukaryotic DNA polymerases in DNA repair synthesis. *Mutation Research* 384: 157-167.
109. Nishida C, Reinhard P, Linn S (1988) DNA repair synthesis in human fibroblasts requires DNA polymerase delta. *Journal of Biological Chemistry* 263: 501-510.
110. Moser J, Kool H, Giakzidis I, Caldecott K, Mullenders LH, et al. (2007) Sealing of chromosomal DNA nicks during nucleotide excision repair requires XRCC1 and DNA ligase III alpha in a cell-cycle-specific manner. *Molecular Cell* 27: 311-323.
111. Bohr VA, Smith CA, Okumoto DS, Hanawalt PC (1985) DNA repair in an active gene: removal of pyrimidine dimers from the DHFR gene of CHO cells is much more efficient than in the genome overall. *Cell* 40: 359-369.
112. Park JS, Roberts JW (2006) Role of DNA bubble rewinding in enzymatic transcription termination. *Proceedings of the National Academy of Sciences* 103: 4870-4875.

113. Tanaka K, Miura N, Satokata I, Miyamoto I, Yoshida MC, et al. (1990) Analysis of a human DNA excision repair gene involved in group A xeroderma pigmentosum and containing a zinc-finger domain. *Nature* 348: 73-76.
114. de Vries A, van Oostrom CT, Hofhuis FM, Dortant PM, Berg RJ, et al. (1995) Increased susceptibility to ultraviolet-B and carcinogens of mice lacking the DNA excision repair gene XPA. *Nature* 377: 169-173.
115. Weinert TA, Hartwell LH (1988) The RAD9 gene controls the cell cycle response to DNA damage in *Saccharomyces cerevisiae*. *Science* 241: 317-322.
116. Parker LL, Piwnica-Worms H (1992) Inactivation of the p34cdc2-cyclin B complex by the human WEE1 tyrosine kinase. *Science* 257: 1955-1957.
117. Mueller PR, Coleman TR, Dunphy WG (1995) Cell cycle regulation of a *Xenopus* Wee1-like kinase. *Molecular Biology of the Cell* 6: 119-134.
118. Peng CY, Graves PR, Thoma RS, Wu Z, Shaw AS, et al. (1997) Mitotic and G2 checkpoint control: regulation of 14-3-3 protein binding by phosphorylation of Cdc25C on serine-216. *Science* 277: 1501-1505.
119. Sanchez Y, Wong C, Thoma RS, Richman R, Wu Z, et al. (1997) Conservation of the Chk1 checkpoint pathway in mammals: linkage of DNA damage to Cdk regulation through Cdc25. *Science* 277: 1497-1501.
120. Toyoshima-Morimoto F, Taniguchi E, Shinya N, Iwamatsu A, Nishida E (2001) Polo-like kinase 1 phosphorylates cyclin B1 and targets it to the nucleus during prophase. *Nature* 410: 215-220.
121. Jackman M, Lindon C, Nigg EA, Pines J (2003) Active cyclin B1-Cdk1 first appears on centrosomes in prophase. *Nature Cell Biology* 5: 143-148.

122. Watanabe N, Arai H, Nishihara Y, Taniguchi M, Hunter T, et al. (2004) M-phase kinases induce phospho-dependent ubiquitination of somatic Wee1 by SCFbeta-TrCP. *Proceedings of the National Academy of Sciences* 101: 4419-4424.
123. Toyoshima-Morimoto F, Taniguchi E, Nishida E (2002) Plk1 promotes nuclear translocation of human Cdc25C during prophase. *EMBO Reports* 3: 341-348.
124. Lee H, Larner JM, Hamlin JL (1997) A p53-independent damage-sensing mechanism that functions as a checkpoint at the G1/S transition in Chinese hamster ovary cells. *Proceedings of the National Academy of Sciences* 94: 526-531.
125. Falck J, Mailand N, Syljuasen RG, Bartek J, Lukas J (2001) The ATM-Chk2-Cdc25A checkpoint pathway guards against radioresistant DNA synthesis. *Nature* 410: 842-847.
126. Despras E, Daboussi F, Hyrien O, Marheineke K, Kannouche PL (2010) ATR/Chk1 pathway is essential for resumption of DNA synthesis and cell survival in UV-irradiated XP variant cells. *Human Molecular Genetics* 19: 1690-1701.
127. Weiss RS, Leder P, Vaziri C (2003) Critical Role for Mouse Hus1 in an S-Phase DNA Damage Cell Cycle Checkpoint. *Molecular and Cellular Biology* 23: 791-803.
128. Johnson RE, Kondratick CM, Prakash S, Prakash L (1999) hRAD30 mutations in the variant form of xeroderma pigmentosum. *Science* 285: 263-265.
129. Tissier A, Frank EG, McDonald JP, Iwai S, Hanaoka F, et al. (2000) Misinsertion and bypass of thymine-thymine dimers by human DNA polymerase iota. *EMBO Journal* 19: 5259-5266.

130. Ziv O, Geacintov N, Nakajima S, Yasui A, Livneh Z (2009) DNA polymerase ζ cooperates with polymerases κ and ι in translesion DNA synthesis across pyrimidine photodimers in cells from XPV patients. *Proceedings of the National Academy of Sciences* 106: 11552-11557.
131. Waters LS, Walker GC (2006) The critical mutagenic translesion DNA polymerase Rev1 is highly expressed during G(2)/M phase rather than S phase. *Proceedings of the National Academy of Sciences* 103: 8971-8976.
132. Parrinello S, Samper E, Krtolica A, Goldstein J, Melov S, et al. (2003) Oxygen sensitivity severely limits the replicative lifespan of murine fibroblasts. *Nature Cell Biology* 5: 741-747.
133. Enright AJ, John B, Gaul U, Tuschl T, Sander C, et al. (2003) MicroRNA targets in *Drosophila*. *Genome Biology* 5: R1.
134. Betel D, Wilson M, Gabow A, Marks DS, Sander C (2008) The microRNA.org resource: targets and expression. *Nucleic Acids Res* 36: D149-153.
135. Guo L, Huang ZX, Chen XW, Deng QK, Yan W, et al. (2008) Differential Expression Profiles of microRNAs in NIH3T3 Cells in Response to UVB Irradiation. *Photochemistry and Photobiology*.
136. Pothof J, Verkaik NS, van IW, Wiemer EA, Ta VT, et al. (2009) MicroRNA-mediated gene silencing modulates the UV-induced DNA-damage response. *EMBO Journal* 28: 2090-2099.
137. Lanni JS, Jacks T (1998) Characterization of the p53-Dependent Postmitotic Checkpoint following Spindle Disruption. *Molecular and Cellular Biology* 18: 1055-1064.

138. Laffin J, Fogleman D, Lehman JM (1989) Correlation of DNA content, p53, T antigen, and V antigen in simian virus 40-infected human diploid cells. *Cytometry* 10: 205-213.
139. Brash DE, Rudolph JA, Simon JA, Lin A, McKenna GJ, et al. (1991) A Role for Sunlight in Skin Cancer: UV-Induced p53 Mutations in Squamous Cell Carcinoma. *Proceedings of the National Academy of Sciences* 88: 10124-10128.
140. Lautenschlager S, Wulf HC, Pittelkow MR (2007) Photoprotection. *The Lancet* 370: 528-537.
141. de Gruijl FR, Sterenborg HJ, Forbes PD, Davies RE, Cole C, et al. (1993) Wavelength dependence of skin cancer induction by ultraviolet irradiation of albino hairless mice. *Cancer Research* 53: 53-60.
142. van Kranen HJ, de Gruijl FR, de Vries A, Sontag Y, Wester PW, et al. (1995) Frequent p53 alterations but low incidence of ras mutations in UV-B-induced skin tumors of hairless mice. *Carcinogenesis* 16: 1141-1147.
143. Fisher M, Kripke M (1977) Systemic alteration induced in mice by ultraviolet light irradiation and its relationship to ultraviolet carcinogenesis. *Proceedings of the National Academy of Sciences* 74: 5.
144. USDA UV-B Monitoring and Research Program. Colorado State University, Fort Collins, Co. 80523.
145. Setlow RB (1974) The Wavelengths in Sunlight Effective in Producing Skin Cancer: A Theoretical Analysis. *Proceedings of the National Academy of Sciences* 71: 3363-3366.

146. Kuluncsics Z, Perdiz D, Brulay E, Muel B, Sage E (1999) Wavelength dependence of ultraviolet-induced DNA damage distribution: Involvement of direct or indirect mechanisms and possible artefacts. *Journal of Photochemistry and Photobiology B: Biology* 49: 71-80.
147. Rogers HW, Weinstock MA, Harris AR, Hinckley MR, Feldman SR, et al. (2010) Incidence Estimate of Nonmelanoma Skin Cancer in the United States, 2006. *Archives of Dermatology* 146: 283-287.
148. De Vries E, Van De Poll-Franse LV, Louwman WJ, De Gruijl FR, Coebergh JWW (2005) Predictions of skin cancer incidence in the Netherlands up to 2015. *British Journal of Dermatology* 152: 481-488.
149. Stern RS (2010) Prevalence of a History of Skin Cancer in 2007: Results of an Incidence-Based Model. *Archives of Dermatology* 146: 279-282.
150. Bickers DR, Lim HW, Margolis D, Weinstock MA, Goodman C, et al. (2006) The burden of skin diseases: 2004: A joint project of the American Academy of Dermatology Association and the Society for Investigative Dermatology. *Journal of the American Academy of Dermatology* 55: 490-500.
151. de Vries A, Berg RJ, Wijnhoven S, Westerman A, Wester PW, et al. (1998) XPA-deficiency in hairless mice causes a shift in skin tumor types and mutational target genes after exposure to low doses of U.V.B. *Oncogene* 16: 2205-2212.
152. (2007) *The Genetic Basis of Human Cancer* Vogelstein B, Kinzler KW, editors. New York: McGraw-Hill.
153. Boveri T (1929) *The Origin of Malignant Tumors* Baltimore, MD: Williams and Wilkins.

154. Borgen A, Darvey H, Castagnoli N, Crocker TT, Rasmussen RE, et al. (1973)
Metabolic conversion of benzo(a)pyrene by Syrian hamster liver microsomes and
binding of metabolites to deoxyribonucleic acid. *The Journal of Medicinal
Chemistry* 16: 502-506.
155. Sims P, Grover PL (1974) Epoxides in polycyclic aromatic hydrocarbon metabolism
and carcinogenesis. *Advanced Cancer Research* 20:165-274.: 165-274.
156. Pelkonen O, Nebert DW (1982) Metabolism of polycyclic aromatic hydrocarbons:
etiologic role in carcinogenesis. *Pharmacological Reviews* 34: 189-222.
157. Chen L, Devanesan PD, Higginbotham S, Ariese F, Jankowiak R, et al. (1996)
Expanded analysis of benzo [a]pyrene-DNA adducts formed in vitro and in mouse
skin: their significance in tumor initiation. *Chemical Research in Toxicology* 9:
897-903.
158. Randerath E, Agrawal HP, Reddy MV, Randerath K (1983) Highly persistent
polycyclic aromatic hydrocarbon-DNA adducts in mouse skin: Detection by 32P-
postlabeling analysis. *Cancer Letters* 20: 109-114.
159. Schurdak ME, Randerath K (1989) Effects of Route of Administration on Tissue
Distribution of DNA Adducts in Mice: Comparison of 7H-Dibenzo(c,g)carbazole,
Benzo(a)pyrene, and 2-Acetylaminofluorene. *Cancer Research* 49: 2633-2638.
160. Yang JL, Maher VM, McCormick JJ (1989) Amplification and direct nucleotide
sequencing of cDNA from the lysate of low numbers of diploid human cells.
Gene 83: 347-354.

161. Zhang Y, Wu X, Guo D, Rechkoblit O, Geacintov NE, et al. (2002) Two-step error-prone bypass of the (+)- and (-)-trans-anti-BPDE-N²-dG adducts by human DNA polymerases eta and kappa. *Mutation Research* 510: 23-35.
162. Day TA, Palle K, Barkley LR, Kakusho N, Zou Y, et al. (2010) Phosphorylated Rad18 directs DNA Polymerase η to sites of stalled replication. *The Journal of Cell Biology* 191: 953-966.
163. Zhang Y, Yuan F, Wu X, Wang Z (2000) Preferential incorporation of G opposite template T by the low-fidelity human DNA polymerase iota. *Molecular and Cellular Biology* 20: 7099-7108.
164. Vaisman A, Tissier A, Frank EG, Goodman MF, Woodgate R (2001) Human DNA polymerase iota promiscuous mismatch extension. *Journal of Biological Chemistry* 276: 30615-30622.
165. Zhang Y, Yuan F, Wu X, Taylor JS, Wang Z (2001) Response of human DNA polymerase iota to DNA lesions. *Nucleic Acids Research* 29: 928-935.
166. Plosky BS, Vidal AE, Fernandez de Henestrosa AR, McLenigan MP, McDonald JP, et al. (2006) Controlling the subcellular localization of DNA polymerases iota and eta via interactions with ubiquitin. *EMBO Journal* 25: 2847-2855.

LIST OF ABBREVIATIONS

7AAD	7-aminoactinomycin D
ANOVA	analysis of variables
BER	base excision repair
BPDE	benzo[a]pyrene dihydrodiolepoxide
BrdU	bromodeoxyuridine
CPD	cyclobutane pyrimidine dimer
FACS	fluorescence activated cell sorting
FDR	false discovery rate
Hprt	hypoxanthine guanine phosphoribosyltransferase
IPA	Ingenuity Pathway Analysis
IVT	in vitro transcription
MED	minimal erythematous dose
NER	nucleotide excision repair
PCNA	proliferating cell nuclear antigen
Pol ζ	DNA polymerase zeta
Pol η	DNA polymerase eta
Pol ι	DNA polymerase iota
Pol κ	DNA polymerase kappa
SNP	single nucleotide polymorphism
SUMO	small ubiquitin-like modifier

TG	6-thioguaning
TLS	translesion synthesis
UTR	untranslated region
UV	ultraviolet radiation
WHO	World Health Organization
XP	xeroderma pigmentosum

CURRICULUM VITAE

BIOGRAPHICAL

Name: Lindsey Jay Stallons **Birth Date:** August 25, 1983
Home Address: 3606 Locust Avenue **Birth Place:** Paducah, Kentucky
Louisville, KY 40299
Home Phone: 502.558.8507 **Citizenship:** USA
Business Address: Dept of Pharmacology **E-Mail:** jay.stallons@gmail.com
& Toxicology
505 S. Hancock St
Room 352F
Louisville, KY 40202
Business Phone: 502.852.2115 **Business Fax:** 502.852.2123

EDUCATION AND TRAINING

UNDERGRADUATE

<i>Dates attended</i>	<i>Name and location of institution</i>	<i>Degree received and date</i>	<i>Major subject</i>
2003 – 2006	University of Louisville Louisville, KY	Bachelor of Science May 2006	Chemistry
2002 – 2003	Centre College Danville, KY	Transfer May 2003	Chemistry

GRADUATE

<i>Dates attended</i>	<i>Name and location of institution</i>	<i>Degree received and date</i>	<i>Major subject</i>
2006 - Present	University of Louisville Louisville, KY	MS – August 2008 Ph.D. – June 2011	Pharmacology & Toxicology

PROFESSIONAL EXPERIENCE

ACADEMIC:

<i>Years inclusive</i>	<i>Name and location of institution, department and mentor / supervisor</i>	<i>Title</i>
2004 - 2005	University of Louisville Dept of Chemistry, Teresa Fan, Ph.D.	Undergraduate Research Asst.

2005 - 2006	University of Louisville Resources for Academic Achievement, Karen Seng	Tutor
2005	University of Louisville Dept of Pharmacology, Glenn McGregor, M.D.	Undergraduate Research Asst.

PUBLICATIONS

1. **LJ Stallons** and WG McGregor, "Translesion Synthesis Polymerases in the Prevention and Promotion of Carcinogenesis," *Journal of Nucleic Acids*, vol. 2010, Article ID 643857, 10 pages, 2010. doi:10.4061/2010/643857. PMID: PMC2945679.
2. B Panchapakesan, R Caprara, V Velasco, J Loomis, B King, P Xu, T Burkhead, P Sethu, **LJ Stallons**, WG McGregor, SN Rai, G Kloecker, and E Wickstrom, "Micro- and nanotechnology approaches for capturing circulating tumor cells," *Cancer Nanotechnology*, 9 pages, 2010. doi: 10.1007/s12645-010-0007-z

PROFESSIONAL ACTIVITIES

Invited Seminar

- 2011 February 9 – Mitchell Cancer Institute, University of South Alabama
DNA polymerase iota causes mutations yet suppresses carcinogenesis after UV exposure; unexpected connections to the G2/M checkpoint

National / International Meetings

- 2007 Platform Presenter, Environmental Mutagen Soc. National Meeting, Atlanta, GA
Evidence from Mutation Spectra that DNA Polymerase eta is the Preferred Translesion DNA Polymerase and May Be Error-Free or Error-Prone
- 2008 Platform Presenter, Environmental Mutagen Soc. National Meeting, Rio Grande, Puerto Rico
Cell Death and Cell Cycle Pathways as Potential Targets for Tumor Suppression by Pol Iota: A Systems Biology Approach

Local / Regional Meetings

- 2005 Poster Presenter, Research Louisville, UofL
Chronic inflammation does not alter patterns of gene expression in carcinogen-initiated lung cancer
- 2006 Poster Presenter, Posters-at-the-Capitol, Frankfort, KY
Chronic inflammation does not alter patterns of gene expression in carcinogen-initiated lung cancer
- 2007 Seminar, Dept. of Pharmacology, University of Louisville
Human DNA polymerase η is error-free when bypassing UV photoproducts but error-prone when bypassing benzo[a]pyrene adducts in vivo.
- 2007 Seminar, Student Meeting of the Ohio Valley Society of Toxicology, Louisville, KY
Human DNA polymerase η is error-free when bypassing UV photoproducts but error-prone when bypassing benzo[a]pyrene adducts in vivo.

- 2007 1st Place Poster, Basic Science Masters Student, Research!Louisville, UofL
DNA polymerase eta is the preferred translesion DNA polymerase and may be error-free or error-prone: evidence from mutation spectra.
- 2007 Poster Presenter, Ohio Valley Society of Toxicology Annual Meeting, Indianapolis, IN
Polη and Polι are required for mutagenic bypass of BPDE lesions in primary murine fibroblasts
- 2007 Poster Presenter, JG Brown Cancer Center Annual Retreat, Louisville, KY
Polη and Polι are required for mutagenic bypass of BPDE lesions in primary murine fibroblasts
- 2008 Poster Presenter, JG Brown Cancer Center Annual Retreat, Louisville, KY
Cell death and cell cycle pathways as potential targets for tumor suppression by pol iota: a systems biology approach
- 2009 Platform Presenter, Graduate Research Symposium, University of Louisville
DNA polymerase iota suppresses UV-induced skin cancer by linking stalled replication forks with cell cycle arrest and apoptotic programs
- 2009 Platform Presenter, Student Meeting of the Ohio Valley SOT, Louisville, KY
DNA polymerase iota suppresses UV-induced skin cancer by linking stalled replication forks with cell cycle arrest and apoptotic programs.
- 2009 Poster Presenter, NIEHS Showcase of Fellows, Cincinnati, OH
DNA polymerase iota suppresses UV-induced skin cancer by linking stalled replication forks with cell cycle arrest and apoptotic programs.
- 2009 Poster Presenter, Research!Louisville, University of Louisville
DNA polymerase iota suppresses UV-induced skin cancer by facilitating DNA damage-induced cell cycle checkpoint arrest and apoptosis.
- 2009 2nd Place Graduate Student Poster, JG Brown Cancer Center Annual Retreat, Louisville, KY
DNA polymerase iota suppresses UV-induced skin cancer by facilitating DNA damage-induced cell cycle checkpoint arrest and apoptosis
- 2010 2nd Place Graduate Student Platform Presentation, Midwest DNA Repair Symposium, Louisville, KY
Bioinformatics analysis implicates DNA polymerase iota is involved in signaling mitotic entry and exit
- 2010 Poster Presenter, Research!Louisville, University of Louisville
Systems biology reveals altered polo-like kinase signaling in polymerase iota-deficient cells after UV
- 2010 Poster Presenter, JG Brown Cancer Center Annual Retreat, Louisville, KY
Systems biology reveals altered polo-like kinase signaling in polymerase iota-deficient cells after UV

Teaching:

Course: Advanced Nursing Contact Hours: 2
Topics: Presented basic pharmacology principles of absorption, distribution, metabolism, and excretion to 50 Master's level nursing students in the Fall of 2009.

Course: Dental Hygiene Contact Hours: 5
Topics: Covered topics including antibiotics, antiseptics, and antiviral/anticancer drugs to 30 undergraduate level students in the Fall of 2010.

Service:

University of Louisville

Co-Founder & Vice President, Pharm/Tox Graduate Student Organization	2009 – 2010
Public Safety Advisory Committee	2009 – 2010
Medical Council Graduate Student Representative	2009 – 2010
Senator, Student Senate, UofL Student Government Association	2009 – 2010
GSC Representative & Academic Policy Board member, UofL Student Senate	2009 – 2010
Vice President, Graduate Student Council (GSC)	2009 – 2010

Departmental Representative, Graduate Student Council	2008 – 2009
Organizer and Founder, Third Thursday Seminar Series, Dept of Pharmacology	2008 – 2009
Graduate Education Committee, Dept. of Pharmacology and Toxicology	2008 – 2009
Departmental Chair Search Committee, Biochemistry & Molecular Biology	2007 – 2009

Mentoring:

University of Louisville
Undergraduates

Brian Sils
Robert Skaggs – Current medical student, U. of Kentucky
Anthony Smith – Current medical student, Pikeville University
Christopher Belcher – Current medical student, U. of Kentucky
Caleb Greenwell
Amanda Hodges – Current medical student, U. of Louisville

RESEARCH

Grant Support History:

<u>Grant Source</u>	<u>Grant Title</u>	<u>Role in Project and % of Effort</u>	<u>Years Inclusive</u>
NHLBI HL007260	Training to Improve Cardiovascular Therapies	T32 Fellow 100% (Postdoc)	6/2011 – 5/2012
NIEHS ES011564	U of L Environmental Health Sciences Training Program T32	T32 Fellow 100% (Predoc)	12/2007 – 11/2010

Current research interests:

- Characterize the cellular function of mammalian DNA polymerase iota
- Understand the cellular roles played by Y family DNA polymerases in response to structurally varied DNA adducts
- Investigate the role of Y family DNA polymerases in UV-induced immunosuppression
- Develop carbon nanotube devices to capture and characterize circulating tumor cells

MEMBERSHIPS in PROFESSIONAL and SCIENTIFIC SOCIETIES

Organization

<i>Year</i>	
	Society of Undergraduate Chemistry Students, University of Louisville
2004 – 2006	
	Vice President
2005 – 2006	
	Environmental Mutagen Society
2007 – Present	
	Ohio Valley Society of Toxicology
2007 – Present	
	American Association for Cancer Research
2008 – Present	

HONORS

<i>Title of award, sponsor</i>	<i>Year</i>
Dean's List, Centre College	2002 – 2003
Dean's List, University of Louisville	2003 – 2006
Cancer Education Program Fellowship, University of Louisville	2005
First Place Poster, Research!Louisville, University of Louisville	2007
Travel Award, Environmental Mutagen Society, Atlanta, Georgia	2007
Travel Award, University of Louisville School of Medicine	2007
Travel Award, University of Louisville Graduate Student Council	2007
Travel Award, University of Louisville Center for Genetics and Molecular Medicine	2008
Travel Award, Environmental Mutagen Society, San Juan, Puerto Rico	2008
Second Place Poster, Brown Cancer Center Retreat, University of Louisville	2009
Second Place Platform Presentation, Midwest DNA Repair Symposium, Louisville, KY	2010
Doctoral Dissertation Completion Award, University of Louisville	2010

COMMUNITY INVOLVEMENT

Co-Captain, OneCorps Community Service Group, Louisville, KY	2006 – 2008
Volunteer, Greyhound Pets of America, Louisville Chapter	2009 – Present

REFERENCES

W. Glenn McGregor, M.D.

Professor of Pharmacology & Toxicology
and Medicine
505 S. Hancock St, Rm 305
Louisville, KY 40202
wgmcgregor@louisville.edu
502.852.2564

J. Christopher States, Ph.D.

Professor of Pharmacology & Toxicology
505 S. Hancock St, Rm 304
Louisville, KY 40202
jcstates@louisville.edu
502.852.5347

Jason Chesney, M.D., Ph.D.

Associate Professor of Medicine, Biochemistry &
Molecular Biology, and Pharmacology
505 S. Hancock St, Rm 424
Louisville, KY 40202
jaches03@louisville.edu
502.852.3679

David W Hein, Ph.D.

Professor and Chair, Pharmacology &
Toxicology
505 S. Hancock St, Rm 303
Louisville, KY 40202
dwhein01@louisville.edu
502.852.6252